WRC RESEARCH REPORT NO. 103

REDUCTION OF AQUEOUS FREE CHLORINE WITH GRANULAR ACTIVATED CARBON

by

Makram T. Suidan
and
Vernon L. Snoeyink

University of Illinois at Urbana-Champaign
Urbana, Illinois

FINAL REPORT

Project No. A-066-ILL

The work upon which this publication is based was supported in part by funds provided by the U. S. Department of the Interior as authorized under the Water Resources Resarch Act of 1964, P. L. 88-379
Agreement No. 14-31-0001-5013

UNIVERSITY OF ILLINOIS
WATER RESOURCES CENTER

2535 Hydrosystems Laboratory
Urbana, Illinois 61801

August 1975

ABSTRACT

REDUCTION OF AQUEOUS CHLORINE WITH
GRANULAR ACTIVATED CARBON

A surface reaction rate expression was developed to describe the heterogeneous reaction between aqueous free chlorine and granular activated carbon. This expression was then incorporated into a pore diffusion model and the relevant partial differential equations with the corresponding boundary conditions were solved for the case of (1) a constant concentration batch reactor and (2) a closed batch reactor. The solutions were then compared to similar batch data in order to evaluate the pore model constants. A packed bed reactor model was then solved using the rate information from the batch mathematical models and experimental data. The predicted results from the packed bed model were then compared to experimental results which were collected using applicable conditions.

The effect of particle size on the rate of removal of free chlorine was investigated both in batch and packed bed column form. The effect of pH on the rate of reaction was studied in the pH range of 4-10. It was found that the pH only affects the rate insofar as it affects the distribution of free chlorine between OCl^- and HOCl.

Temperature effects were also studied in the range 2°-35°C. The effect of temperature on the surface dissociation rate constant was found to correspond to the Arrhenius law.

Suidan, Makram T. and Vernon L. Snoeyink
REDUCTION OF AQUEOUS FREE CHLORINE WITH GRANULAR ACTIVATED CARBON
Final report to the Office of Water Resources Research, Department of the Interior on Annual Allotment Project A-066-ILL, August 1975.

KEYWORDS: dechlorination/mathematical model/pore diffusion/packed bed model

ACKNOWLEDGEMENT

This report represents the thesis of Makram T. Suidan, submitted in partial fulfillment of the requirements for the degree of Doctor of Philosophy in Environmental Engineering in Civil Engineering at the University of Illinois at Urbana-Champaign, 1975.

The authors wish to thank Drs. Roger A. Schmitz, Jon C. Liebman and Arthur R. Robinson whose interest and many valuable suggestions contributed a great deal towards the completion of this investigation. The input provided by Drs. Edward S. K. Chian, Paul A. Jennings, Mr. Gerald E. Quindry and Mr. David L. Dunn is gratefully acknowledged.

This study was supported, in part, by funds provided by the United States Department of the Interior as authorized under the Water Resources Research Act of 1964, Public Law 88-379.

The numerical analysis was carried out using the IBM 360/75 computer system of the Computer Services Office of the University of Illinois, Urbana, Illinois.

TABLE OF CONTENTS

LIST OF FIGURES

NOTATION

A	Packed bed cross-sectional area	L^2
A_p	Pore surface area per unit weight of carbon	L^2/M
C	Free chlorine concentration per unit volume of solution	M/L^3
C_o	Initial, bulk or influent free chlorine concentration for closed batch, constant concentration batch and packed bed reactor	M/L^3
C^*	Reactive sites concentration per unit surface area of carbon	$SITE/L^2$
$CHOCl^*$	Adsorbed free chlorine concentration per unit surface area of carbon	$SITE/L^2$
CO^*	Oxidized sites concentration per unit surface area of carbon	$SITE/L^2$
C^*	Total sites concentration per unit surface area of carbon	$SITE/L^2$
CCBR	Constant concentration batch reactor	
D_A	Packed bed axial dispersion coefficient	L^2/T
D_c	Free chlorine pore diffusion coefficient	L^2/T
d_p	Diameter of straight cylindrical pore	L
F	Dimensionless free chlorine concentration in packed bed model	
G	Dimensionless free chlorine concentration in pore model	
H	Packed bed residence time	T

h	Dimensionless position variable used in packed bed numerical solution	
J_i	Constant i in expression for R(X,C)	
k	First order reaction rate constant in Magee's packed bed column reactor	T^{-1}
k_1	Free chlorine-activated carbon adsorption rate constant	L^2/T SITE
k_2	Free chlorine-activated carbon desorption rate constant	M/L T SITE
k_3	Surface reaction dissociation rate constant	M/L T SITE
k_4	Adsorption-desorption equilibrium constant	M/L^3
k_7	Numerator constant in SSO expression	SITE/M
k_8	$k_4 \cdot V_P$	
k_9	$k_7 \cdot L_p^2/D_c$	
k_{10}	Dimensionless constant in SSO expression	
k_d	First order rate of decay constant	T^{-1}
L_b	Packed bed length	L
L_p	Pore half length	L
M	Number of segments into which packed bed is sub-divided for numerical solution purposes	
m	Mass of carbon per unit reactor volume	M/L^3
N	Number of segments into which half pore is divided for numerical solution purposes	
n	2 x number of pores per unit weight of carbon	M^{-1}

p	Dimensionless position in time used in packed bed numerical solution	
P	Free chlorine mass concentration per unit mass of carbon	
P_e	Peclet number	
P_o	Initial or bulk free chlorine concentration per unit mass of carbon for closed batch or CCBR models	
pK_a	Negative $\log_{10}$ of equilibrium constant	
Q	Mass of free chlorine reacted per unit mass of carbon	
q	Dimensionless position in time used in numerical solution of pore model	
R	Dimensionless rate term in pore model	
R_c	Surface reaction rate	$M/L^3\ T$
R_d	Rate of free chlorine decay in blank Reactor	$M/L^3\ T$
R_{rc}	Rate of chlorine removal for a concentration of carbon equal to m	$M/L^3\ T$
R_{rp}	$R_{rc}V_p$	T^{-1}
R(X,C)	Free chlorine mass removal rate per unit mass of carbon	T^{-1}
r	Dimensionless position in space used in numerical solution of pore model	
S	Rate of free chlorine mass applied per unit mass of carbon in packed bed reactor	T^{-1}
SIT	SST x L_p^2/D_c	
SSO	Oxidized sites per unit mass of carbon x $k_3 d_p/4$	T^{-1}

SST	Total reactive sites per unit mass of carbon x $k_3 dp/4$	T^{-1}
$\overline{T}$	Absolute temperature	°K
t	Cumulative time for batch or column run	T
t*	Bed residence time in Magee's model	T
v	Axial velocity through packed bed reactor	L/T
V_p	Pore volume per unit mass of carbon	L^3/M
W	Free chlorine mass reacted per unit surface area	M/L^2
X	Total free chlorine reacted per unit mass of carbon	
Y	Position variable in pore model	L
z	Distance variable in packed bed column model	L
C	Change from mean concentration, C_o, allowed in CCBR experiments	M/L^3
$\Delta H°$	Enthalpy of Reaction	ML^2/T^2
Δh	Dimensionless distance step used in numerical solution of packed bed reactor model	
Δp	Dimensionless time step used in numerical solution of packed bed reactor model	
Δq	Dimensionless time step used in numerical solution of pore model	
Δr	Dimensionless distance step used in numerical solution of pore model	
α	Dimensionless position variable in packed bed model	
ε	Packed bed porosity	

μ	Absolute viscosity of solution	M/L·T
θ	Dimensionless time variable in pore model	
ξ	Dimensionless position variable in pore model	
τ	Dimensionless time variable in packed bed model	
γ	$\tau-\alpha$	

I. INTRODUCTION

Free chlorine has been used in water treatment for many years. Its primary use is for disinfection, although it has a number of other applications, such as ammonia removal and taste and odor control. Free chlorine residual is sometimes in excess of desired levels, and consequently it has to be removed or reduced in concentration. This may be the case, for example, after breakpoint chlorination, especially of wastewater. A number of industries also require chlorine free water because of the interference of chlorine with some industrial processes. These and many other reasons illustrate the importance of having a well understood process for the removal of free chlorine from water.

A. Literature Review

A number of processes have been developed for eliminating or reducing free chlorine residuals from water, the use of sulfur compounds being the most common. Activated carbon, hydrogen peroxide, ammonia and ferrous sulfate have also been used. Snoeyink and Suidan (1975) conducted an intensive literature review of the subject of dechlorination and some of the material in this section was taken from that review.

1. Dechlorination with Sulfur Compounds

The most common procedure for reducing free chlorine residual involves the use of sulfur compounds with sulfur in the +IV oxidation state. Sulfur dioxide is the most popular among the S(+IV) species, the major

reason for which appears to be the cost of using it. Dean (1974) has estimated that the cost of chlorination of a secondary effluent for disinfection followed by dechlorination with SO_2 will be on the order of 1.2 to 1.3 times as great as chlorination alone.

Sulfur dioxide is generally purchased as a liquid which is then converted to a gas in preparation for adding it to water. The gas dissolves readily in water forming sulfurous acid

$$SO_2 + H_2O \rightleftarrows H_2SO_3 \qquad 1.1$$

The H_2SO_3 partially ionizes to give HSO_3^- and $SO_3^=$, with the relative concentrations of these species being dependent on pH. Sodium bisulfite, $NaHSO_3$, and sodium sulfite, Na_2SO_3, are salts which are also used as a source of S(+IV) for dechlorination but these are generally more expensive and less stable than SO_2 (Laubusch, 1971). A major advantage in using SO_2 is that the equipment used for feeding it is the same as that used for dosing chlorine (White, 1972). This similarity serves to cut down on equipment variability in a plant and thus to reduce operational difficulties.

According to White (1972), hypochlorous acid reacts with SO_2 as follows:

$$SO_2 + H_2O + HOCl \rightarrow 3\,H^+ + SO_4^= + Cl^- \qquad 1.2$$

with similar reactions being applicable when the other S(+IV) species are used. Using Equation 1.2 as a basis for calculation, it can be shown that 0.9 mg of SO_2 is required per mg of chlorine, as Cl_2, reduced. Similarly, 2.1 mg of alkalinity as $CaCO_3$ is required to react with the H^+ produced by

the reaction. If the H^+ resulting from hydrolysis of gaseous Cl_2 when it is added to the water is included, a total of 2.8 mg of alkalinity is required per mg of chlorine. There is some evidence that the required S(+IV) dose is a function of the composition of the water (Gagen, 1941).

The kinetics of S(+IV) dechlorination are very fast. White (1972) states that it reacts nearly instantaneously with free chlorine. A search of the available literature has not revealed information on the effect of pH, temperature and composition of the water on the kinetics. Because of the very rapid reaction kinetics, mixing is the most important parameter to be considered when S(+IV) compounds are to be used for dechlorination.

The reaction between S(+IV) and oxygen

$$O_2 + 2\ SO_2 + 2\ H_2O \rightarrow 4\ H^+ + 2\ SO_4^{=} \qquad 1.3$$

is important and merits careful consideration. The extent to which it proceeds will increase the S(+IV) dose, but, more importantly, depletion of dissolved oxygen may necessitate a costly reaeration step if dechlorination is being applied prior to discharge of a treated wastewater to receiving waters. It also indicates the importance of avoiding any overdose of S(+IV), which may be difficult in certain situations.

Sodium thiosulfate, $Na_2S_2O_3$, can also be used in dechlorination but it reacts more slowly than the S(+IV) compounds and it can contribute to sensory effects involved with taste and odor (Baker, 1964). It is usually employed for dechlorinating water samples prior to bacteriological analysis.

2. Dechlorination with Hydrogen Peroxide, Ammonia and Ferrous Sulfate

Hydrogen peroxide has not been extensively used for dechlorination

although it may have some potential in this respect. According to Mishchenko *et al.* (1960), the following reaction will take place.

$$HOCl + H_2O_2 \rightarrow O_2\,(aq) + H^+ + Cl^- + H_2O \qquad 1.4$$

This reaction is not thermodynamically limited (ΔG° = -36.3 kcal at 25°C) but the kinetics of the reaction with free chlorine have not been well defined. In view of the lack of information about the use of this compound for dechlorination, it is obvious that much more remains to be learned if the feasibility of using it is to be fully assessed.

According to White (1972) as well as others, ammonia and ferrous sulfate can be used as dechlorinating agents. Ammonia can be used to eliminate free chlorine via the breakpoint reaction,

$$2\,NH_3 + 3\,HOCl \rightarrow N_2 + 3\,H^+ + 3\,Cl^- + 3\,H_2O \qquad 1.5$$

or it can be used to convert free chlorine to combined chlorine. A very long reaction time, approximately 20 minutes in the pH range 7 to 7.5, must be allotted for the breakpoint reaction, however (White, 1972).

Ferrous ion, Fe^{+2}, can also be used as a dechlorinating agent, but its use is limited to situations where dechlorination is followed by a solids removal step. When oxidized by chlorine, Fe^{+2} is converted to Fe^{+3} which is very insoluble and which serves as a good coagulant. Sedimentation and/or filtration would be required to remove it from the water. According to White (1972), Fe^{+2} reacts readily with free chlorine.

3. Dechlorination with Activated Carbon

a. Free Chlorine - Activated Carbon Reactions

Activated carbon has been used for dechlorination for some time. The process was first installed in a municipal water treatment plant at Reading, England in 1910. It appears to have been used predominantly for the removal of free chlorine, although reference has been made to the fact that it will also remove combined chlorine (Magee, 1956). Magee (1956) was the first to conduct an intensive study of this process but despite the advancement which he and others following him have made, much remains to be learned about it.

Investigators (Magee, 1956; Puri, 1970) have studied the reaction between free chlorine and carbon and according to their findings, it can be described by the following equation:

$$C^* + HOCl \rightarrow CO^* + H^+ + Cl^- \qquad 1.6$$

where C^* represents the activated carbon and CO^* represents a surface oxide on the carbon. Magee (1956) showed that when free chlorine is initially contacted with activated carbon, there is an initial buildup of Cl-containing species on the carbon surface. After a period of time, however, the chlorides produced in the reaction are stoichiometrically equal to the free chlorine removed from the aqueous solution in the reactor. Snoeyink *et al.* (1974) also observed similar results.

The hydrogen ion produced in accordance with Equation 1.6 is important because it may necessitate a pH adjustment step subsequent to

dechlorination. The problem of a pH decrease becomes more severe if chlorine gas is used as the source of chlorine. Chlorine gas hydrolyzes to produce H^+ when added to water. The stoichiometry of the reaction in Equation 1.6 requires further study with respect to production of H^+, however. Based on this equation, it is predicted that no H^+ will be produced if OCl^- reacts in place of HOCl. However, Olson and Binning (1974) and Snoeyink *et al.* (1974) noticed a pH drop when OCl^- reacted, the reason for which was not determined. It may be attributable to the formation of a surface oxide in the form of a carboxyl group which subsequently ionizes to produce the H^+, however (Olson and Binning, 1974). In experiments carried out by the author, no H^+ production was observed when the carbonate system was in equilibrium with the atmosphere. Thus, the drop in pH observed by Olson and Binning (1974) and Snoeyink *et al.* (1974) could be attributed to CO_2 dissolution from the atmosphere.

The production of surface oxides via Equation 1.6 is important because of their effect on the dechlorination reaction as well as on the adsorption of organic compounds by the carbon. Magee (1956) attributed the gradual reduction in efficiency of dechlorination of a carbon bed to the gradual poisoning of the carbon surface with these oxides. He also observed that these oxides were unstable to a certain degree because CO and CO_2 were released to the solution. That this does occur is fortunate because it probably results in extended life of the carbon for dechlorination.

Using the analytical procedure of Boehm (1966), Snoeyink *et al.* (1974) studied the accumulation of acidic surface oxides as a function of the amount of free chlorine reacted. As the amount of chlorine reacted

increases, the surface concentration of NaOH titratable oxides reached a plateau as can be seen in Figure 1.1. At the plateau value, approximately 15 mmoles free chlorine (1.06 g as Cl_2) have reacted per gram of carbon. Many of the titratable oxides were relatively volatile in nature and could be removed by drying at 105°-110°C or, alternatively, by drying and outgassing, as shown in Figure 1.1. The same study showed that the oxides removed by this procedure had little effect on adsorption of phenolic compounds.

Only a small fraction of the oxides which were produced via Equation 1.6 were titratable with NaOH. On the basis of the reaction stoichiometry, a one-to-one correspondence between oxides produced and chlorine reacted is expected. Such was not the case, however. Only 1.5-2 mmoles of titratable oxides were formed for 15 mmoles reacted per gram; also the increase in oxides was not linear but reached a plateau. Some of the oxides were probably evolved while others were not titratable with NaOH. It was also found possible to nearly double the concentration of NaOH titratable oxides by using three sequential treatments of the carbon with 15 mmoles chlorine per gram, with each treatment being followed by drying of the carbon.

The surface oxides which result from reaction with chlorine also affect adsorption of organic compounds. Figure 1.2 (Snoeyink *et al.*, 1974) shows the decrease in capacity of carbon for p-nitrophenol as a function of the amount of chlorine reacted. Each treatment with chlorine was followed by drying of the carbon at 105°-110°C prior to the adsorption studies. The value at 60 mmoles/g was obtained by using carbon which had been reacted with 15 mmoles chlorine per gram four times and dried after each treatment. The decrease in capacity may possibly be attributed to destruction of the

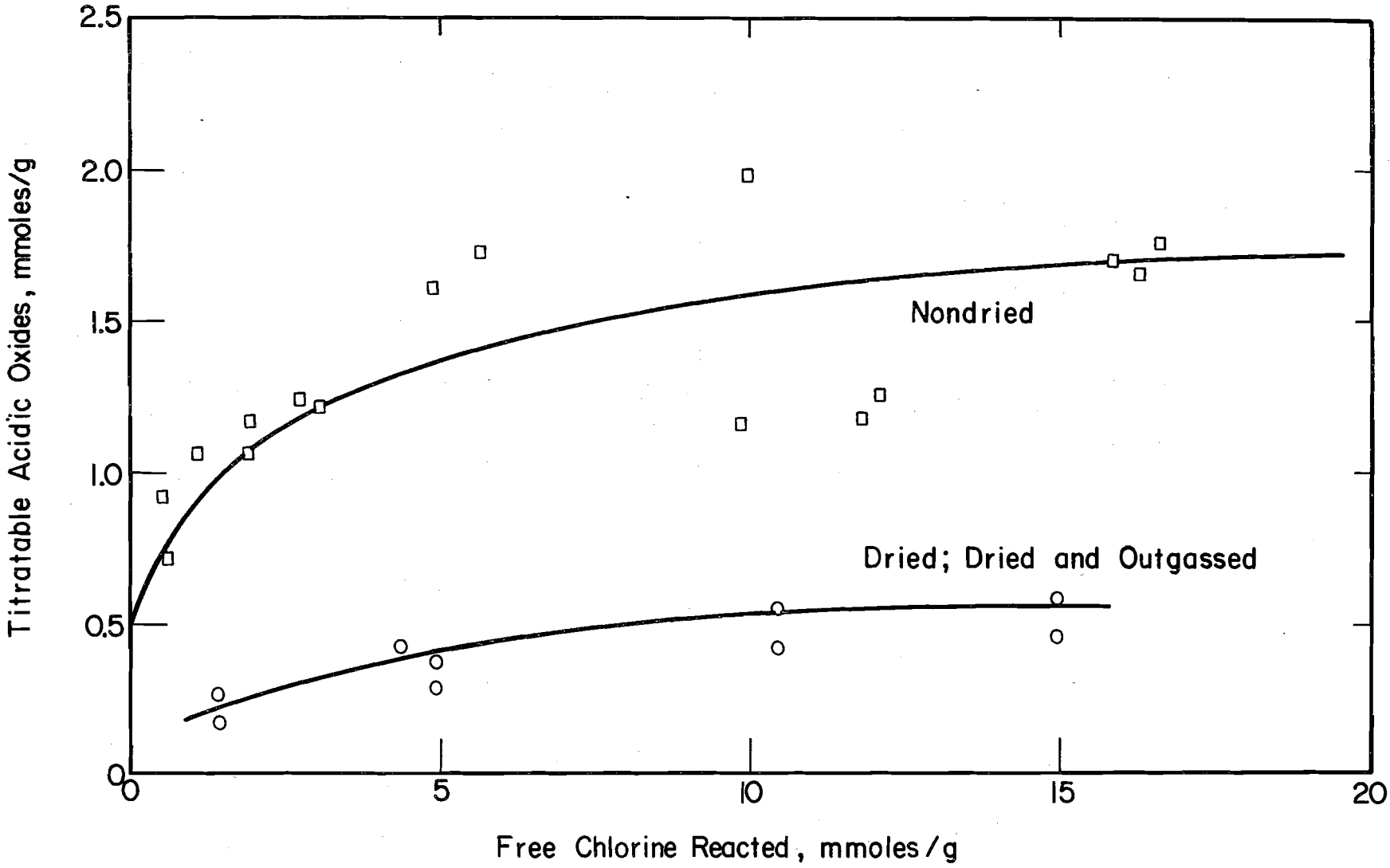

FIG. I.I NaOH TITRATABLE SURFACE OXIDES PRODUCED BY THE REACTION OF FREE CHLORINE WITH ACTIVATED CARBON

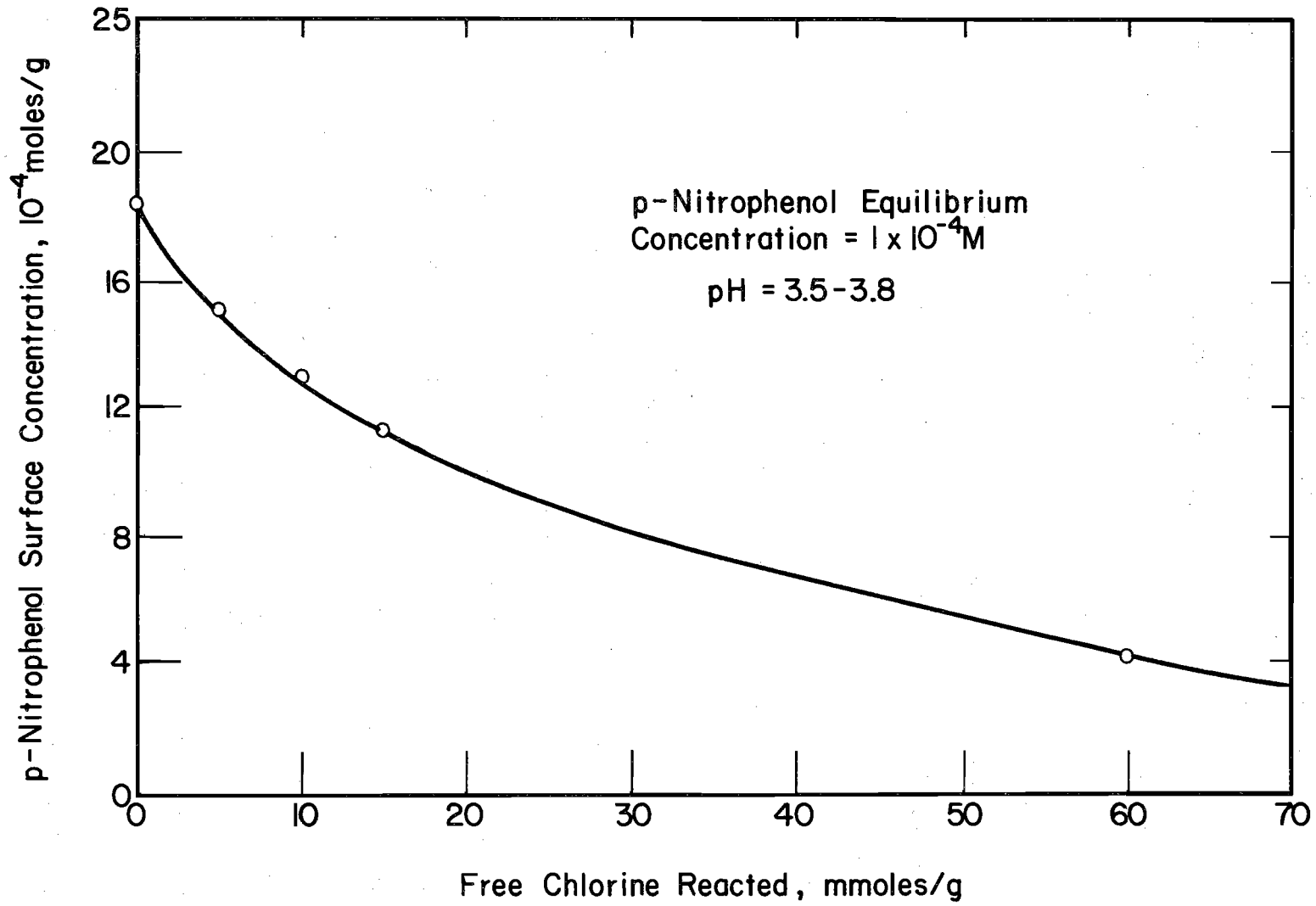

FIG. 1.2 REDUCTION IN p-NITROPHENOL ADSORPTION CAPACITY AS A FUNCTION OF THE AMOUNT OF FREE CHLORINE REACTED

carbonyl functional groups or to pore blockage by the surface oxides. These results are generally consistent with those of Coughlin *et al.* (1968). The effect on adsorption of other types of organic compounds may well be different than was observed for p-nitrophenol, especially if the compound will react specifically with the surface oxides which are formed.

In batch systems, a distinct brown color was found in solution after reaction of approximately 15 mmoles chlorine per gram of carbon (Snoeyink *et al.*, 1974). Boehm (1966) similarly found brown colloidal matter in suspension after extensive oxidation of carbon. Olson and Binning (1974) observed a similar material and noted that a certain portion of it was not adsorbable by carbon. Snoeyink and Suidan (1975) observed that this color appeared in the effluent from a carbon dechlorination bed after about 3 grams free chlorine, as Cl_2, had reacted per gram of carbon in the bed. It should be noted, however, that the amount of chlorine which must react before the color is produced is near the amount that reacts during the life of a typical dechlorination bed (as defined by a preset breakthrough concentration) as given by Hagar and Flentje (1965). If alternative designs of the bed are used, the production of color by the carbon bed, rather than the appearance of chlorine in the effluent of the bed, may signal the need for regeneration or replacement of the carbon.

b. Dechlorination Bed Life and Regeneration

There is little quantitative information available on the life of dechlorination beds or on procedures which will allow the prediction of bed life under different conditions. One exception is the set of curves presented

by Hagar and Flentje (1965) as reproduced in Figure 1.3, although no information is given on the procedures which were used to develop these curves. Using a concentration of 0.01 mg/ℓ chlorine to define breakthrough, Hagar and Flentje found bed life to be a significant function of influent chlorine concentration, hydraulic loading rate, temperature, pH, and particle size of the activated carbon. Calculations made from these curves show that at an influent concentration of 1 mg/ℓ of free chlorine, 1 g of 8 x 30 U.S. standard mesh carbon will react with 0.28 and 2.1 g chlorine when loaded at rates of 2 and 1 gpm/ft^3, respectively, while 1 g of 12 x 40 mesh carbon will react with 2.1 and 12.5 g chlorine when hydraulic loading rates of 2 and 1 gpm/ft^3 are used, respectively. If 2.1 g chlorine react per g of carbon at the 1 gpm/ft^3 loading rate, a bed life of 12.5 years is predicted for a 2.5 foot bed depth. This period of time is very long, however, and it is expected that adsorption of organics which would cause a decrease in dechlorination efficiency would necessitate regeneration much before the 12.5 years.

Care must be exercised in using Figure 1.3. If Equation 1.6 correctly represents the reaction, only 5.9 g free chlorine can react per g carbon before each carbon atom has combined with an oxygen atom if activated carbon is assumed to be 100 percent carbon. But if each carbon atom can accept 2 oxygen atoms, then 17.7 g chlorine/g carbon represents the maximum. The type of oxide formed is important in this respect. If the reaction were to proceed to these limits, all the carbon would have been converted to CO or CO_2. Prior to complete conversion, however, the carbon particles would fragment with the smaller particles escaping from the bed

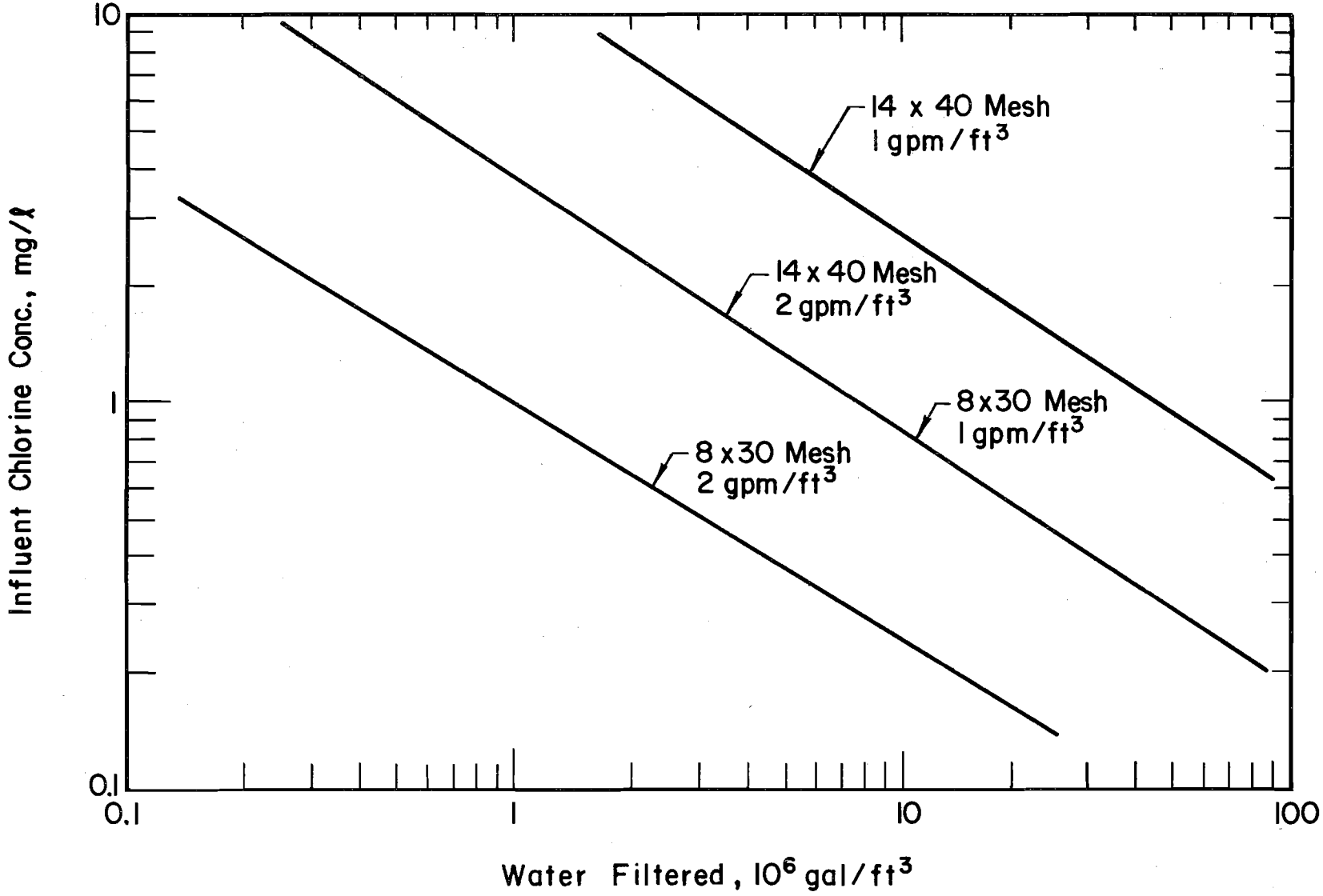

FIG. 1.3 DECHLORINATION BED LIFE

and the dark color, as noted above, would also be produced. It is not apparent that Figure 1.3 takes these latter phenomena into account.

One possible mechanism of reaction which could significantly affect bed life and which merits discussion concerns the catalytic destruction of HOCl by carbon as follows:

$$2\ HOCl \rightarrow 2\ H^{+} + 2\ Cl^{-} + O_2 \qquad 1.7$$

This reaction is thermodynamically favored as can be shown by free energy calculations. Preliminary monitoring of dissolved oxygen during dechlorination has shown no significant change in concentration, however, thus reducing the probability that this reaction is important (Snoeyink and Suidan, 1975). Magee (1956) similarly found no increase in dissolved oxygen concentration during dechlorination.

The original activated carbon dechlorination efficiency can be regenerated by heating the carbon to temperatures in excess of 500°-700°C (Magee, 1956). Boehm (1966) and Puri (1970) noted that carbon must be heated in an inert atmosphere to a temperature exceeding 1000°C in order to evolve all oxides, thus indicating that elimination of all oxides is not necessary to reestablish the original dechlorination efficiency.

A large weight loss may be noted during regeneration. The very extensive surface area of carbon can hold a large number of oxides and the carbon evolved with the oxides can be significant. If Equation 1.6 is correct, for example, each part by weight of free chlorine requires 0.17 parts by weight of carbon. Because many of the oxides formed as products are attached to the carbon, a very significant portion of the weight loss will take place during the regeneration step.

Stuchlik (Smisek and Cerny, 1970) reports that carbon in pressure dechlorinators can be regenerated by steam treatment. The exhausted bed is first washed with a basic solution to remove the acid which has formed during the dechlorination reaction. Then 105°-110°C steam, 1 atm gauge pressure, is introduced at the top of the bed. Several hours are required for the steam to heat the bed; steaming is continued for about 1 hr after steam first appears in the effluent of the bed. After steaming, the carbon is rinsed and returned to operation. Stuchlik indicates that regeneration treatments after the first regeneration are necessary after successively shorter time intervals and after a time the carbon will require replacement. He also notes that in gravity fed dechlorinators, some recovery of capacity can be achieved by washing with caustic solution.

c. Rate of Reaction and Modeling of Dechlorination Beds

Magee (1956) studied the rate of reaction of free chlorine with carbon in a column apparatus and claimed that his results generally agree with the surface reaction being the rate limiting step. He observed that an initial stage, which he called a diffusion controlled stage, was in effect prior to initiation of the surface reaction rate controlled step. The initial phase was observed to last for approximately 1000 bed volumes when the inlet concentration of free chlorine was 30 mg/ℓ as Cl_2. Subsequent to this initial period, he found that the removal rate could be described by the first order rate equation,

$$\frac{dC}{dt^*} = - kC \qquad 1.8$$

which, for the initial conditions of concentration $C = C_o$ at time $t^* = 0$ integrates to,

$$C = C_o e^{-kt^*} \qquad 1.9$$

The time parameter, t^*, in this case represents the time of contact of the chlorinated water with carbon.

Although Magee's (1956) model is based upon the surface reaction being the rate limiting step, it is not apparent that the diffusion controlled step can be eliminated from an accurate model which describes the reaction. Magee found that the reaction rate constant was inversely proportional to the particle size of carbon, an observation which is inconsistent with the surface reaction being rate controlling because the total surface area of an adsorbent generally varies very little with particle size. What Magee failed to note was that the inverse proportionality between k and particle diameter indicates a diffusion controlled mechanism in the case of a first order surface reaction (Levenspiel, 1972). Additionally, Magee reported that the reaction rate doubled for a temperature increase of 20°C for the range 0 to 90°C. This temperature effect corresponds to an activation energy of 5.5 to 8.6 kcal/mole, values which correspond to those generally attributed to a diffusion controlled reaction rate (Helfferich, 1962).

Magee (1956) found the rate constant to be an important function of pH, with the value at pH 4-5.5 being four times greater than the value at pH 8.5-10; marked differences in the efficiency of different types of carbon were also observed.

Magee's (1956) model does not take into account the poisoning, or reduction in reaction rate, which occurs as the extent of the reaction increases. The data on which he based his model were taken after a significant amount of chlorine had reacted with the carbon and it was assumed that a further reduction in rate as the reaction proceeded would be negligible. Equation 1.9 thus predicts that a dechlorination bed operating under a given set of conditions will produce a given quality of effluent indefinitely, and this prediction is contrary to observed results.

Kovach (1971) proposed the use of bed half-length (bed length required to reduce the influent concentration by one half) for the design of activated carbon dechlorination beds. No information was provided on how his data were collected. As stated previously, Magee (1956), and Snoeyink and Suidan (1975) observed that dechlorination columns operate at an unsteady state, at least initially. Consequently, it is meaningless to even propose the use of bed half-length for the design of such reactors.

B. Objective of Study

Preliminary investigations indicate that the design of activated carbon dechlorination reactors on a steady state basis is very erroneous and may lead to excessive over-design. The objective of this study was to develop a theoretically sound model for the dechlorination process.

The model utilized a proposed theoretically derived surface reaction rate expression based on Langmuir-Hinshelwood kinetics. This reaction rate expression was incorporated into a pore diffusion model. Closed and constant concentration batch reactor data were then used to evaluate

constants in the proposed model. Once the constants were evaluated, the pore model was incorporated in a packed bed model to predict the time varying effluent quality from an activated carbon dechlorination bed. The predicted breakthrough curves were then tested against experimental data to verify the validity of the proposed approach.

The pore model includes a particle diameter term, and the model was tested for particle diameter effects by comparing experimental data with predicted results.

Hypochlorous acid dissociates in water according to

$$HOCl \rightleftarrows H^+ + Cl^- \qquad 1.10$$

Because of the effect of pH on the composition of free chlorine, model constants were evaluated for different pH values.

Finally, since both the diffusivity and the surface reaction rate are functions of temperature, temperature effects were also evaluated.

II. THEORETICAL ANALYSIS

The reaction between aqueous free chlorine and granular activated carbon is heterogeneous in nature. A free chlorine molecule has first to migrate to an activated carbon site. This transport involves bulk and surface film transport which are functions of the hydrodynamics of the reactor and finally pore diffusion, since activated carbon is highly porous with practically all the reactive surface situated inside the granule. In this study, it was assumed that the major resistance to free chlorine transport occurred in the activated carbon pore. This assumption was verified experimentally by running identical closed batch chlorine-activated carbon experiments under different mixing conditions. For low mixing rates, the rate of free chlorine reduction increased with increasing mixing rates. As the mixing rate was further increased, the concentration vs. time curves coincided indicating that above a minimum mixing intensity, no appreciable bulk or surface film transport resistance was present. In all batch experiments carried out in this study, the mixing intensity was maintained within the range where no external transport resistance was observed. It was further assumed that the outward diffusion of reaction product from the activated carbon pores did not interfere with the forward free chlorine diffusion. This assumption is usually true in dilute systems such as the one studied here.

The assumption that all resistance to transport occurred within the activated carbon pores is very commonly employed in the study of reactor kinetics. Petersen (1965) stated that "concentration differences between the bulk fluid phase and the external surface of a catalytic pellet

owing to external diffusion limitations is never observed in the absence of corresponding larger concentration gradients within the pellet."

A. Surface Reaction Rate Expression

The reaction between free chlorine and activated carbon can be described by (Magee, 1956; Puri, 1970):

$$C^* + HOCl \rightarrow CO^* + H^+ + Cl^- \qquad 1.6$$

where C* represents an activated carbon reaction site and CO* represents a surface oxide on the carbon. The above reaction is heterogeneous and it was assumed that it proceeds by a simple reversible adsorption-desorption step followed by a simple irreversible dissociation step.

$$C^* + HOCl \underset{k_2}{\overset{k_1}{\rightleftarrows}} CHOCl^* \qquad 2.1$$

$$CHOCl^* \xrightarrow{k_3} CO^* + H^+ + Cl^- \qquad 2.2$$

where CHOCl* represents an adsorbed free chlorine molecule and k_1, L^2/SITE•T, K_2, M/SITE•T•L and k_3, M/SITE•T•L are rate constants. Here L, M, T and SITE stand for length, mass, time and surface site, respectively.

Some of the reactive carbon sites are oxidized as the surface reaction proceeds. Magee (1956) observed that some of these oxides were released to the solution as CO_2 and CO. When such a release occurred, it was assumed that the site was regenerated. As a result, the total number of surface sites, C_t^*, remains constant. A material balance on the surface sites yields

$$C_t^* = C^* + CO^* + CHOCl^* \qquad 2.3$$

In the above equation, the symbols refer to the concentrations of the respective species. The units for all four surface species are SITE/L^2.

In this study, the dissociation step of the surface reaction was assumed to be rate limiting, and consequently the adsorption-desorpation step was assumed to be at equilibrium. This is expressed by

$$K_1 C^* C = k_2 CHOCl^* \qquad 2.4$$

where C represents the free chlorine concentration, M/L^3. When the term for C* as expressed in Equation 2.3 is substituted in Equation 2.4, CHOCl* is solved to be

$$CHOCl^* = \frac{k_1 C}{k_1 C + k_2} (C_t^* - CO^*) \qquad 2.5$$

Since the adsorption-desorption step was assumed to be at equilibrium, then the rate of production of chloride ions is equal to the rate of free chlorine removal, $-R_c$. This is expressed by

$$R_c = \frac{-k_3 C}{C + k_4} (C_t^* - CO^*) \qquad 2.6$$

where R_c represents the rate of free chlorine generation, M/L^3·T, and k_4 represent the adsorption-desorption equilibrium constant, M/L^3 given by k_2/k_1.

Activated carbon contains impurities such as oxygen, hydrogen and metals in addition to carbon in the form of graphitic microcrystallites. In addition, the surface structure of the carbon probably varies along the pores

due to strains acquired during manufacture. In this study, however, the carbon surface was assumed to be homogeneous. It was also assumed that chloride and hydrogen ions produced by the surface reaction do not occupy any of the reactive sites. As a result, they were not included in an overall reactive sites material balance.

B. Model for Reaction within Carbon Pores

The pores of an activated carbon granule are a series of tortuous, interconnected paths of varying cross-sectional areas. Consequently, it would not be feasible to describe diffusion within each or any of the pores. In this study, it was assumed that the pore volume of a carbon granule was made up of straight cylindrical open ended pores of length 2 L_p and diameter d_p. The half length, L_p, of each such pore being equal to one-sixth the average diameter of the granule (Levenspiel, 1972). Both open ends of a pore are exposed to the bulk free chlorine concentration. Because of that, symmetry exists in a pore and, consequently, it is sufficient to consider only half of such a pore for the purpose of analysis (Figure 2.1).

Let Y be the position variable as measured from pore mouth, and consider a differential element of width ΔY positioned at a distance Y from the pore mouth. A material balance on C leads to

$$\left\{\begin{matrix}\text{Flux of}\\ \text{C in}\end{matrix}\right\} + \left\{\begin{matrix}\text{Rate of Generation}\\ \text{of C}\end{matrix}\right\} - \left\{\begin{matrix}\text{Flux of}\\ \text{C out}\end{matrix}\right\} = \left\{\begin{matrix}\text{Rate of Accumulation}\\ \text{of C}\end{matrix}\right\} \qquad 2.7$$

which could be rewritten explicitly as

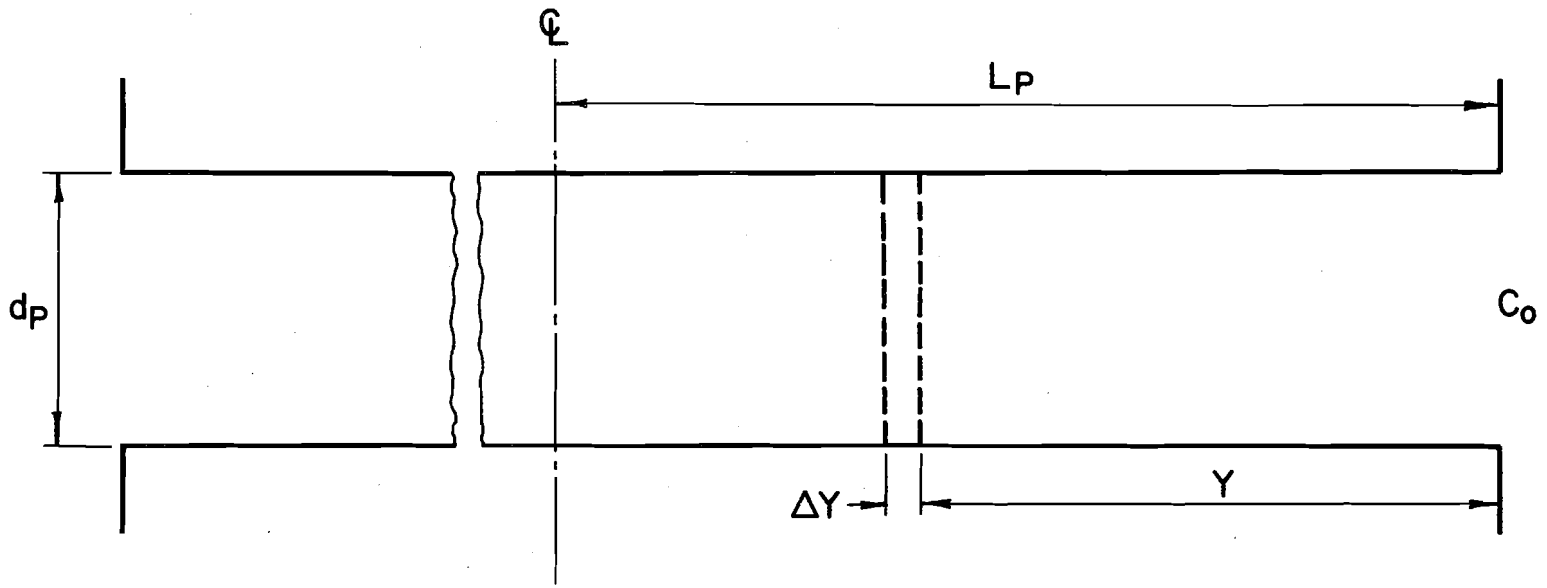

FIG. 2.1 SCHEMATIC DIAGRAM OF CARBON PORE

$$\left(\frac{-\pi d_p^2}{4} \cdot D_c \cdot \frac{\partial C}{\partial Y}\Big|_Y\right) + \left(R_c \cdot \frac{\pi d_p^2}{4} \cdot \Delta Y\right) - \left(\frac{-\pi d_p^2}{4} \cdot D_c \cdot \frac{\partial C}{\partial Y}\Big|_{Y + \Delta Y}\right)$$

$$= \left(\frac{\pi d_p^2}{4} \cdot \Delta Y \cdot \frac{\partial C}{\partial t}\right) \qquad 2.8$$

where D_c represents the diffusivity of free chlorine in the pore, L^2/T, and t represents the time dimension. Dividing by ΔY and letting ΔY tend to zero, Equation 2.8 reduces to

$$\frac{\partial C}{\partial t} = R_c + D_c \frac{\partial^2 C}{\partial Y^2} \qquad 2.9$$

Let W be the mass of free chlorine reacted per unit area of pore surface, M/L^2. Then a differential material balance on C and W yields

$$\frac{\partial W}{\partial t} = - \frac{R_c d_p}{4} \qquad 2.10$$

Let n be the number of half pores per unit weight of activated carbon, V_p be the pore volume per unit weight of carbon, L^3/M, given by $\left(\frac{\pi d_p^2}{4}\right)$ (L_p) (n), and A_p be the pore surface area per unit weight of carbon, L^2/M, given by (πd_p) (L_p) (n). Multiplying Equation 2.9 by V_p, Equation 2.10 by A_p and substituting Equation 2.6 for R_c leads to

$$\frac{\partial P}{\partial t} = - \frac{P}{P + k_8} (SST - SSO) + D_c \frac{\partial^2 P}{\partial Y^2} \qquad 2.11$$

$$\frac{\partial Q}{\partial t} = \frac{P}{P + k_8} (SST - SSO) \qquad 2.12$$

where P and Q represent the mass concentration of free chlorine per unit mass of carbon and the mass of free chlorine reacted per unit mass of carbon, respectively. Similarly SST and SSO represent the number of total and oxidized reactive sites per unit mass of carbon, respectively, each multiplied by the quantity $\frac{k_3 d_p}{4}$. Also, k_8 is equal to k_4 multiplied by V_p.

The surface reaction terms in Equations 2.11 and 2.12 are a function of the oxidized reactive sites, SSO. Snoeyink *et al.* (1974) presented data describing the accumulation of NaOH titratable surface oxides as a function of the amount of chlorine reacted per unit weight of carbon. Their data, as reproduced in Figure 1.1, could not be used to arrive at a theoretical expression for SSO since only some of these oxides were measurable by their technique and because their data represent an average effect over a carbon granule and not a localized effect as SSO represents. As a result, an empirical expression was adopted for SSO which describes the general shape of the data shown in Figure 1.1.

$$SSO = \frac{k_7 Q}{1 + k_{10} Q} \qquad 2.13$$

In addition it allows for more free chlorine to react with the carbon without much increase in the surface oxides once the level of these surface oxides became appreciable. This is in agreement with Magee's (1956) observation that more CO_2 and CO was in the effluent from packed bed activated carbon reactors as the influent free chlorine concentration to these reactors was increased.

Substituting the expression for SSO given by Equation 2.13 into Equations 2.11 and 2.12 leads to the general pore model

$$\frac{\partial P}{\partial t} = - \frac{P}{P + k_8} \left(SST - \frac{k_7 Q}{1 + k_{10} Q}\right) + D_c \frac{\partial^2 P}{\partial Y^2} \qquad 2.14$$

$$\frac{\partial Q}{\partial t} = \frac{P}{P + k_8} \left(SST - \frac{k_7 Q}{1 + k_{10} Q}\right) \qquad 2.15$$

C. Boundary Conditions and Reactor Mathematical Models

The pore mathematical model developed in the previous section describes the reaction and transport mechanisms taking place inside the pores of activated carbon granules. To solve these equations, however, boundary conditions are needed to relate the conditions in the bulk of the solution to those inside a pore. In addition, initial conditions are also required to describe the state of the system just prior to the start of the reaction.

The initial conditions needed to solve Equations 2.14 and 2.15 are independent of the type of reactor under consideration and depend on the state of P and Q at the start of an experiment. Assuming that fresh carbon was used, then the initial condition on Q becomes

$$Q = 0; \quad \text{for } t = 0, \quad 0 \leq Y \leq L_p \qquad 2.16$$

The initial condition on P was obtained from the steady state solution of Equation 2.14 with Q set to zero. The use of such an initial condition assumes that the concentration profile for P inside a pore develops relatively fast compared to the speed of the surface reaction. This initial condition is given by

$$D_c \frac{d^2P}{dY^2} - \frac{P\ SST}{P + k_8} = 0; \quad \text{for } t = 0, \quad 0 \leq Y \leq L_p \qquad 2.17$$

The pore model used in this study assumes a straight cylindrical pore with both open ends exposed to the bulk free chlorine concentration. Because of the symmetry of such a pore, the boundary condition at the half length of a pore is given by

$$\frac{\partial P}{\partial Y} = 0; \quad \text{for } t \geq 0, \quad Y = L_p \qquad 2.18$$

The second boundary condition describes the concentration P at the pore mouth. This boundary condition is a function of the type of reactor for which the pore diffusion model is solved.

1. Batch Reactors

a. Constant Concentration Batch Reactor

The constant concentration batch reactor, CCBR, assumes that the bulk solution is infinite in volume thus resulting in a constant concentration of free chlorine in the bulk solution. Consequently, the boundary condition at pore mouth for a CCBR is given by

$$\left.\begin{array}{l} C = C_o \\ \text{or } P = P_o \end{array}\right\}, \quad \text{for } t \geq 0, \quad Y = 0 \qquad 2.19$$

where C_o is the free chlorine concentration in the bulk, M/L^3 and P_o is given by $V_p \times C_o$.

The mathematical model for a CCBR is therefore given by Equations 2.14, 2.15, 2.16, 2.17, 2.18 and 2.19.

b. Closed Batch Reactor

A closed batch reactor, sometimes known as a simple or finite batch reactor, assumes a finite bulk solution volume in which the activated carbon is well mixed. When the pore diffusion model is solved for such a reactor, the boundary condition at pore mouth requires a free chlorine material balance to supply a link between the carbon pore phase and the bulk solution phase. Because of this, an expression, R_{rc}, for the rate of free chlorine removal from the solution phase is needed. This expression is given by

$$R_{rc} = \frac{m\ V_p\ D_c}{L_p} \left.\frac{\partial C}{\partial Y}\right|_{Y = 0} \qquad 2.20$$

where m represents the concentration of activated carbon per unit reactor volume, M/L^3 and R_{rc} has the units of $M/L^3 \cdot T$. The rate of chlorine removal, R_{rp}, expressed in terms of P is given by

$$R_{rp} = \frac{m\ V_p\ D_c}{L_p} \left.\frac{\partial P}{\partial Y}\right|_{Y = 0} \qquad 2.21$$

where R_{rp} has the units T^{-1} and is equal to $R_{rc} \times V_p$.

The rate of chlorine removal, R_{rc}, due to activated carbon was summed over time in conjunction with the rate of chlorine disappearance, R_d, owing to factors other than activated carbon to provide the pore mouth boundary condition for a closed batch reactor.

$$C = C_o + \int_o^t \left(\frac{m V_p D_c}{L_p} \frac{\partial C}{\partial Y}\Big|_{Y=0} - R_d\right) d_t; \text{ for } t \geq 0, Y = 0 \qquad 2.22$$

R_d has the units of M/L^3 T. Equation 2.22 expressed in terms of P becomes

$$P = P_o + \int_o^t \left(\frac{m V_p D_c}{L_p} \frac{\partial P}{\partial Y}\Big|_{Y=0} - V_p R_d\right) d_t; \text{ for } t \geq 0, Y = 0 \qquad 2.23$$

where C_o represents the initial bulk concentration of free chlorine and P_o is given by $V_p \times C_o$.

The mathematical model for a closed batch reactor is therefore given by Equations 2.14, 2.15, 2.16, 2.17, 2.18 and 2.23.

c. Nondimensionalized Batch Models

The two batch reactor models developed above were nondimensionalized using the dimensionless time, θ; distance, ξ; and concentration, G, variables. These dimensionless variables were defined as

$$\theta = \frac{t D_c}{L_p^2} \qquad 2.24$$

$$\xi = \frac{Y}{L_p} \qquad 2.25$$

and

$$G = \frac{P}{P_o} \qquad 2.26$$

Substituting the above dimensionless variables in the CCBR model leads to

$$\frac{\partial G}{\partial \theta} = -\frac{G}{GP_o + k_8}\left(SIT - \frac{k_9 Q}{1 + k_{10} Q}\right) + \frac{\partial^2 G}{\partial \xi^2} \qquad 2.27$$

$$\frac{\partial Q}{\partial \theta} = \frac{GP_o}{GP_o + k_8}\left(SIT - \frac{k_9 Q}{1 + k_{10} Q}\right) \qquad 2.28$$

$$Q = 0; \text{ for } \theta = 0,\ 0 \leq \xi \leq 1 \qquad 2.29$$

$$\frac{\partial^2 G}{\partial \xi^2} - \frac{G\ SIT}{GP_o + k_8} = 0; \quad \text{for } \theta = 0,\ 0 \leq \xi \leq 1 \qquad 2.30$$

$$\frac{\partial G}{\partial \xi} = 0; \text{ for } \theta \geq 0, \quad \xi = 1 \qquad 2.31$$

and

$$G = 1; \quad \text{for } \theta \geq 0, \quad \xi = 0 \qquad 2.32$$

where SIT and k_9 are two dimensionless variables obtained from SST and k_7, respectively, through multiplication of each by the quantity $\frac{L_p^2}{D_c}$.

The nondimensionalized mathematical model for a closed batch reactor is identical to the CCBR model except for the boundary condition given by Equation 2.32 which is replaced by

$$G = 1 + \int_0^{\theta} \left(m V_p \left.\frac{\partial G}{\partial \xi}\right|_{\xi = 0} - \frac{V_p L_p^2}{P_o D_c} R_d\right) d\theta; \text{ for } \theta \geq 0,\ \xi = 0 \qquad 2.33$$

2. Packed Bed Column Reactor

When the pore diffusion model is solved in conjunction with a packed bed reactor model, then the pore mouth free chlorine concentration

is obtained through a material balance on free chlorine in the liquid phase of the reactor. The rate of chlorine reduction, in this case, is still expressed by Equation 2.20.

The column reactor considered in this study is a packed bed reactor with axial dispersion. It consists of a cylindrical tube, tightly packed with activated carbon. Aqueous chlorine was pumped at a steady rate into one end of the column and out the other.

In most dechlorination applications, a very low effluent chlorine concentration is desirable. Consequently, an axial dispersion term is needed in the mathematical model of such a bed to better predict the lower effluent concentrations from such a reactor (Levenspiel, 1972). The importance of axial dispersion is discussed in more detail in the section on Results and Discussion.

To develop the governing equation describing the free chlorine concentration levels along a packed bed reactor, consider the schematic diagram for such a reactor as given in Figure 2.2. Let A represent the cross sectional area of the bed, L^2, L_b represent the depth of the bed, L, and z be the position variable as measured from the entrance end of the bed. A differential material balance on free chlorine leads to

$$\{\text{C in by Bulk Transport}\} + \{\text{C in by Axial Dispersion}\} - \{\text{C out by Bulk Transport}\} - \{\text{C out by Axial Dispersion}\}$$

$$+ \{\text{C Generated by Carbon}\} = \{\text{Rate of Accumulation of C}\} \qquad 2.34$$

which could be rewritten explicitly as

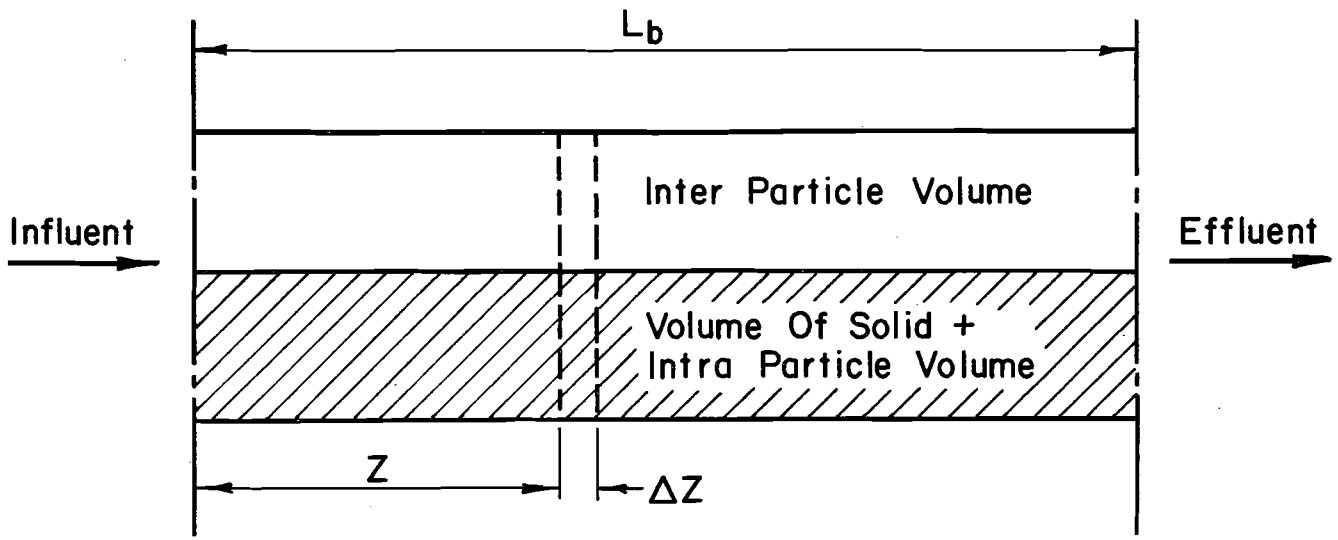

FIG. 2.2 SCHEMATIC DIAGRAM OF PACKED BED COLUMN REACTOR

$$(v \cdot A \cdot \varepsilon \cdot C)_z + (A \cdot \varepsilon \cdot D_A \cdot [-\frac{\partial C}{\partial z}])_z - (v \cdot A \cdot \varepsilon \cdot C)_{z+\Delta z} - (A \cdot \varepsilon \cdot D_A \cdot [-\frac{\partial C}{\partial z}])_{z+\Delta z}$$

$$+ (\frac{m\ V_p\ D_c}{L_p} \frac{\partial C}{\partial Y}\Big|_{Y=0} \cdot A \cdot \Delta z) = (A \cdot \varepsilon \cdot \Delta z \frac{\partial C}{\partial t}) \qquad 2.35$$

where C represents the free chlorine concentration, M/L^3, v represents the actual liquid velocity through the packed bed, L/T, ε represents the interparticle porosity of the packed carbon and D_A represents the axial dispersion coefficient, L^2/T. It is important to note that C and P are related by $P = C\ V_p$ and that Equation 2.35 is valid only at $Y = 0$. Dividing Equation 2.35 by Δz and letting Δz tend to zero leads to

$$\frac{\partial C}{\partial t} = \frac{m\ V_p\ D_c}{\varepsilon\ L_p} \frac{\partial C}{\partial Y}\Big|_{Y=0} + D_A \frac{\partial^2 C}{\partial z^2} - v \frac{\partial C}{\partial z} \qquad 2.36$$

The boundary conditions for a packed bed reactor with axial dispersion have been the subject of controversy for some time. The boundary conditions adopted in this study assume that the packed bed extends from $z = -\infty$ to $z = +\infty$ with the reactive activated carbon situated between $z = 0$ and $z = L_b$. It was also assumed that the bed was packed with an inert or nonreactive material in the regions $-\infty < z \leq 0$ and $L_b \leq z < \infty$. The inert packing was of the same particle size as the activated carbon and, consequently, no sudden changes in the flow regime are encountered at $z = 0$ and $z = L_b$. These boundary conditions as developed by Bischoff (1961) are

$$v\ C_o = v\ C - D_A \frac{\partial C}{\partial z}; \quad \text{for } t \geq 0,\ z = 0 \qquad 2.37$$

and $$\frac{\partial C}{\partial z} = 0; \quad \text{for } t \geq 0,\ z = L_b \qquad 2.38$$

where C_o represents the influent free chlorine concentration. The initial condition on C is obtained from the steady state solution of Equations 2.17, 2.18, 2.36, 2.37 and 2.38 and is represented by

$$D_A \frac{\partial^2 C}{\partial z^2} - v \frac{\partial C}{\partial z} + \frac{m V_p D_c}{\varepsilon L_p} \frac{\partial C}{\partial Y}\Big|_{Y=0} = 0; \text{ for } t = 0,\ 0 \leq z \leq L_b \qquad 2.39$$

In conclusion the mathematical model for the packed bed reactor is given by Equations 2.14, 2.15, 2.16, 2.17, 2.18, 2.36, 2.37, 2.38 and 2.39.

a. Approximate Rate Expression

The packed bed reactor mathematical model consists of a system of three nonlinear partial differential equations. The numerical solution of such a system of equations is rather complicated and costly in computer time. In an attempt to simplify this model, it was observed that after verifying the applicability of the two batch mathematical models to both closed and constant concentration batch data, calculations based on the models showed that for the same total mass of chlorine reacted per unit weight of carbon, X, the rates of chlorine removal were nearly identical when the bulk concentrations were the same. To illustrate this fact, the two models were solved for values of m, L_p, D_c, SIT, k_8, k_9 and k_{10} equal to 10 mg/ℓ, 0.0035 cm, 6×10^{-4} cm^2/min, 0.007, 0.000017, 2.66 and 380, respectively. The initial concentration used in the closed batch model was 30 mg/ℓ and the CCBR model was solved for bulk concentrations of 20 and 10 mg/ℓ. For a bulk

concentration of 20 mg/ℓ and a value of X equal to 0.966 g/g, the two predicted rates were 0.004475 and 0.004472 mg/ℓ-min for the closed and constant concentration batch models, respectively. When X was 1.896 g/g and for a bulk concentration of 10 mg/ℓ, the two rates predicted by the two models were identical at 0.001563 mg/ℓ-min.

Based on this observation an expression, R(X,C), was developed to express the rate of reduction of chlorine mass per unit mass of carbon, T^{-1}. This expression is a function of the bulk chlorine concentration, C, and the mass of chlorine reacted per unit mass of carbon, X. This expression was developed according to the following procedure:

(i) The solutions of the batch models were used in conjunction with similar batch experimental data in order to determine values for the constants SIT, k_8, k_9 and k_{10}.

(ii) The constants thus determined were then used in the CCBR mathematical model to determine the rate of chlorine removal as a function of X for four different bulk concentrations 5, 10, 20 and 30 mg/ℓ.

(iii) The information from step (ii) was then plotted on a log-log scale and fitted to the empirical expression

$$R(X,C) = \frac{J_1 \cdot C}{(J_2 + C)[1 + J_3 \cdot EXP(-J_4 \cdot C) \cdot X]^{J_5} [1 + (J_6 \cdot EXP(J_7 \cdot C) \cdot X)^{J_8}]^{J_9}} \qquad 2.40$$

In the above expression, the $J_{i's}$, i = 1,9 are positive constants and J_5, J_8 and J_9 are related by

$$J_5 + J_8 \cdot J_9 = 1 \qquad 2.41$$

The terms $J_3 \cdot EXP(-J_4 \cdot C)$ and $J_6 \cdot EXP(J_7 \cdot C)$ are equivalent to the inverses of the first and second breakpoints as shown in Figure 2.3.

b. Modified Packed Bed Reactor Model

The use of the algebraic rate expression R(X,C), to express the rate of free chlorine removal in a packed bed reactor model makes Equation 2.36 independent of the pore diffusion equations and, accordingly, the packed bed mathematical model reduces to

$$\frac{\partial C}{\partial t} = -\frac{m}{\varepsilon} R(X,C) + D_A \frac{\partial^2 C}{\partial z^2} - v \frac{\partial C}{\partial z} \qquad 2.42$$

$$\frac{\partial X}{\partial t} = R(X,C) \qquad 2.43$$

$$X = 0; \text{ for } t = 0, \quad 0 \leq z \leq L_b \qquad 2.44$$

$$D_A \frac{\partial^2 C}{\partial z^2} - v \frac{\partial C}{\partial z} - \frac{m}{\varepsilon} R(0,C) = 0; \text{ for } t = 0, \; 0 \leq z \leq L_b \qquad 2.45$$

$$v C_o = v C - D_A \frac{\partial C}{\partial z}; \quad \text{for } z = 0, \; t \geq 0 \qquad 2.37$$

and

$$\frac{\partial C}{\partial z} = 0; \quad \text{for } z = L_b, \; t \geq 0 \qquad 2.38$$

c. Nondimensionalized Packed Bed Reactor Model

The packed bed mathematical model was nondimensionalized using

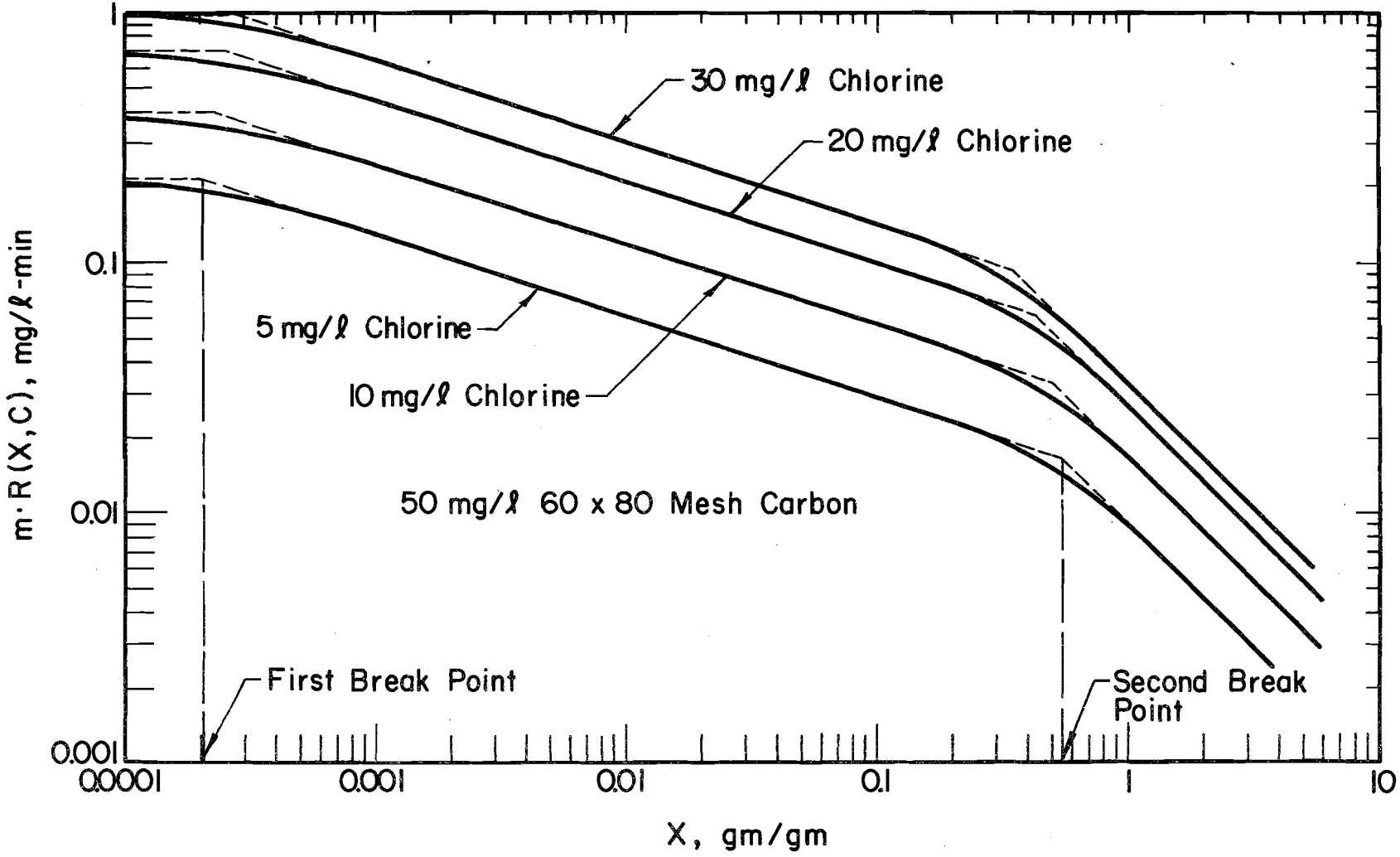

FIG. 2.3 CHLORINE REDUCTION RATE vs X IN A CCBR, pH 4, 23°C

the dimensionless time, τ; distance, α; and concentration, F, variables. These dimensionless variables were defined as

$$\tau = \frac{t\ v}{L_b} \qquad 2.46$$

$$\alpha = \frac{z}{L_b} \qquad 2.47$$

$$F = \frac{C}{C_o} \qquad 2.48$$

Substituting the above dimensionless variables in the packed bed reactor mathematical model leads to

$$\frac{\partial F}{\partial \tau} = -\frac{1}{S} R(X,F) + \frac{1}{P_e} \frac{\partial^2 F}{\partial \alpha^2} - \frac{\partial F}{\partial \alpha} \qquad 2.49$$

$$\frac{\partial X}{\partial \tau} = H\ R(X,F) \qquad 2.50$$

$$X = 0; \text{ for } \tau = 0,\ 0 \leq \alpha \leq 1 \qquad 2.51$$

$$\frac{1}{P_e} \frac{\partial^2 F}{\partial \alpha^2} - \frac{\partial F}{\partial \alpha} - \frac{1}{S} R(0,F) = 0; \text{ for } \tau = 0,\ 0 \leq \alpha \leq 1 \qquad 2.52$$

$$1 = F - \frac{1}{P_e} \frac{\partial F}{\partial \alpha}; \text{ for } \tau \geq 0,\ \alpha = 0 \qquad 2.53$$

and

$$\frac{\partial F}{\partial \alpha} = 0; \quad \text{for } \tau \geq 0, \quad \alpha = 1 \qquad 2.54$$

where S, given by $\frac{v\ C_o\ \varepsilon}{m\ L_b}$, represents the mass of free chlorine applied per unit time per unit mass of carbon; H, given by $\frac{L_b}{v}$, represents the average residence time of the solution in the bed and P_e represents the Peclet number and is given by $\frac{VL_b}{D_A}$. The units for S and H are T^{-1} and T, respectively, and P_e is dimensionless. The Peclet number is a measure of the degree of mixing in the reactor. When P_e is small, the packed bed reactor approaches a completely mixed reactor and when P_e tends to infinity, it approaches a plug flow reactor.

d. Plug Flow Packed Bed Reactor Model

Under certain flow conditions, the axial dispersion coefficient, D_A, and accordingly the mixing term given by the inverse of the Peclet number take small values. In such a case, the contribution of D_A to the solution of the packed bed model becomes negligible and, consequently, it may be more convenient to solve the packed bed model with D_A set to zero, leading to a plug flow reactor. The mathematical model describing such a reactor is obtained from the packed bed with axial dispersion mathematical model by setting D_A equal to zero. Thus the nondimensionalized plug flow mathematical model is given by

$$\frac{\partial F}{\partial \tau} + \frac{\partial F}{\partial \alpha} = -\frac{1}{S} R(X,F) \qquad 2.55$$

$$\frac{\partial X}{\partial \tau} = H\ R(X,F) \qquad 2.56$$

$$X = 0;\ \text{for}\ \tau < \alpha,\ \alpha > 0 \qquad 2.57$$

$$F = 0; \quad \text{for } \tau < \alpha, \ \alpha > 0 \qquad 2.58$$

$$F = 1; \quad \text{for } \alpha = 0, \ \tau > 0 \qquad 2.59$$

where F, X, S, H, τ and α are the same as defined previously.

III. EXPERIMENTAL MATERIALS AND METHODS

A. Activated Carbon

The activated carbon used in this study was bituminous base Filtrasorb 400 (Calgon Corporation, Pittsburgh, PA). The activated carbon was prepared by mechanical grinding followed by sieving into a number of particle size ranges. The carbon was then washed with deionized water, first in a beaker and then in a fluidized bed, to eliminate fines. It was subsequently dried at 105°-110°C. The specific characteristics of the carbon are given in the manufacturer's bulletin (Calgon Corporation, 1969).

B. Free Chlorine Measurement

The DPD Ferrous Titrimetric Procedure (*Standard Methods*, 1970) was used to determine the concentration of aqueous chlorine. For experiments run at pH 10.0, samples were acidified prior to free chlorine measurements. A 5 ml buret was used for the titration.

This analytical technique was found to be accurate and reproducible down to a free chlorine concentration of 0.1 mg/ℓ, as Cl_2. For chlorine concentrations higher than 3 mg/ℓ, as Cl_2, the samples were diluted in order to lower the measured concentrations to a range of 1-2 mg/ℓ, as Cl_2, where the end point of the titration was best detected.

C. Color Measurement

A quantitative measure of the brown color of the solution was made for one CCBR and one column experiment. This measurement was made at

270 nm with an ACTA III UV-visible Spectrophotometer using a 10 cm light path (Beckman Instruments, Inc., Fullerton, CA). These measurements were evaluated relative to the blank and influent chlorine solution as was applicable.

The appearance of brown color was also visually detected in some CCBR and packed bed experiments.

D. Free Chlorine Solutions

Stock free chlorine solutions were prepared by making appropriate dilutions of the household bleach, Clorox. Free chlorine solutions were prepared by adding measured volumes of the stock free chlorine solution, and 5 ml of a pH 7.4 phosphate buffer (14.3 g KH_2PO_4 plus 68.8 g K_2HPO_4/ℓ of buffer solution) per liter of deionized water. The carbonate system of the solutions was always set close to equilibrium with the atmosphere at the operating pH of the reactor by the addition of calculated amounts of Na_2CO_3 and $NaHCO_3$. Adjustments of pH were made as necessary using HCl and NaOH solutions. A Beckman Electromate pH Meter (Beckman Instruments, Inc., Fullerton, CA) was used for pH measurement.

E. Experimental

1. Batch Experiments

For the experiments run at room temperature, no temperature control was used and the temperature varied between 22.5°-23.5°C with 23°C as a mean. For experiments run at 35°C a Magni Whirl Constant Temperature Bath (Blue M Electric Co., Blue Island, IL) was used and for experiments at 2°C, a constant temperature cold room was used.

For batch experiments carried out at pH 4.0, where the buffer capacity of the solutions is weak, a Fisher Automatic Titrimeter (Fisher Scientific Co., Pittsburgh, PA) was used to maintain constant pH during the run. A 0.5 M NaOH solution was used to control pH in this case. For other pH values investigated, 7.6 and 10.0, the buffer capacity of the solutions was sufficiently strong to permit manual pH control. All batch reactors were covered with foil to exclude light and to thus prevent photodecomposition of the chlorine.

Two types of batch experiments were carried out in this study, closed and constant concentration.

a. Closed Batch Experiments

Four liters of solution were used; the only substance added to the reactor after starting the test was NaOH for pH control. A blank reactor containing all reagents except activated carbon was run to determine the rate of disappearance of free chlorine owing to factors other than reaction with activated carbon.

The reactors, including the blank, were mixed using T-line Laboratory Stirrers (Talboys Engineering Corp., Emerson, NJ) and a Teflon stirring rod. The speed of mixing was controlled by a variable Autotransformer (STACO, Inc., Dayton, OH). The stirring speed was maintained at 764-917 rpm as measured by a Biddle Indicator (James G. Biddle Co., Plymouth Meeting, PA).

After the solutions were mixed for about 3 hours, activated carbon was added to the reactors; the initial concentration of chlorine was measured just prior to carbon addition.

b. Constant Concentration Batch Experiments

The second type of batch experiment carried out in this study was a constant concentration batch reactor, CCBR. In this type of experiment, only two liters of solution were used and both the reactor and the blank were mixed at 610 rpm using the same equipment described in the previous section.

All the CCBR experiments were conducted at room temperature, 23°C, and at pH 4.0. The pH was maintained at 4.0 using the Fisher Automatic Titrimeter described previously.

Activated carbon was added to the reactors after the solutions were mixed for 3 hours. The initial free chlorine concentration was measured just prior to carbon addition. In this experiment, the free chlorine concentration was maintained constant at C_o, and the rate of reaction was determined as a function of the mass of chlorine reacted per unit weight of carbon, X. This was accomplished by allowing the free chlorine concentration in the bulk to drop from $C_o + \Delta C$ to $C_o - \Delta C$ and then adding more stock chlorine solution to bring the concentration back to $C_o + \Delta C$. The values used for ΔC were about 0.5-1.0 mg/ℓ. The rate of chlorine reduction was estimated from a few measurements of chlorine concentration as this concentration dropped from $C_o + \Delta C$ to $C_o - \Delta C$. A stock chlorine solution, buffered and maintained at pH 4.0, and another pH 4.0 solution which was buffered but void of any chlorine, were used to bring the chlorine concentration in the reactor back to $C_o + \Delta C$, and to maintain the volume of the solution in the reactor constant. Both the estimated rate and the value of X were

adjusted by subtracting the effect of chlorine decay as observed in the blank reactor.

2. Packed Bed Column Experiments

The other type of experiment was the upflow packed bed reactor. The influent solution was prepared in 60 liter batches and it was stabilized by mixing for at least 3 hours prior to applying it to the carbon. An FMI positive displacement lab pump (Fluid Metering, Inc., Oyster Bay, NY) was used to provide a steady influent flow rate. Tygon tubing was used for the transmission of the influent and effluent flows. The carbon columns were made from Plexiglass. A sufficiently large ratio of column diameter to particle diameter was used to avoid wall effects. In the case of 18 x 20 U.S. Standard mesh size carbons this ratio was 27.6 while it was 73.8 for the 60 x 80 carbon. A minimum depth of 10 column diameters of Ottawa sand was packed ahead of and after the carbon in the column. This sand had the same particle size as the activated carbon and was inert to chlorine. Its purpose was to control the flow regime through the carbon section of the reactor and as such justify the boundary conditions used in the packed bed with axial dispersion mathematical model.

IV. RESULTS AND DISCUSSION

The procedure followed in this study was to fit the numerical solution of the batch mathematical models to corresponding experimental batch data. The constants SIT, k_8, k_9 and k_{10} were evaluated through a trial and error fit of the data. The diffusivity coefficient, D_c, was assigned the value 6×10^{-4} cm^2/min at 23°C. This value is an order-of-magnitude estimate for similar molecules in liquids (Fogler, 1974) and was used for both HOCl and OCl^-. (Calculation of D_c for HOCl by the Wilke-Chang model, which also gives an order-of-magnitude estimate [Bird *et al.*, 1960] gave a value of 1.12×10^{-3} cm^2/min). The value used for V_p was 0.94 cc/g as obtained from the manufacturer's bulletin (Calgon Corp., 1969). The value of L_p was always taken as one-sixth of the arithmetic mean of the particle size range.

A. Rate of Chlorine Disappearance from Blank Reactor

The rate of disappearance of free chlorine from the blank reactors was observed to follow first order kinetics rather closely. The results from two blank experiments are shown in Figure 4.1. The data exhibiting the higher slope represent a 4 liter, pH 4.0 and 35°C blank experiment, while the data from the second experiment were obtained at pH 4.0 and 23°C. As a result of the linearity shown by the data on a semi-log plot, the term R_d for the decay rate in the boundary condition appearing in Equations 2.22, 2.23 and 2.33 was replaced by

$$R_d = - k_d C \qquad 4.1$$

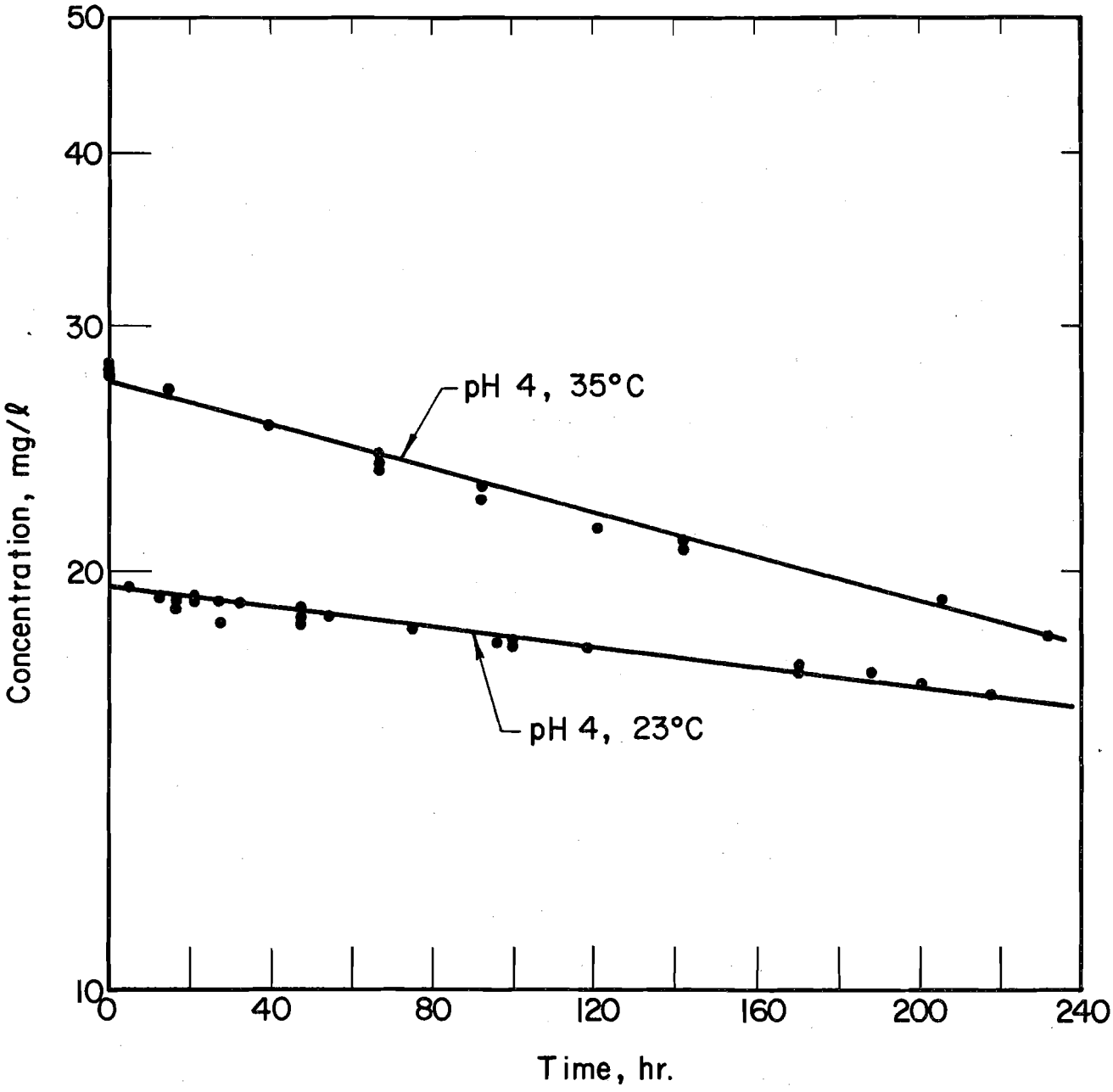

FIG. 4.1 RATE OF CHLORINE DISAPPEARANCE IN BLANK REACTOR

where k_d is the first order rate constant, T^{-1}, and C is the free chlorine concentration, M/L^3. The value of k_d for the pH 4.0, 35°C experiment was calculated to be 0.00003 min^{-1}, while it was found to be 0.0000134 min^{-1} for the pH 4.0, 23°C experiment. Similar data were obtained for pH 10.0 blank experiments carried out at 23° and 35°C.

The values of k_d calculated from the two pH 10.0 blank experiments were equal to the value obtained from the 23°C, pH 4.0 data. At pH 4.0, HOCl is the predominant free chlorine species while it is OCl^- at pH 10.0. Since the same value of k_d was obtained at these two pH values at 23°C, it was assumed that this same value holds at intermediate pH values where the chlorine solution is made up of mixtures of the two free chlorine species. Also, since the same value of k_d was obtained for the two pH 10.0 experiments at 23° and 35°C, it was assumed that this same value holds for blank experiments carried out at the same pH but at 2°C.

Blank experiments were also carried out in conjunction with CCBR experiments. In this case, however, the value of R_d at only one concentration, namely C_o, was needed.

B. Experiments at pH 4.0 and 23°C

1. Batch Studies

Four different constant concentration batch reactor, CCBR, experiments were carried out at pH 4.0 and 23°C (Figures 4.2, 4.3, 4.4 and 4.5). In all four experiments, 50 mg/ℓ of 60 x 80 mesh carbon were used. The bulk concentrations, C_o, in these four experiments were maintained at an average concentration of 30, 20, 10 and 5 mg/ℓ. The bulk concentration in

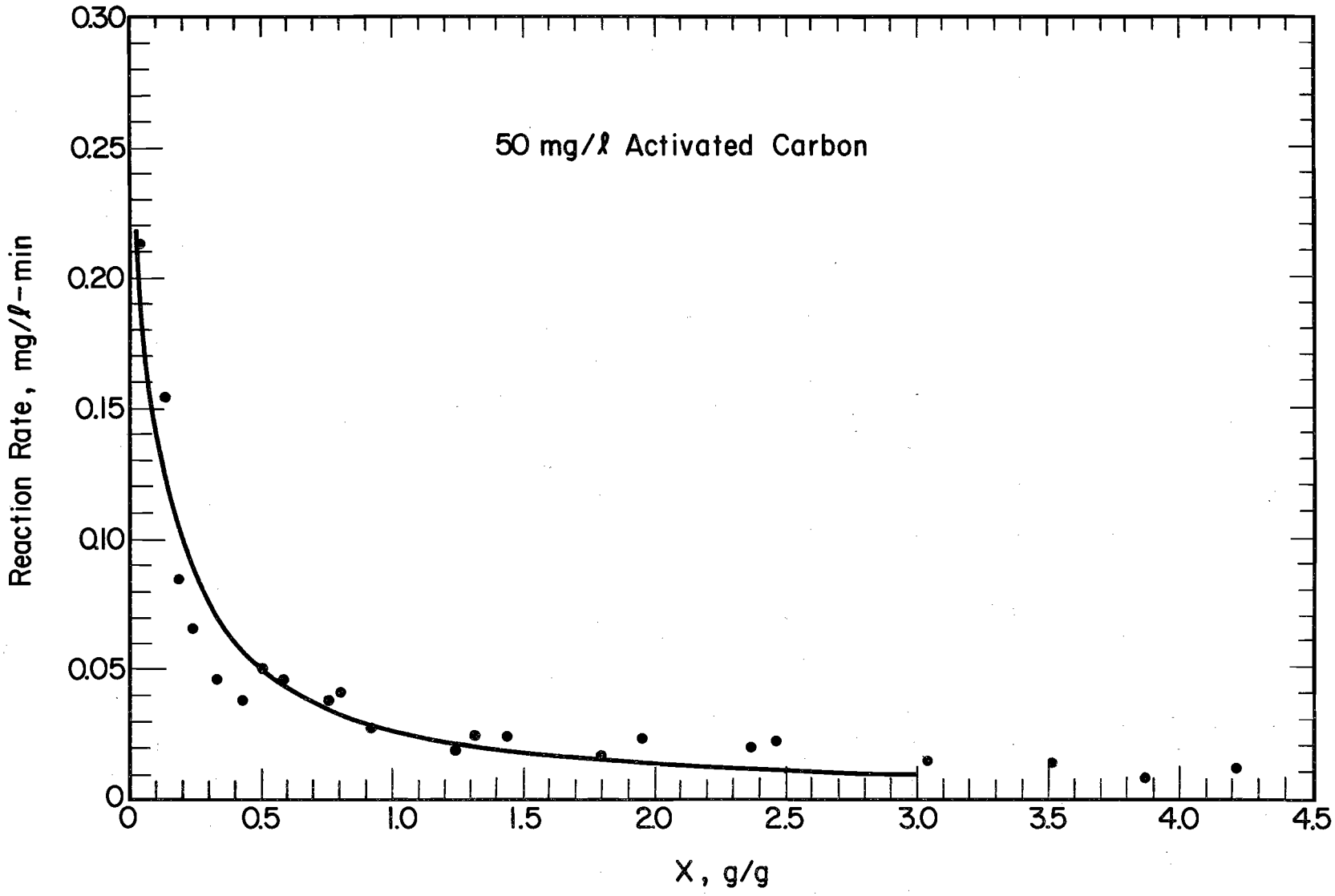

FIG. 4.2 CHLORINE-CARBON (60 x 80 MESH) REACTION IN A 30 MG/L, AS Cl_2, CCBR, pH 4, 23°C

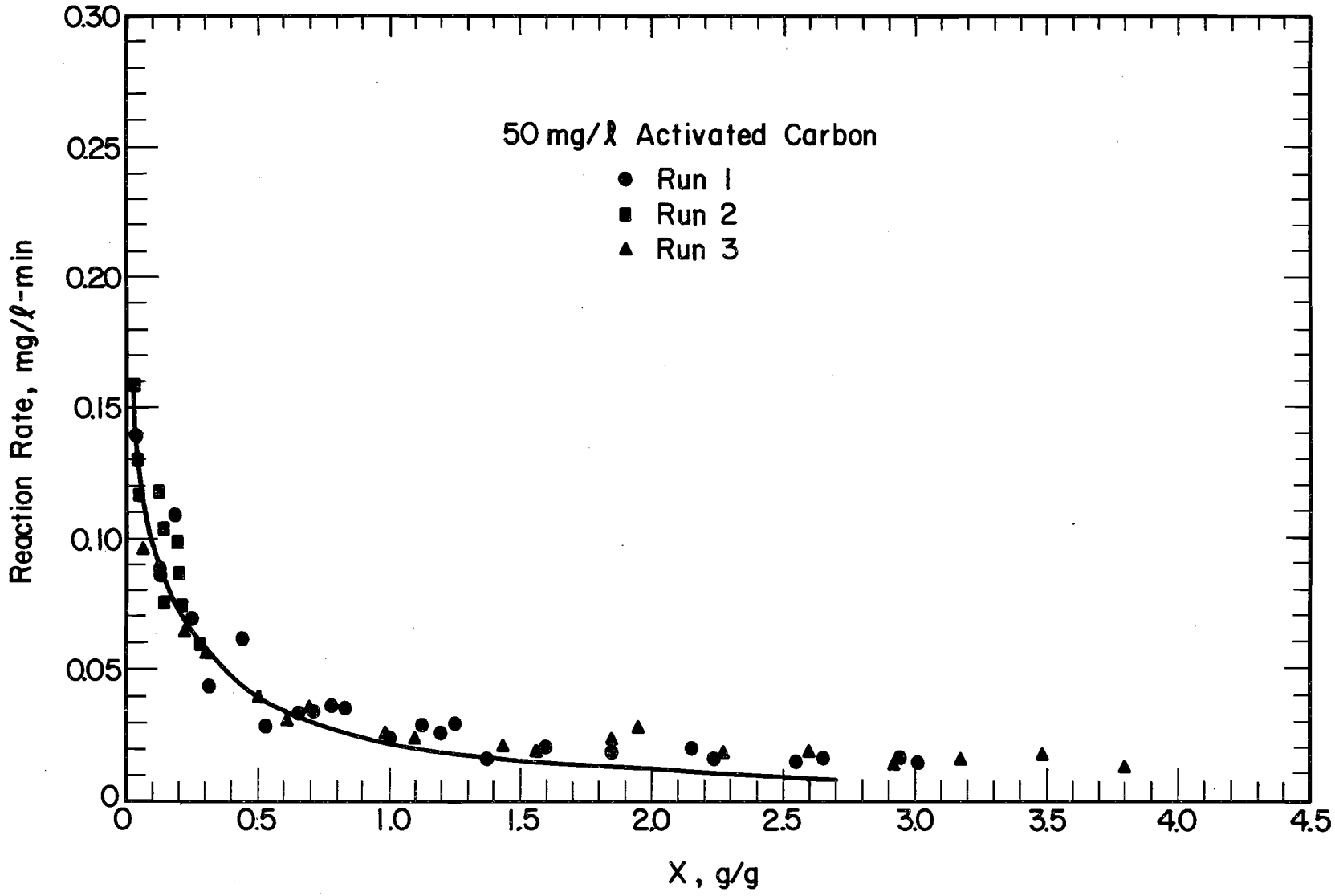

FIG. 4.3 CHLORINE-CARBON (60 x 80 MESH) REACTION IN A 20 MG/L, AS Cl_2, CCBR, pH 4, 23°C

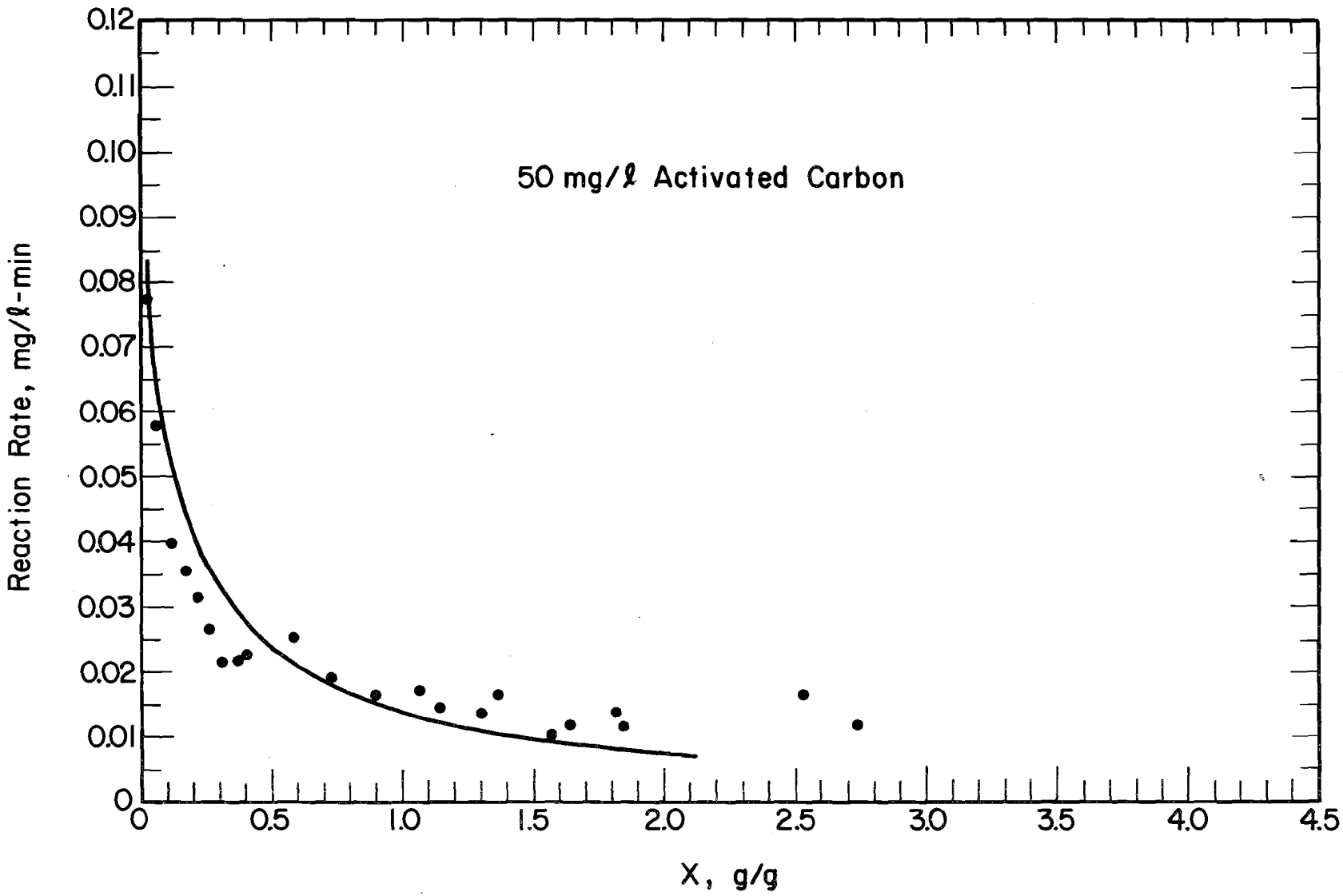

FIG. 4.4 CHLORINE-CARBON (60 x 80 MESH) REACTION IN A 10 MG/L, AS Cl_2, CCBR, pH 4, 23°C

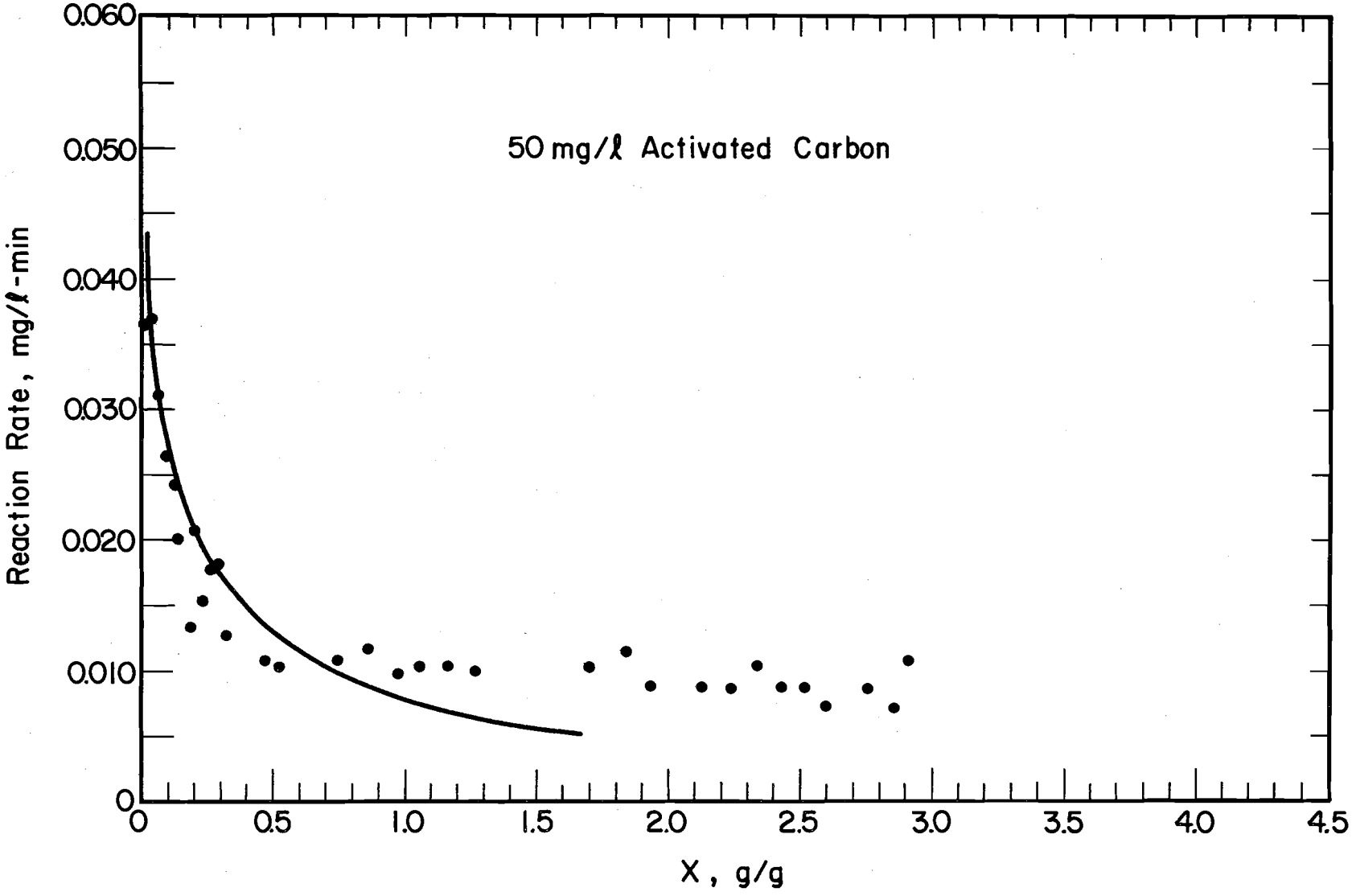

FIG. 4.5 CHLORINE-CARBON (60 x 80 MESH) REACTION IN A 5 MG/L, AS Cl_2, CCBB, pH 4, 23°C

each of these experiments was allowed to vary between $C_o + \Delta C$ and $C_o - \Delta C$ in order to arrive at an estimate of the rate of chlorine removal. The values of ΔC used were 1.0, 0.75, 0.5 and 0.5 mg/ℓ for the 30, 20, 10 and 5 mg/ℓ bulk concentration CCBR experiments, respectively.

The 20 mg/ℓ bulk concentration experiment (Figure 4.3) was repeated three times to test the reproducibility of the data. This reproducibility was considered to be very satisfactory.

Consistent with the surface reaction rate expression given by Equation 2.6, the rate of Chlorine removal for a specific value of X increased with increasing bulk concentration. The ratio of this increase was high when the 10 and 5 mg/ℓ data were compared (Figures 4.4 and 4.5) but tended to decrease as the bulk concentration increased as is evident from the 30 and 20 mg/ℓ data (Figures 4.2 and 4.3).

Brown color appeared in solution after the reaction of 4.2 and 3.8 grams of free chlorine per gram of carbon in the 30 and 20 mg/ℓ bulk concentration CCBR experiments shown in Figures 4.2 and 4.3. The other two CCBR experiments carried out at bulk concentrations of 10 and 5 mg/ℓ (Figures 4.4 and 4.5) were stopped prior to the emergence of any visible brown color.

The continuous curves in Figures 4.2, 4.3, 4.4 and 4.5 represent the rate of chlorine removal for 50 mg/ℓ of 60 x 80 mesh carbon as a function of X, as predicted by the mathematical model for the CCBR. The values of the model constants for these curves were 0.0035 cm, 0.007, 0.000017, 2.66 and 380 for L_p, SIT, k_8, k_9 and k_{10}, respectively.

In the case of the 5 mg/ℓ bulk concentration experiment (Figure 4.5), the model underestimated the rate for values of X greater than 1 g/g.

No attempt was made to correct for this because data from other pH 4.0, 23°C experiments were well predicted using the above model constants.

Two closed batch experiments were carried out at pH 4.0 and a temperature of 23°C. In both experiments, the initial concentration of free chlorine, as Cl_2, and the activated carbon concentration were 30 mg/ℓ and 10 mg/ℓ, respectively. The carbon used in both experiments was 60 x 80 mesh size. Figure 4.6 shows the results of the two experiments and it can be noted that reproducibility is excellent.

The same values of the model constants used in predicting the CCBR data in Figures 4.2, 4.3, 4.4 and 4.5 when used in the closed batch reactor mathematical model resulted in the continuous curve in Figure 4.6. The value used for k_d, in this case, was 0.0000134 min^{-1} as explained earlier.

As can be seen from Figures 4.2, 4.3, 4.4, 4.5 and 4.6, the two batch mathematical models were able to predict rather closely the experimental batch data when both models employed the same values of the model constants.

2. Particle Size Effect Studies

To test the ability of the pore diffusion mathematical model to predict particle size effects, another constant concentration batch experiment was carried out at pH 4.0 and 23°C. The bulk free chlorine concentration in this case was maintained on the average at 30 mg/ℓ; 50 mg/ℓ of 45 x 50 mesh carbon were used. The results of this experiment are shown in Figure 4.7. This experiment was stopped when brown color was observed in solution. This brown color became visible after 3.6 grams of chlorine had reacted per gram of activated carbon. In this experiment a quantitative

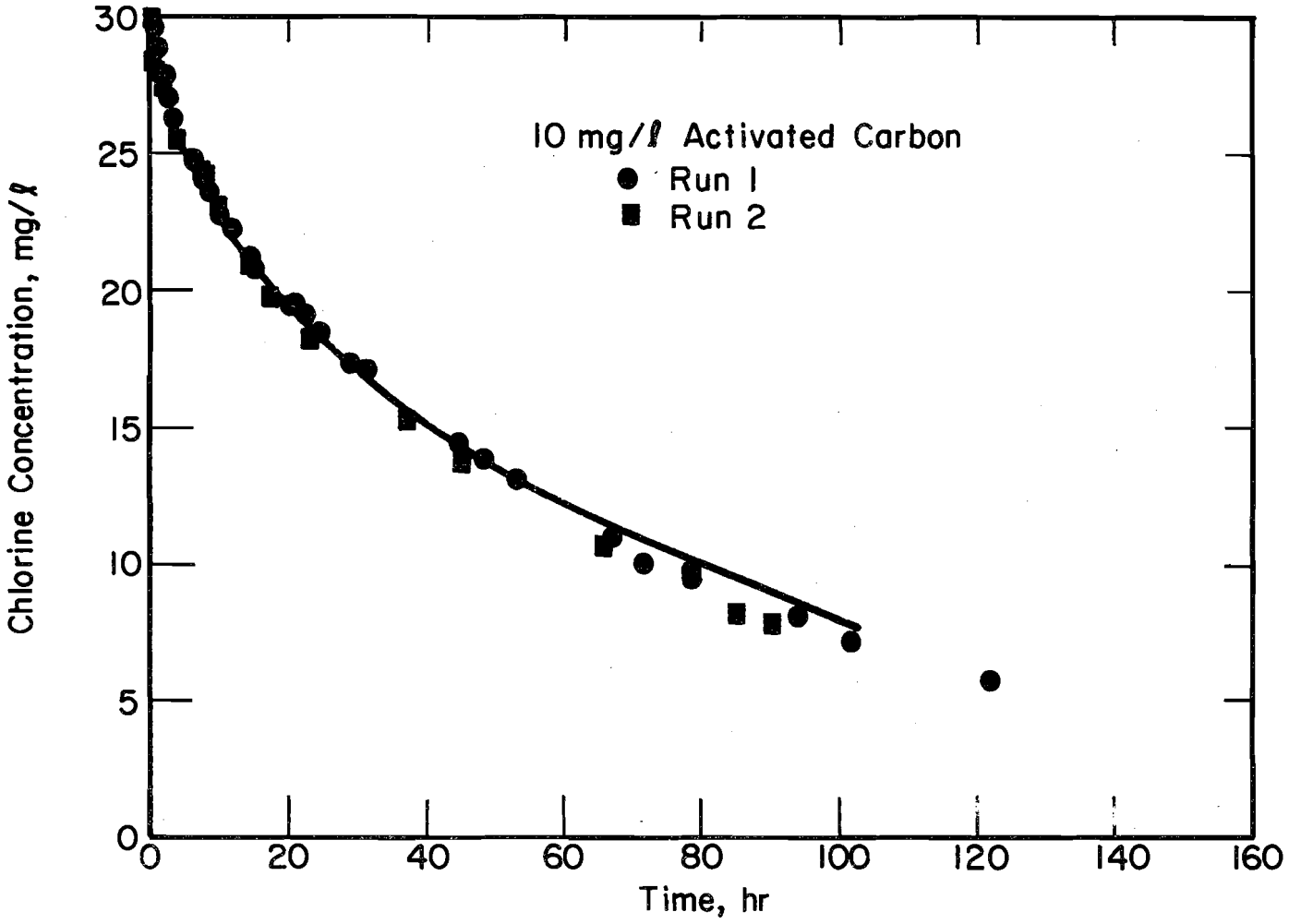

FIG. 4.6 CHLORINE-CARBON (60 x 80 MESH) REACTION IN A CLOSED BATCH REACTOR, pH 4, 23° C

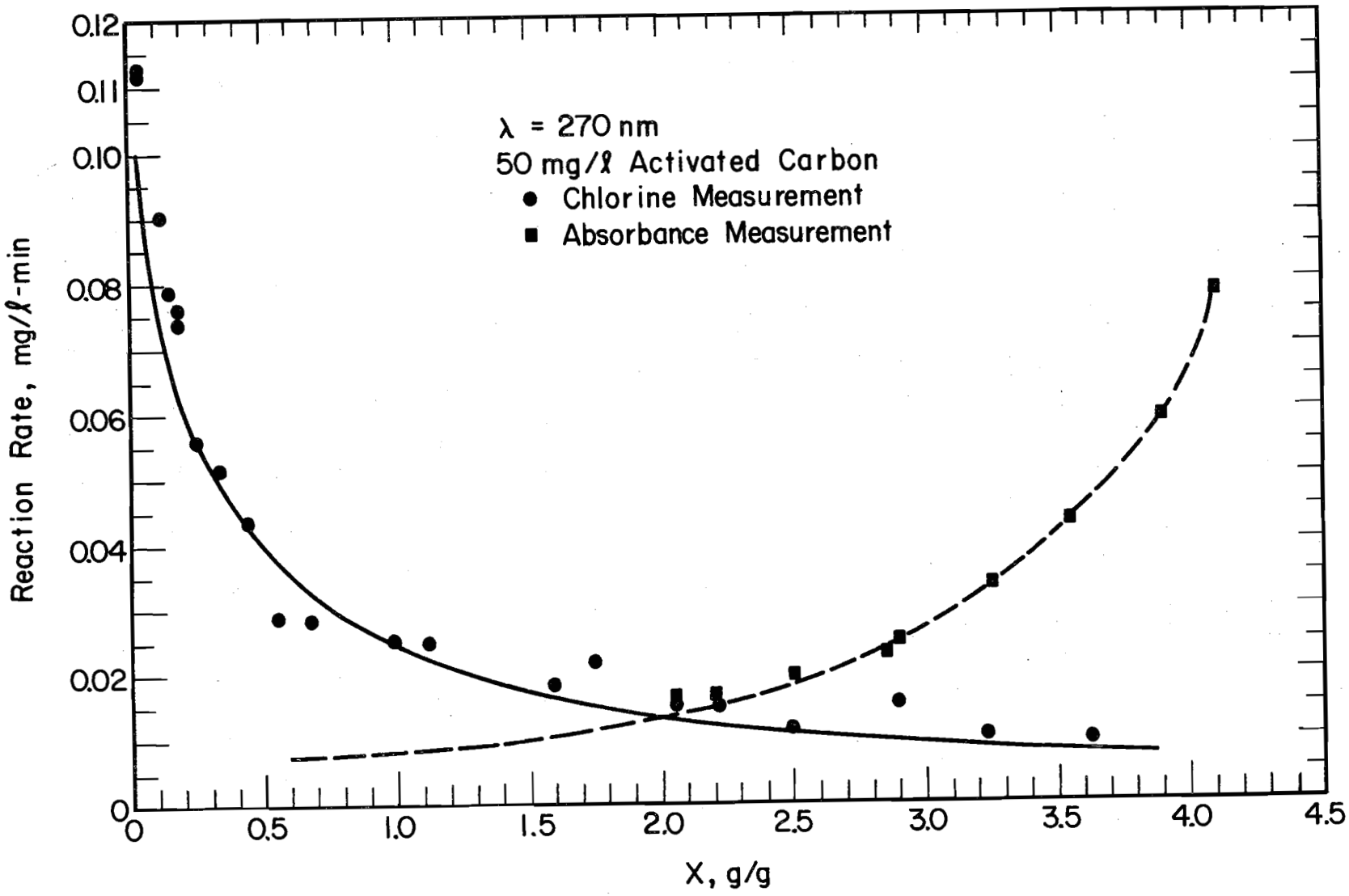

FIG. 4.7 CHLORINE - CARBON (45 x 50 MESH) REACTION IN A 30 MG/L, AS Cl_2, CCBR, pH 4, 23°C

measure of the color of the samples was made at 270 nm using a 10 cm light path (Figure 4.7). The absorbance of the free chlorine solution prior to the addition of carbon was 0.14. At the point when brown color became visible (X = 3.6) the absorbance of the solution was 0.91.

The model constants k_8 and k_{10} are independent of L_p whereas SIT and k_9 are directly proportional to the square of L_p (see section II,C.2.c). Consequently, the values of SIT and k_9 for the 45 x 50 mesh carbon (L_p = 0.0055 cm) were evaluated from the corresponding values of SIT and k_9 for the 60 x 80 mesh carbon to be 0.01728 and 6.568 respectively.

The above values of the model constants were used to predict the rate of free chlorine removal vs. X curve for the 45 x 50 mesh carbon and the results are shown as a continuous curve in Figure 4.7. As is obvious from the figure, a rather good correspondence was obtained between the experimental and predicted data indicating that the model is valid for predicting particle size effects.

It is interesting to note for both the experimental and predicted data in Figures 4.2 and 4.7 that at low values of X, the rate of free chlorine removal for the 60 x 80 mesh carbon is appreciably larger than that for the 45 x 50 mesh carbon. When X is zero, the effectiveness factor (the ratio of the actual rate to that rate obtained if all the carbon surface was exposed to the bulk free chlorine concentration) for the 60 x 80 mesh carbon was computed to be 0.0921 while that for the 45 x 50 mesh carbon was found to be 0.0586. This difference, however, tends to decrease as X increases; the mathematical model predicts that when 3 grams of chlorine have reacted with one gram of carbon, the rate for the 45 x 50 mesh carbon

is 97.3 percent that of the 60 x 80 mesh carbon and the corresponding effectiveness factors were computed to be 0.94 and 0.966, respectively. This observation is consistent with the fact that as the effective reactivity of the surface decreases, the effectiveness factor for both particle sizes tends towards one. Also, since the initial effectiveness factor was found to be much lower than one, a mathematical model that does not include pore diffusion effects would not be in order.

To further check on the ability of the pore model to predict particle size effects, a closed batch experiment was carried out at pH 4.0 and 23°C, with 45 x 50 mesh size carbon. The initial free chlorine concentration and activated carbon concentration were 30 mg/ℓ and 10 mg/ℓ, respectively, and the results are shown in Figure 4.8.

The continuous curve in Figure 4.8 represents the concentration levels as predicted by the closed batch mathematical model for the same values of SIT, k_8, k_9 and k_{10} used in the CCBR mathematical model to predict the 45 x 50 mesh carbon data in Figure 4.7. The value used for k_d was once more 0.0000134 min^{-1}. Examination of Figure 4.8 shows that the model underestimated the effect of particle size but the discrepancies were not drastic.

3. Packed Bed Studies

Activated carbon packed bed experiments were carried out in order to evaluate the accuracy of the packed bed mathematical model for predicting the behavior of such reactors.

The data shown in Figure 4.9 represent the effluent concentration

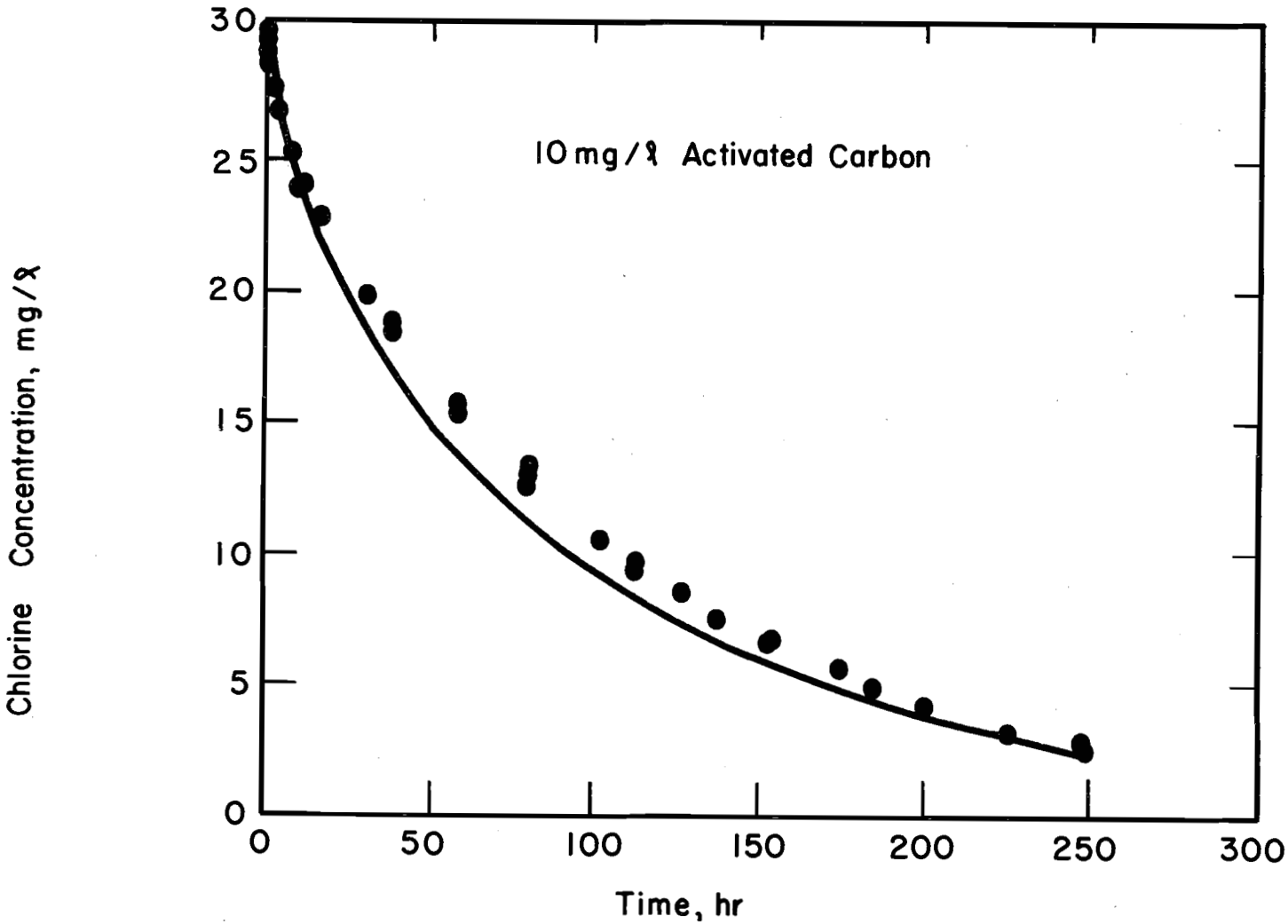

FIG. 4.8 CHLORINE–CARBON (45x50 MESH) REACTION IN A CLOSED BATCH REACTOR, pH 4, 23° C

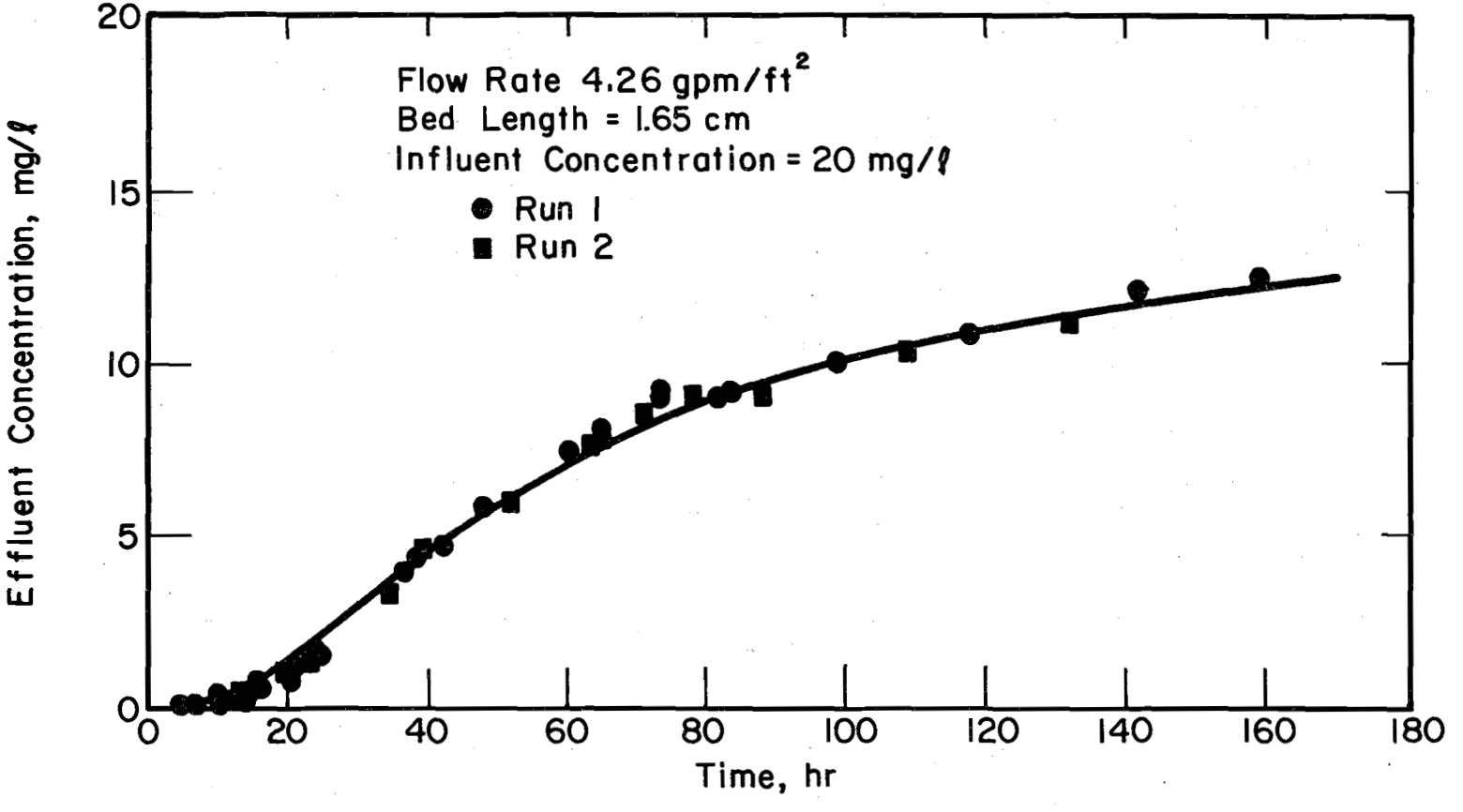

FIG. 4.9 CHLORINE BREAKTHROUGH CURVE, pH 4, 23°C, 60 x 80 MESH CARBON

vs. time for a packed bed experiment wherein the influent concentration, pH, temperature and flow rate were 20 mg/ℓ, 4.0, 23°C and 32.78 cc/min (4.26 gpm/ft^2), respectively. The carbon, 1.49 g of 60 x 80 mesh, was packed in a 1.55 cm internal diameter column. The length of the carbon portion of the bed, L_b was 1.65 cm. The bed porosity was assumed to be 0.43 based on previous determinations made using particles of similar shape (Fair *et al.*, 1968). Initially, the effluent pH rose to 5.2, apparently owing to adsorption of protons by the carbon, and after about one hour it decreased to 3.6. After this initial period, the pH steadily increased towards 4.0. Brown color was observed in the effluent after about 275 hours at which time an average of 3.45 grams of chlorine, as Cl_2, had reacted with each gram of carbon. Using the constant concentration batch reactor model, it was predicted that 3.6 grams of free chlorine, as Cl_2, would have reacted with a gram of carbon exposed to 20 mg/ℓ of free chlorine (column influent concentration).

The four predicted curves for the 60 x 80 mesh carbon shown in Figures 4.2, 4.3, 4.4 and 4.5 were used to obtain the algebraic fit, R(X,C). Using this algebraic fit and an axial dispersion coefficient, D_A, of 1 cm^2/min (Levenspiel, 1972), the packed bed mathematical model was solved to predict the breakthrough curve for the same conditions used in obtaining the data in Figure 4.9. The predicted curve shown as a continuous line in the same figure followed the data rather well indicating the validity of using batch data to predict column performance.

The packed bed mathematical model was also solved for values of the axial dispersion coefficient, D_A, of 2, 3 and 4 cm^2/min. The solutions

were initially different from the solution shown in Figure 4.9 but after about 40 hours, this difference became negligible. The value of D_A of 1 cm^2/min was selected since it gave better fit of the data. All the data presented in this study were correlated using this model.

This model was also solved assuming plug flow (i.e., $D_A = 0$). This solution required the use of a different numerical technique, as outlines in Appendix A, which proved to be more costly than the solution including the axial dispersion term. No appreciable difference was observed between the solutions for D_A equal to zero and D_A equal to 1 cm^2/min.

To further test the ability of the model to predict particle size effects, another packed bed experiment was run, this time using 18 x 20 mesh carbon (see Figure 4.10). The influent concentration, pH and temperature in this experiment were the same as the previous column experiment. The flow rate was 83.9 cc/min (4.06 gpm/ft^2); 8.92 g of carbon were packed in a 2.54 cm internal diameter column yielding a bed length of 4 cm.

Initially, the effluent pH rose to 5.3 and after one hour it dropped to 3.5. Afterwords, the pH rose steadily towards 4.0. Brown color was observed in the effluent after about 395 hours at which time an average of 2.3 grams of chlorine, as Cl_2, had reacted with each gram of carbon. Using the CCBR model, it was predicted that 2.84 grams of chlorine as Cl_2 would have reacted with a gram of carbon located at the entrance of the column under conditions of operation of the bed.

Assuming that the internal particle porosity does not vary with particle size, and using an experimentally determined value for m (weight of activated carbon per unit volume of packed bed), the bed porosity in this

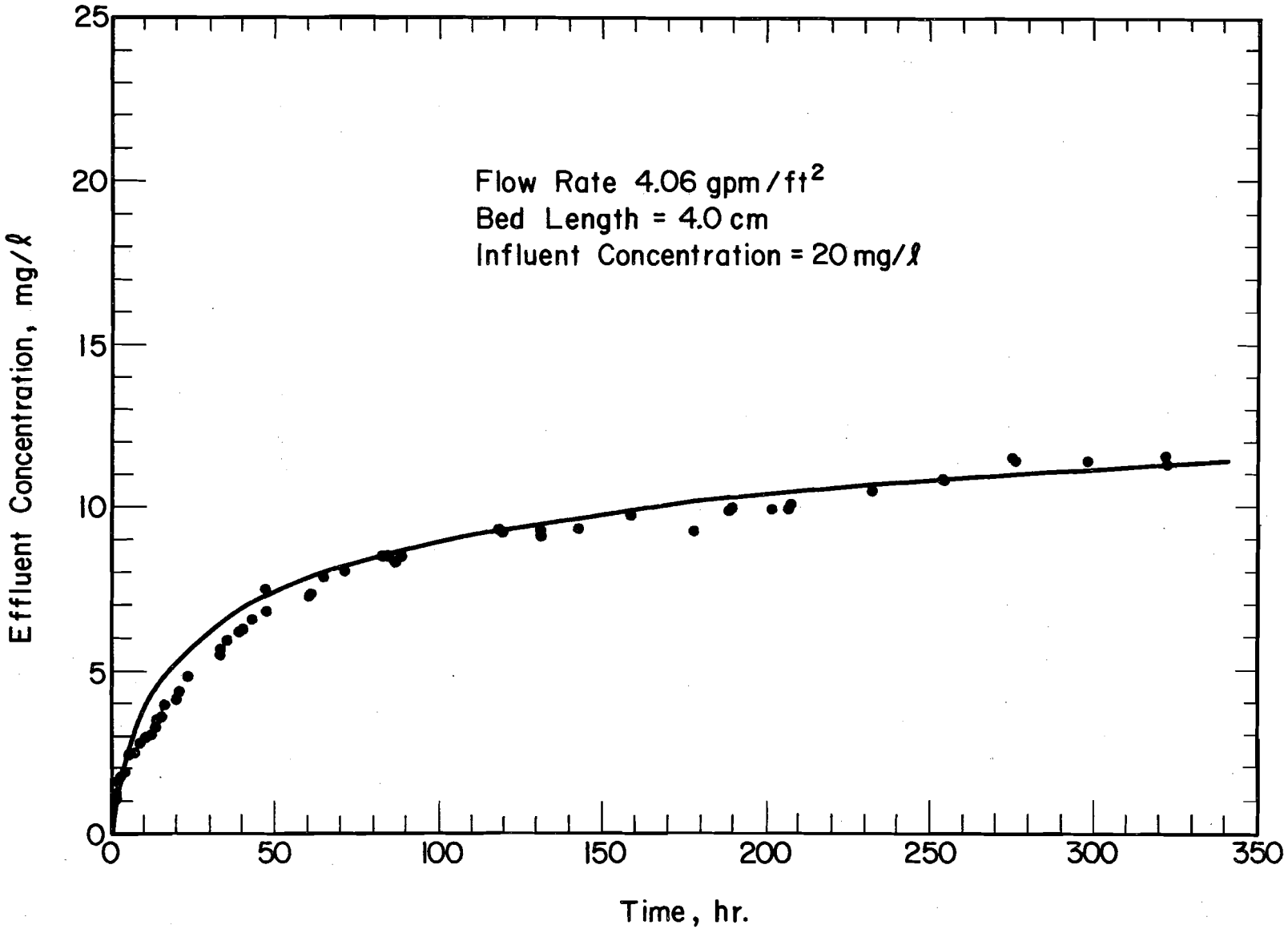

FIG. 4.10 CHLORINE BREAKTHROUGH CURVE, pH 4, 23°C, 18 x 20 MESH CARBON

case was calculated, based on the 60 x 80 mesh carbon bed porosity to be 0.476.

The pore length, L_p, for the 18 x 20 mesh carbon is 0.0153 cm. For this pore length, SIT and k_9 were calculated to be 0.1343 and 51.05, respectively. The constants k_8 and k_9 remain unchanged at 0.000017 and 380 respectively, as they are independent of pore length. Using these values, the algebraic fit, R(X,C), was obtained using four CCBR model runs at bulk concentrations of 5, 10, 20 and 30 mg/ℓ. This algebraic fit was then used along with an axial dispersion coefficient of 1 cm^2/min in the packed bed mathematical model to predict the breakthrough curve for the same conditions applicable to the data in Figure 4.10.

The predicted curve is shown in Figure 4.10 as a continuous line. Correspondence between the predicted curve and the data was rather good, once more indicating the validity of the model in predicting particle size effects.

It is interesting to add here that for fresh carbon, an effectiveness factor of 0.0209 was computed for the 18 x 20 mesh carbon. This effectiveness factor increased as the reaction proceeded and was 0.625 when 3 grams of free chlorine had reacted with one gram of carbon.

Unfortunately, no quantitative measurement of color was made for the packed bed column experiments in Figures 4.9 and 4.10. The data shown in Figure 4.11 represent the effluent concentration vs. time from a 60 x 80 packed bed experiment carried out at 23°C for which color measurements were made, however.

Eight grams of carbon were packed in 2.54 cm internal diameter

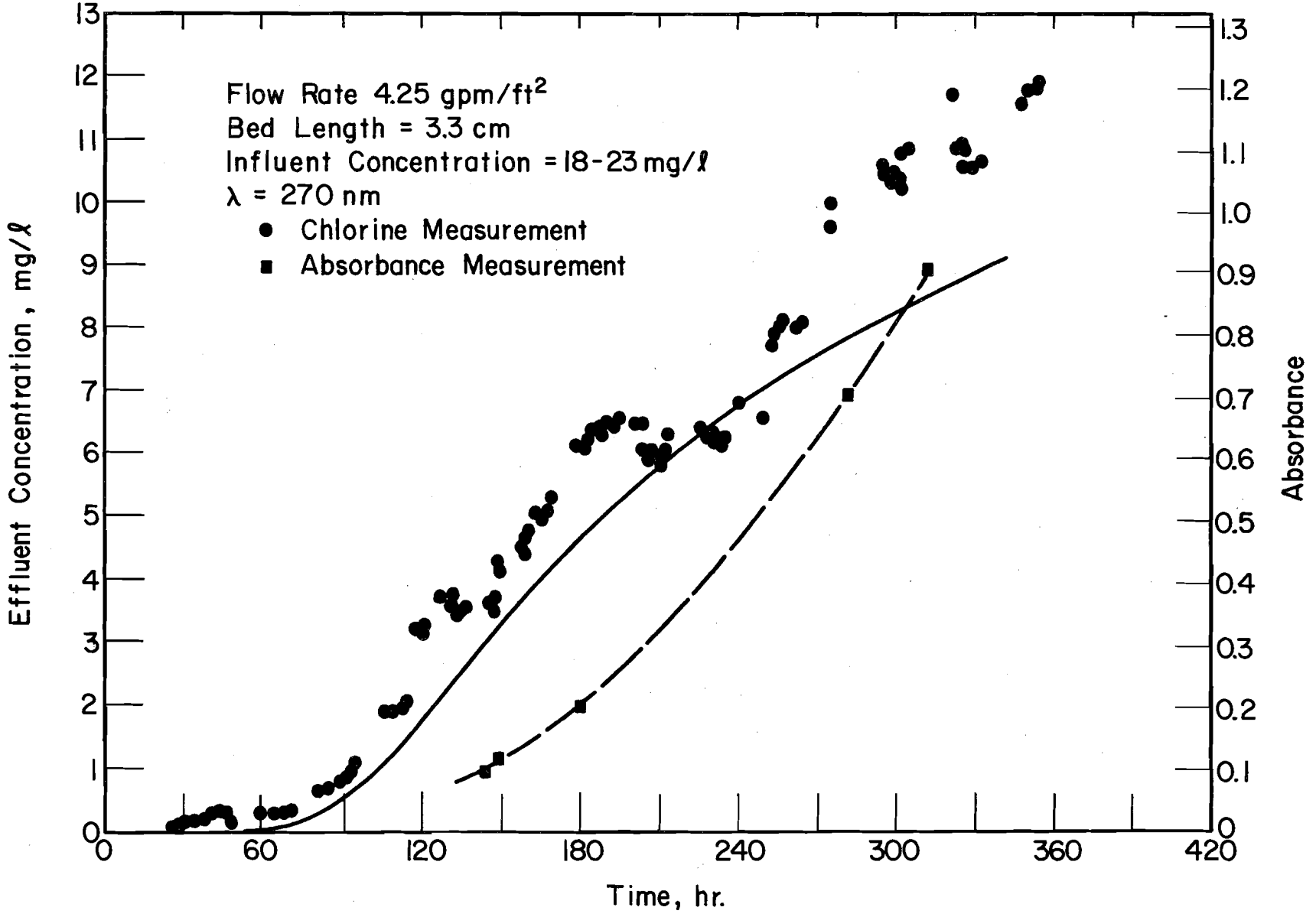

FIG. 4.11 CHLORINE AND COLOR BREAKTHROUGH CURVE, pH 3.2-5.8, 23°C, 60 x 80 MESH CARBON

column. The average length of the carbon portion of the bed was 3.3 cm and the influent flow rate was maintained at 87.5 cc/min (4.25 gpm/ft^2). In this experiment the carbon was held in place by a layer of glass wool on each side. The glass wool was in turn supported by tightly packed 0.2 cm glass beads. The influent free chlorine concentration varied between 18 and 23 mg/ℓ, and the influent pH ranged from 3.2 to 5.8. This experiment was very crudely prepared as it was intended for the purpose of preliminary investigation only. It is reported here only because color measurements of the effluent samples were made. The absorbance, a measure of the organic matter present and the color, of the effluent solution vs. time is shown in Figure 4.11.

Brown color was observed in the effluent after about 288 hours, at which time the absorbance of the effluent was measured at 0.7. By the time brown color became visible in the column effluent, an average of 3.15 grams of chlorine, as Cl_2, had reacted with each gram of carbon. It is interesting to note that in the case of the 60 x 80 mesh carbon packed bed experiment shown in Figure 4.9, brown color was observed in the effluent after 275 hours which is rather close to the 288 hours required for color emergence in this experiment. Using the constant concentration batch reactor model, it was predicted that 3.605 g of free chlorine, as Cl_2, would have reacted with a gram of carbon located at the entrance of the column if it were assumed that both influent concentration and pH were held constant at 20 mg/ℓ and 4.0.

When the results of this experiment were compared to the other pH 4, 60 x 80 mesh carbon column experiment shown in Figure 4.9, it was

found that just prior to the emergence of brown color in the effluent, the amount of chlorine reacted per gram of carbon located at the mouth of the bed was almost the same. However, the average amount of chlorine reacted per gram of carbon in the bed was much lower due to the fact that the carbon column used for the results shown in Figure 4.11 was about twice as long as the one used in the experiment shown in Figure 4.9. Based on this observation, it could be stated that more efficient use of the carbon is attained by resorting to shorter carbon columns.

This column experiment was continued after brown color was observed in the effluent. As the experiment proceeded, the color in the effluent turned to black and became much more intense as the carbon in the bed started to fragment and leave the bed in the effluent. After about 360 hours, the experiment was stopped after a high head loss developed in the bed.

Using the algebraic fit, R(X,C), developed for the 60 x 80 mesh carbon, pH 4, and 23°C column experiment in Figure 4.9, an axial dispersion coefficient, D_A of 1 cm^2/min and a bed porosity, ε, of 0.43, the packed bed model was solved to predict the breakthrough curve assuming an influent concentration of 20 mg/ℓ. The predicted curve is shown as a continuous line in Figure 4.11. A rather good correlation between the predicted curve and the data was obtained considering the crude manner in which this experiment was carried out. Note that beyond 288 hours, color was observed in the effluent and eventually carbon fines began appearing in the effluent. Beyond this point, the model is not expected to predict the effluent quality as it does not account for carbon fines leaving the bed. As can be

seen from Figure 4.11, the predicted values are much lower than the experimental data in this range.

C. Experiments at pH 10.0 and 23°C

HOCl is a weak acid with a pK_a of 7.6 at 23°C (Morris, 1968) and, accordingly, at pH values above 7.6, OCl^- is the predominant species of free chlorine. In order to determine how this species reacts with carbon, experiments were carried out at a pH of 10.0.

1. Batch Studies

Three closed batch reactor experiments were carried out at pH 10.0 and 23°C and the results are shown in Figure 4.12. In this case, 4.21 g $NaHCO_3$ and 0.53 g Na_2CO_3 were added per liter of solution to minimize pH changes owing to entry of CO_2 into the solution from the atmosphere. In all three experiments 20 mg/ℓ of 60 x 80 mesh activated carbon were added. Initial free chlorine concentrations were 37.0, 28.6 and 13.6 mg/ℓ.

The diffusion coefficient, D_c, for OCl^- was assumed to be the same as that used for HOCl, namely 6×10^{-4} cm^2/min. For a value of L_p equal to 0.0035 cm, corresponding to 60 x 80 mesh carbon, the closed batch model was solved to predict the concentration levels in the reactor as a function of time. The values of the model constants for this case were found to be 0.0018, 0.000017, 0.684, 380 and 0.0000134 min^{-1} for SIT, k_8, k_9. k_{10}, and k_d, respectively, and the results are shown in Figure 4.12. As is obvious from Figure 4.12, a rather good prediction was obtained for the three concentration vs. time curves. The values of k_8 and k_{10} were

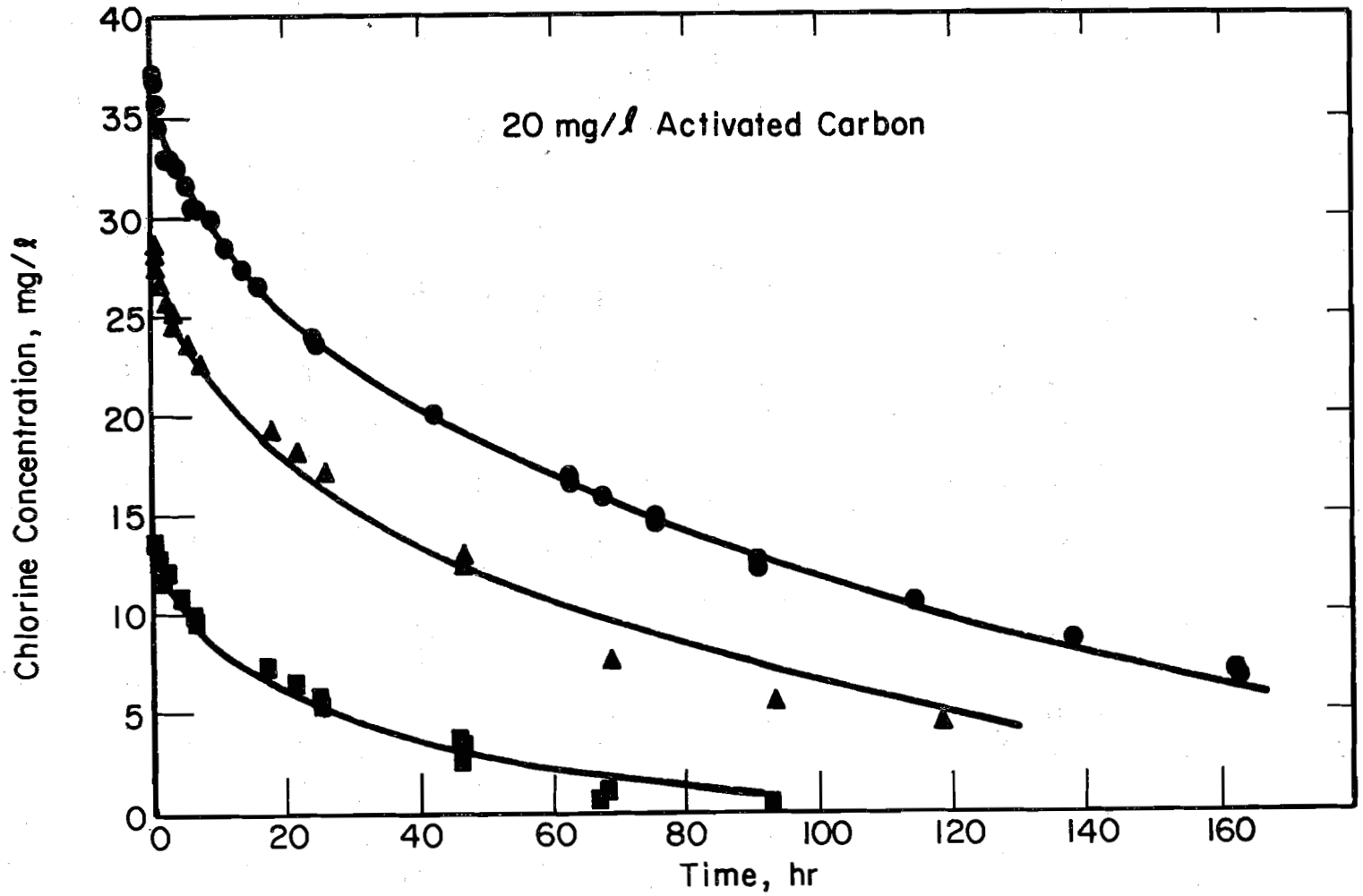

FIG. 4.12 CHLORINE CARBON (60 x 80 MESH) REACTION IN A CLOSED BATCH REACTOR, pH 10, 23°C

not changed from those used to describe the pH 4, 23°C data. It is possible, however, that an equally good fit could have been obtained if all four constants, SIT, k_8, k_9 and k_{10}, had values other than were used for the pH 4, 23°C data.

2. Packed Bed Studies

The data shown in Figure 4.13 represent a breakthrough curve for a packed bed experiment with an influent pH of 10.0. The influent concentration, temperature, and flow rate were 20 mg/ℓ, 23°C and 32.78 cc/min (4.26 gpm/ft^2), respectively. The carbon, 2.35 grams of 60 x 80 mesh, was packed in a 1.55 cm internal diameter column. The length of the carbon portion of the bed, L_b, was 2.6 cm and the porosity was again assumed to be 0.43. The effluent pH remained at 10.0 with no noticeable variation during the run. The experiment was stopped after 250 hours prior to the appearance of brown color.

Using the values for the constants obtained from the batch data at pH 10.0, the algebraic expression, R(X,C), was obtained. Using this expression and an axial dispersion coefficient of 1 cm^2/min, the packed bed model was solved; the predicted breakthrough curve is shown as a continuous line in Figure 4.13. In this case the quality of the prediction is not quite as good as was observed at pH 4.0, but it is considered satisfactory for most purposes.

D. Experiments at pH 7.6 and 23°

The pK_a of the HOCl is 7.6 at 23°C (Morris, 1968). The solution

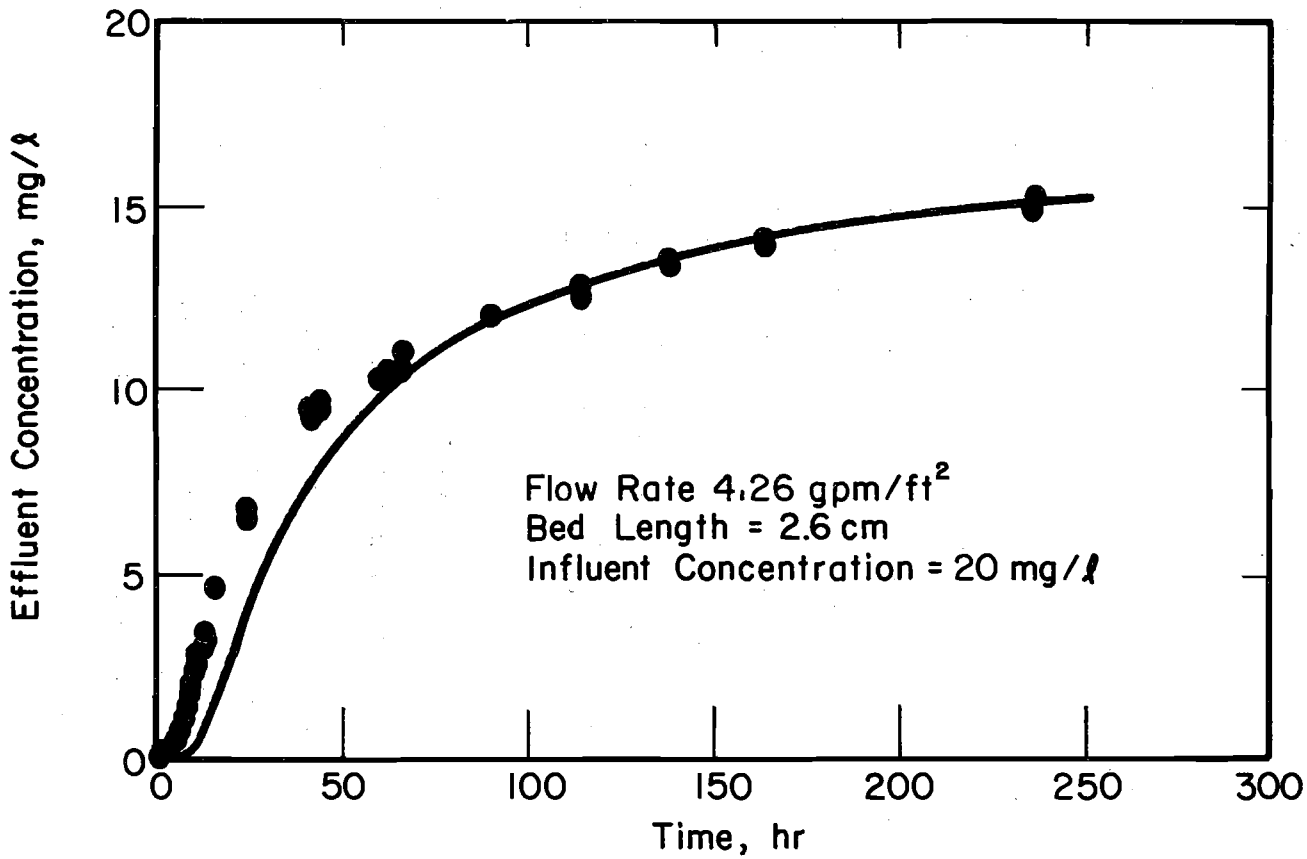

FIG. 4.13 CHLORINE BREAKTHROUGH CURVE, pH 10, 23°C, 60 x 80 MESH CARBON

pH of 7.6 was selected for testing because the concentrations of HOCl and OCl^- are equal in such a solution and because it was desired to determine the applicability of the model to mixtures of these species.

Three closed batch experiments were carried out at this pH and temperature. Carbonate salts, 0.01675 g/ℓ of $NaHCO_3$ and 4.22×10^{-5} g/ℓ of Na_2CO_3 were added to set the solution at equilibrium with the atmosphere. In the first experiment, the results of which are shown in Figure 4.14, 10 mg/ℓ of 60 x 80 mesh carbon were used in conjunction with an initial free chlorine concentration of 33.9 mg/ℓ. In the other two experiments shown in Figure 4.15, 15 mg/ℓ of the same carbon were used with initial free chlorine concentrations of 30.0 and 14.76 mg/ℓ.

The diffusion coefficient, D_c, for HOCl and OCl^- were assumed to be 6×10^{-4} cm^2/min. As a result, this same value was used when both these species existed together in solution. Analysis of experimental data showed that the values of k_8, k_{10}, and k_d were the same at pH 4.0 as at pH 10.0; consequently, the same values were used in solving the closed batch reactor model at pH 7.6. A rather good fit of the data was obtained for values of SIT and k_9 of 0.0044 and 1.672, respectively. These values represent the average of the values of SIT and k_9 at pH 4.0 and 10.0, thus leading to the conclusion that the pH effect is dependent only on the relative distribution of HOCl and OCl^-. Magee (1956) presented values of the first order rate constant, k (see Equation 1.8) vs. pH and his data are consistent with this conclusion.

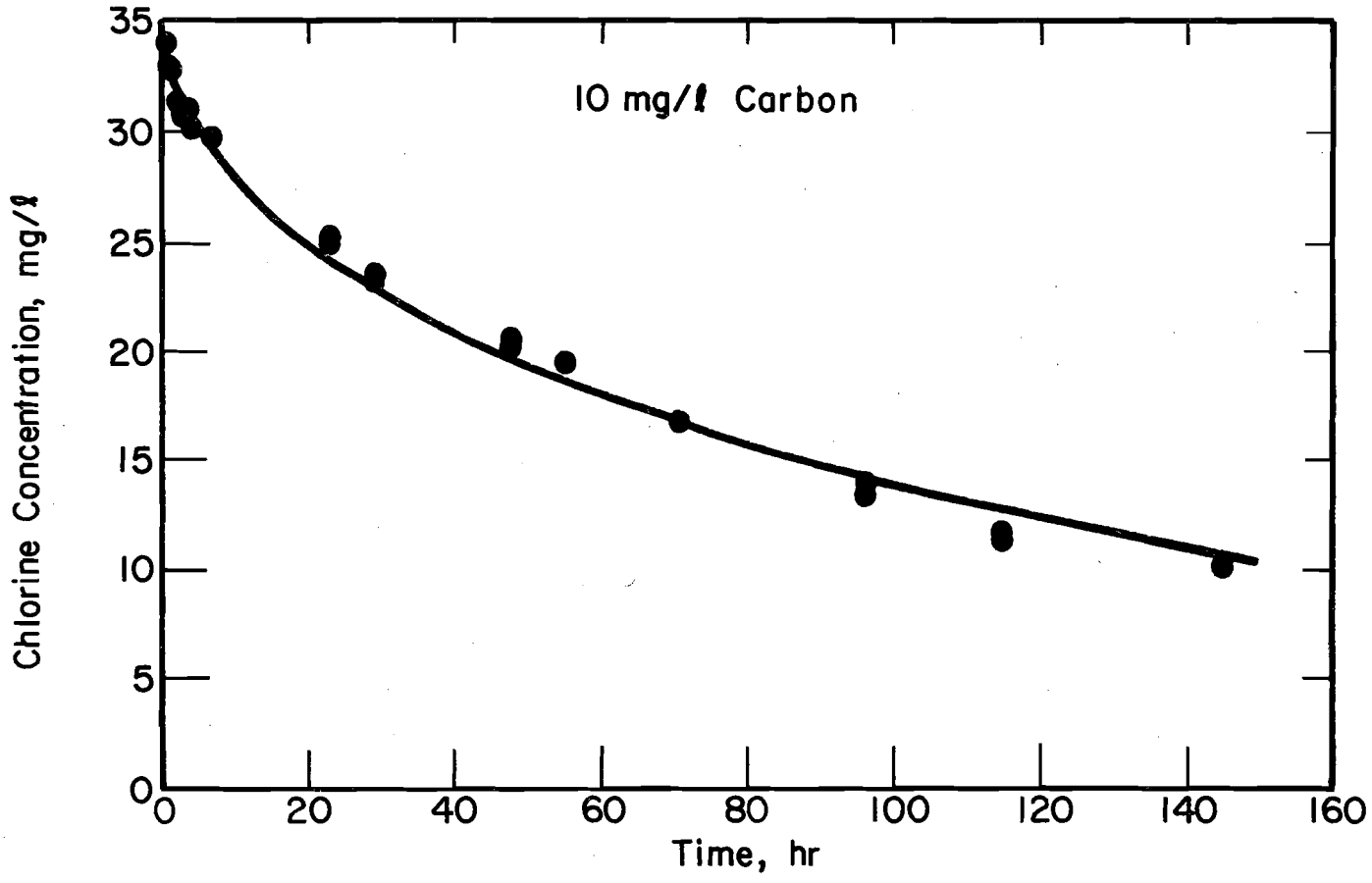

FIG.4.14 CHLORINE-CARBON (60 x 80 MESH) REACTION IN A CLOSED BATCH REACTOR, pH 7.6, 23°C

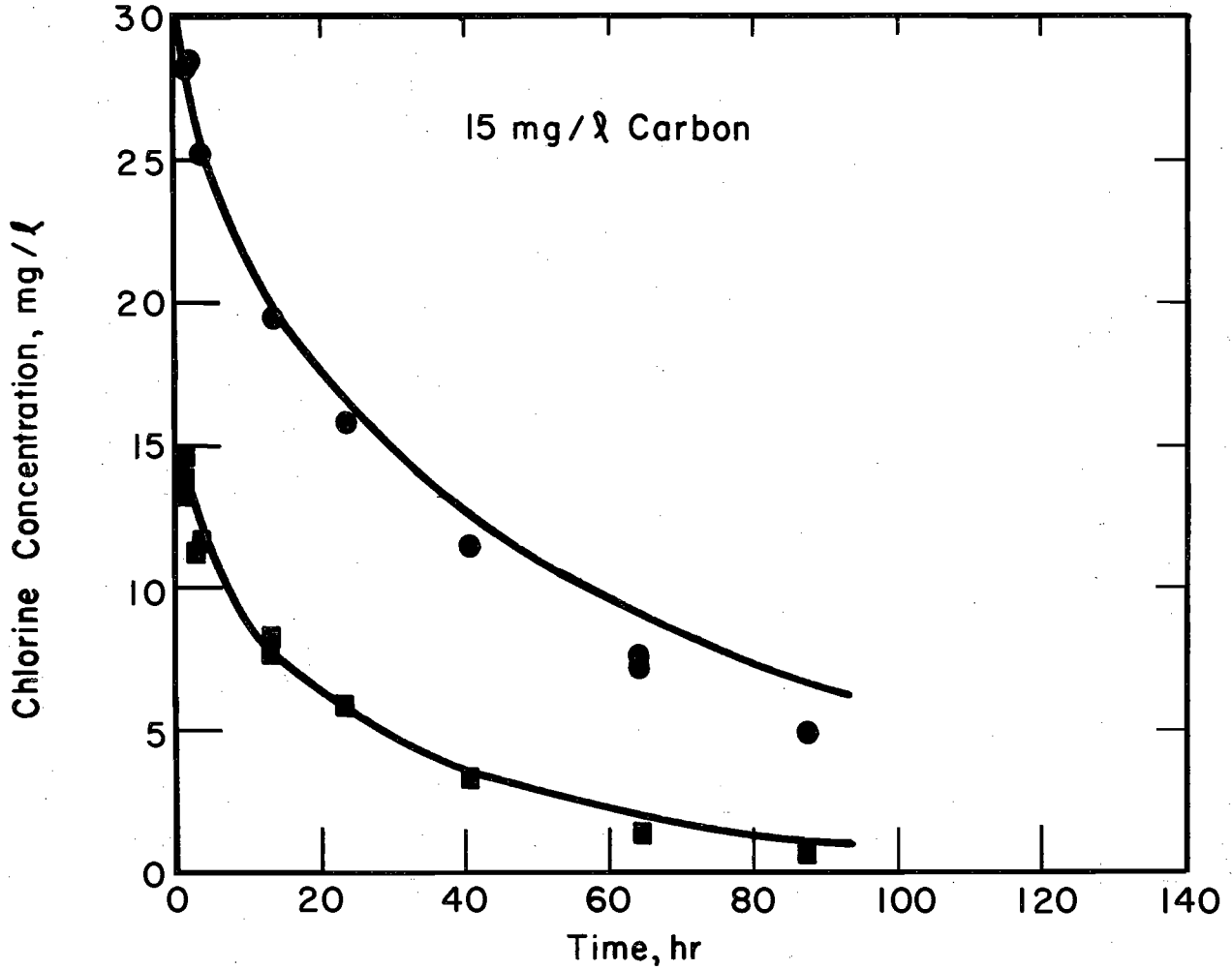

FIG. 4.15 CHLORINE–CARBON (60 x 80 MESH) REACTION IN A CLOSED BATCH REACTOR, pH 7.6, 23° C

E. Temperature Effect Studies at pH 4.0 and 10.0

Temperature is expected to affect both the diffusivity and the reaction rate constants. The effect of temperature on diffusivity in a pore was assumed to be similar to that in free solution. The expression used for predicting the effect of temperature on D_c was (Fogler, 1974)

$$D_c(\bar{T}_2) = D_c(\bar{T}_1) \cdot \frac{\mu_1}{\mu_2} \frac{\bar{T}_2}{\bar{T}_1} \qquad 4.2$$

where μ is the viscosity, M/L·T, and $\bar{T}$ is the absolute temperature, °K.

Two closed batch experiments were run at pH 10.0 and 35°C as shown in Figure 4.16. The initial free chlorine concentrations were 38.1 and 24.8 mg/ℓ. Two other experiments were carried out at the same pH but at a temperature of 2°C as shown in Figure 4.17. In this case the initial free chlorine concentrations were 39.3 and 24.4 mg/ℓ. All four experiments were performed with 20 mg/ℓ of 60 x 80 mesh carbon.

The viscosity of water at 2°C, 23°C and 35°C is 1.6728, 0.9358 and 0.7225 centipoises, respectively (Perry, 1950). Using these values and a base value for D_c of 6 x 10^{-4} cm^2/min at 23°C, the values of D_c were calculated, using Equation 4.2, to be 3.12 x 10^{-4} and 8.04 x 10^{-4} cm^2/min at 2°C and 35°C, respectively. The closed batch model was solved to predict the concentration levels and to determine the remaining constants; a rather good fit was obtained for SIT and k_9 values of 0.0009 and 0.342 at 2°C, and 0.00267 and 1.0157 at 35°C, respectively. The values of k_8 and k_{10} were the same as for the pH 4.0 and 10.0 studies at 23°C. The first order

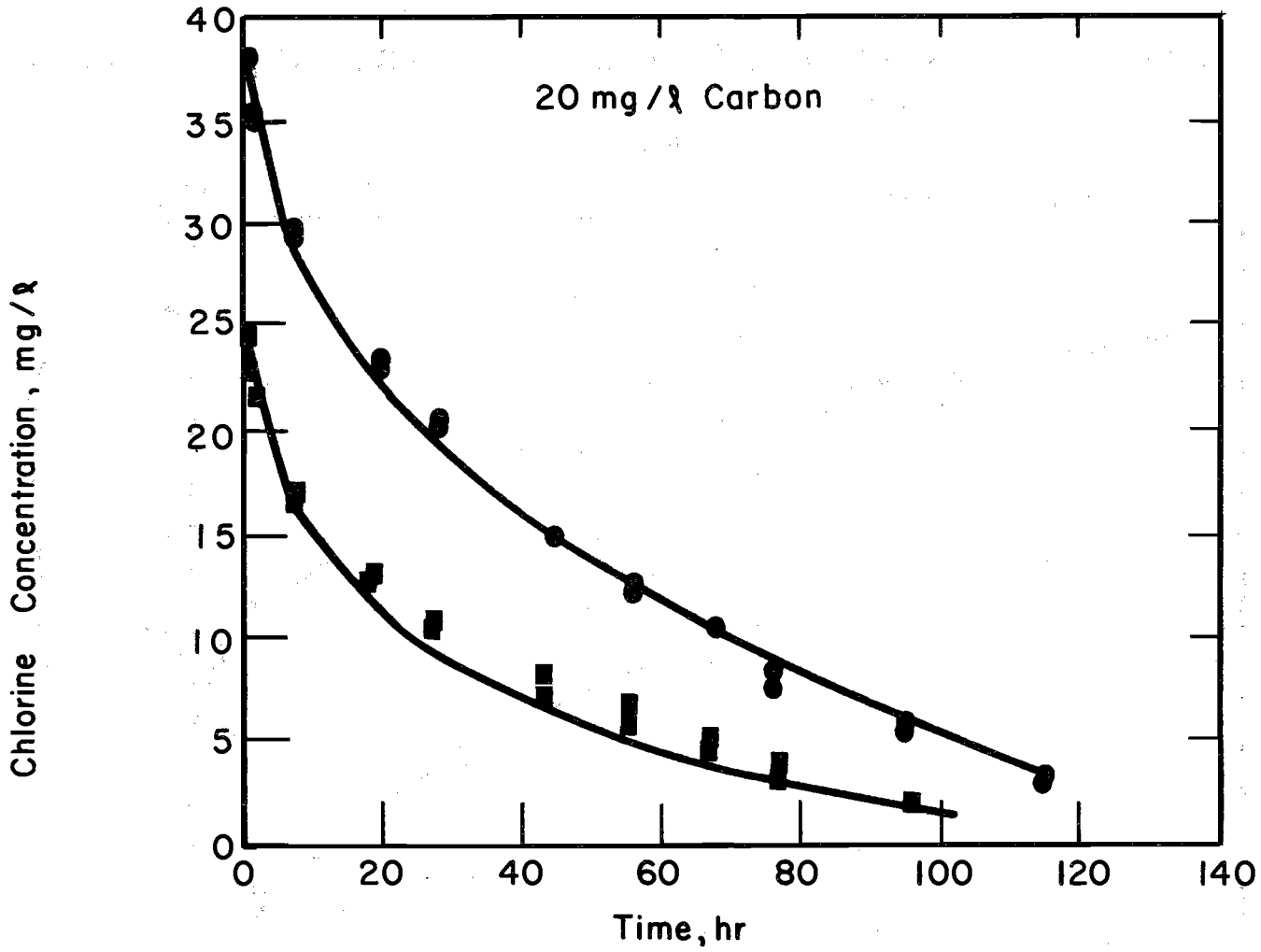

FIG. 4.16 CHLORINE—CARBON (60 x 80 MESH) REACTION IN A CLOSED BATCH REACTOR, pH 10, 35° C

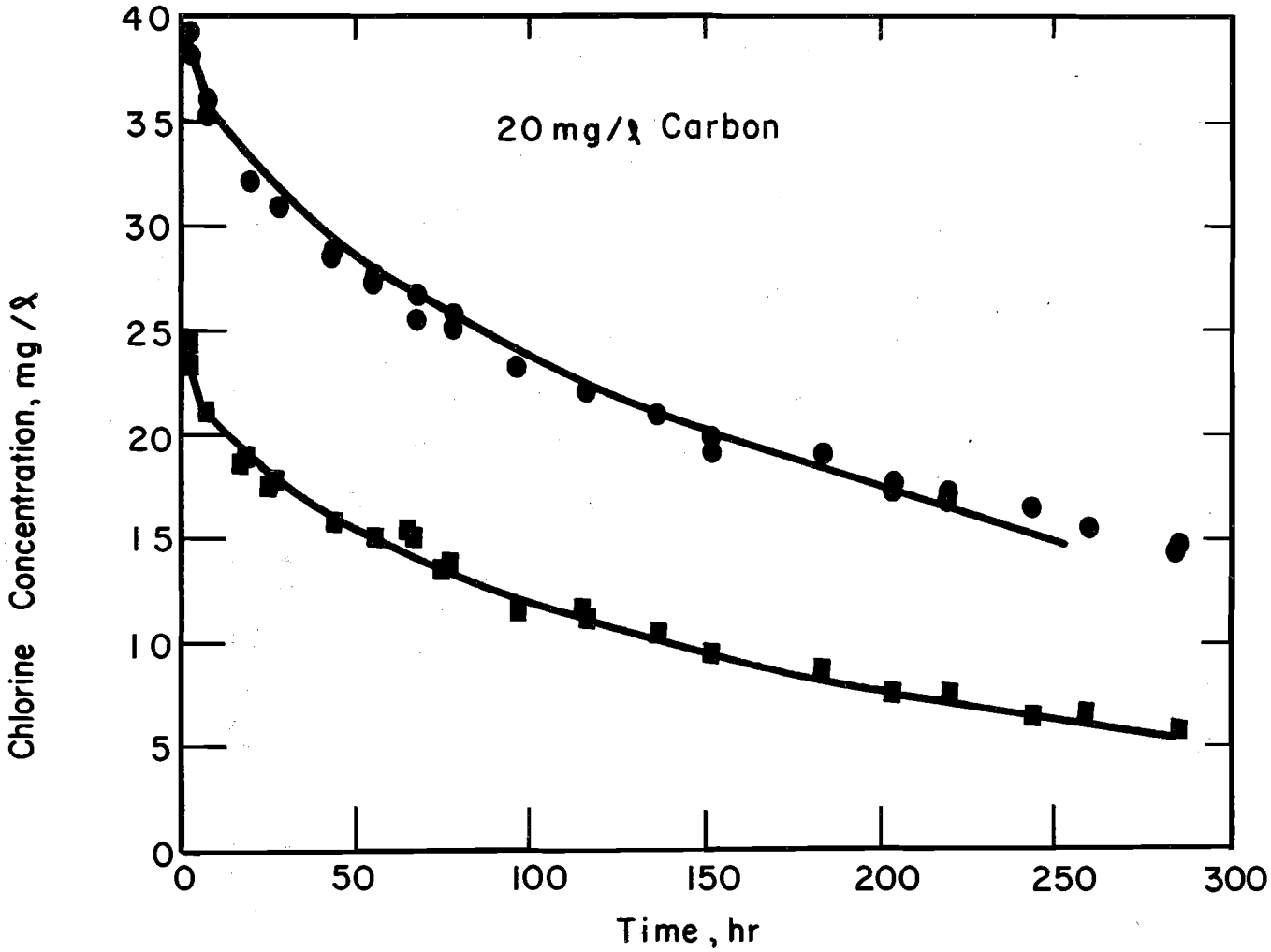

FIG. 4.17 CHLORINE–CARBON (60 x 80 MESH) REACTION IN A CLOSED BATCH REACTOR, pH 10, 2° C

rate of decay constant, k_d, was found to be essentially the same, 0.0000134 min^{-1}, for the three different temperatures at pH 10.0.

Two other closed batch experiments were carried out at pH 4.0 and a temperature of 35°C. In the first experiment 20 mg/ℓ of 60 x 80 mesh carbon was used and the initial free chlorine concentration was 37.8 mg/ℓ. The results are shown in Figure 4.18. Only 10 mg/ℓ of 60 x 80 mesh carbon was used in the second experiment shown in Figure 4.19; the initial free chlorine concentration was 27.3 mg/ℓ. The rate of decay at pH 4.0 and 35°C was found to be higher than that at 23°C at the same pH; k_d was evaluated to be 0.00003 min^{-1} in this case.

A good fit of the data was obtained when the finite batch model was solved for values of SIT and k_9 of 0.01039 and 3.947, respectively, as is apparent in Figures 4.18 and 4.19. In this case also, the values of k_8 and k_{10} were the same as at 23°C.

SIT and k_9 cannot be regarded as surface reaction rate constants because they both include the term L_p^2/D_c. Consequently, in order to study the effect of temperature on the surface reaction rate SST and k_7 are the proper terms to be analyzed. Figure 4.20 shows an Arrhenius plot of the temperature data, $\log_{10}$ SST vs. $1/\bar{T}$. The three values of SST available at pH 10.0 fall on a straight line, and the two values of SST at pH 4.0 form a line parallel to the previous one. Based on these limited data, the activation energy for k_3, the only rate constant which is part of SST, can be calculated to be 5.3 kcal. The constant, k_8, contains the adsorption-desorption equilibrium constant, k_4, and it likely varies with temperature. In this study, however, it was assumed that k_8 and k_{10} did not vary with

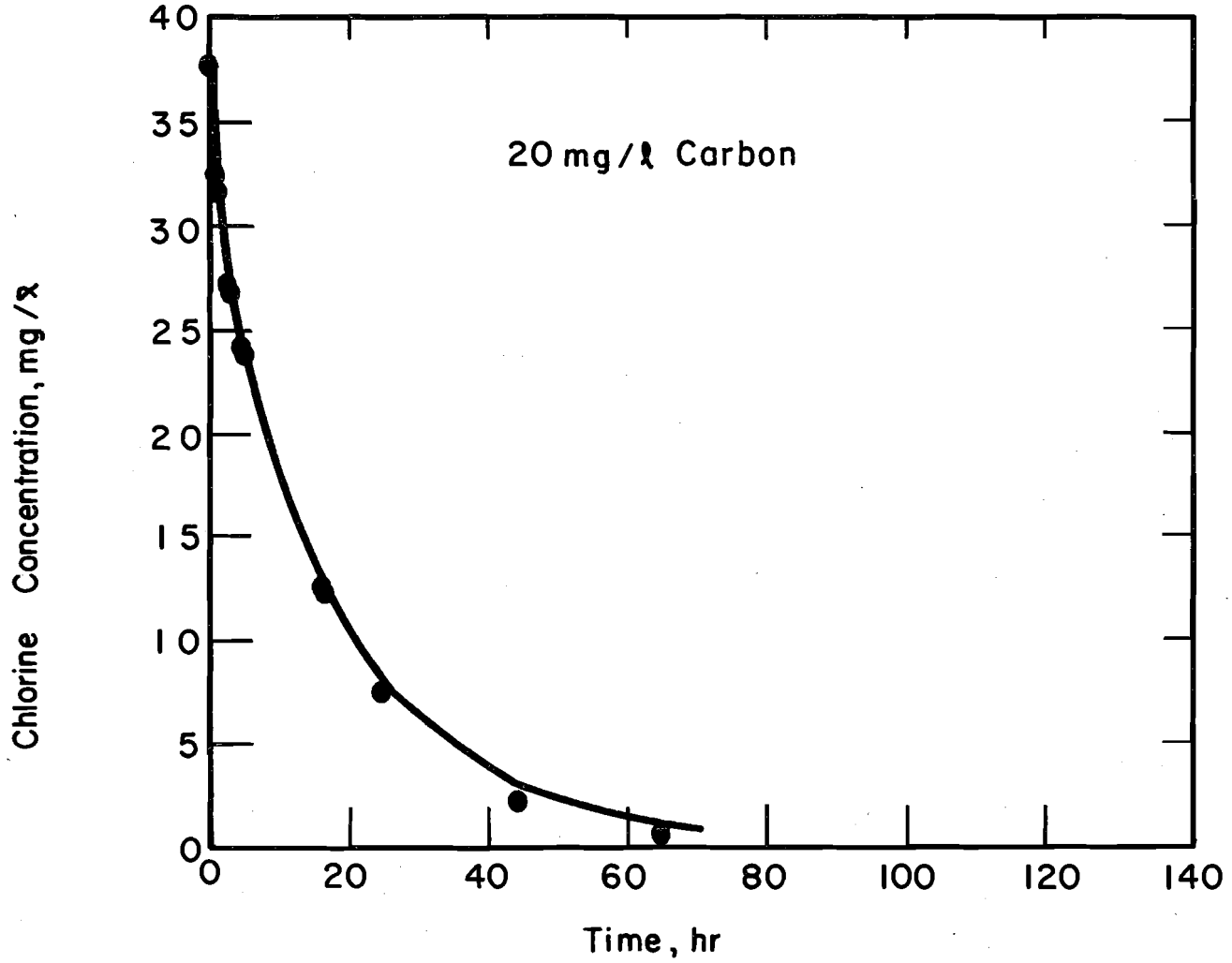

FIG. 4.18 CHLORINE–CARBON (60 x 80 MESH) REACTION IN A CLOSED BATCH REACTOR, pH 4, 35° C

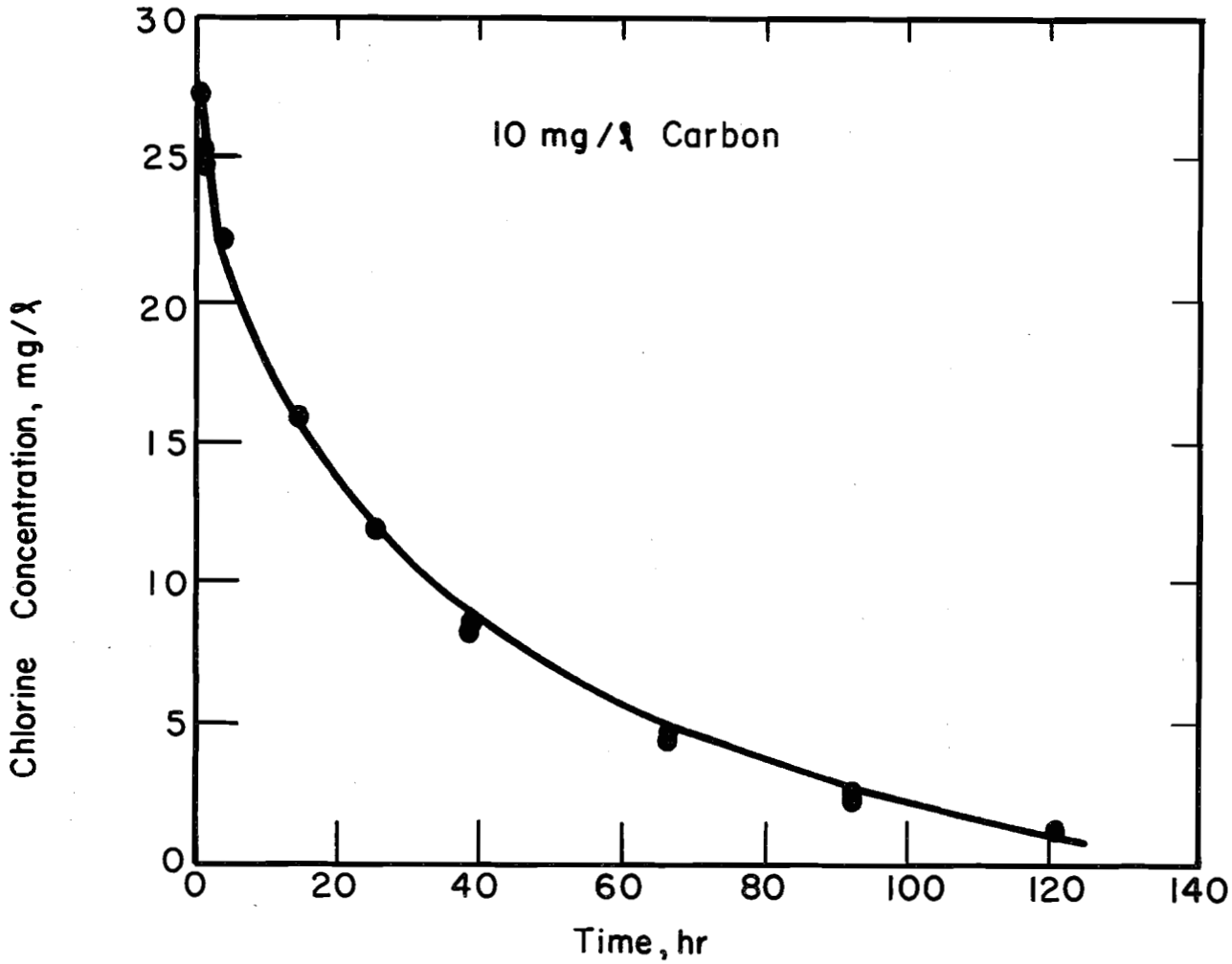

FIG. 4.19 CHLORINE-CARBON (60x80 MESH) REACTION IN A CLOSED BATCH REACTOR, pH 4, 35°C

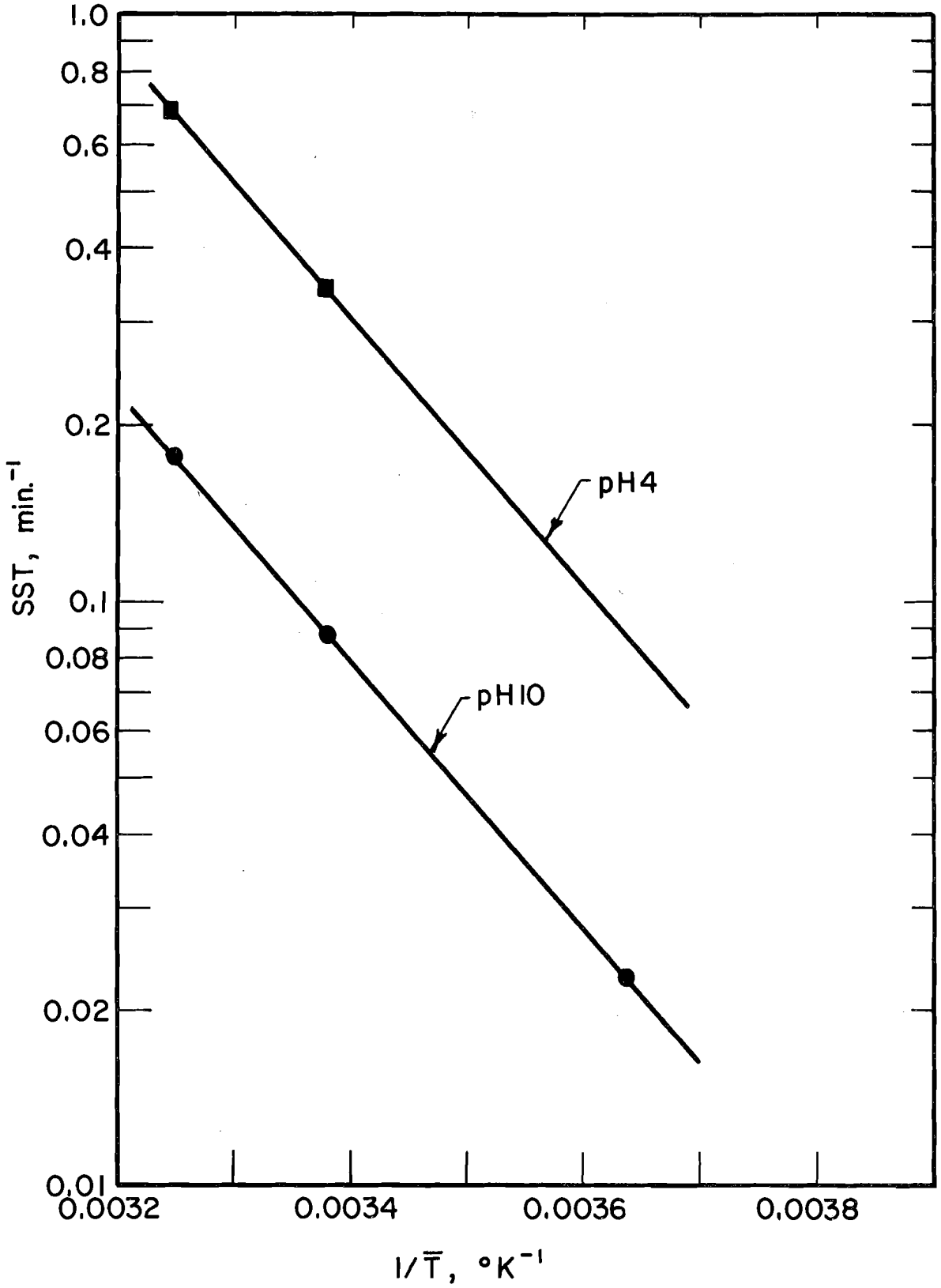

FIG. 4.20 EFFECT OF TEMPERATURE ON THE PARAMETER SST

temperature in fitting the data; thus, the variation observed in k_3 included the effect of temperature on k_8 and k_{10}, if any.

F. Prediction of Model Constants for Different pH and Temperature Values

The pH was observed to influence the reaction rate only as far as it affects the distribution of free chlorine between HOCl and OCl^-. This was an unexpected result because it was thought that the hydrogen ion concentration would affect the surface functional groups on the carbon, thereby influencing the reaction rate. The fraction of free chlorine in the HOCl form is given by $1/[1 + 10^{(pH - pK_{\bar{T}})}]$ while the remaining fraction represents the OCl^- to total free chlorine ratio. $pK_{\bar{T}}$ is the negative $\log_{10}$ of the equilibrium constant evaluated at temperature $\bar{T}$.

Having established the pH and temperature effects, expressions were developed to give SST, min^{-1}, and k_7, min^{-1}, as functions of temperature and pH

$$SST(pH,\bar{T}) = 5.325 \times 10^{7} \frac{[0.343 + 0.0882 \times 10^{(pH - pK_{\bar{T}})}]}{[1 + 10^{(pH - pK_{\bar{T}})}]} \exp \frac{(-5266)}{\bar{T}} \qquad 4.3$$

$$k_7(pH,\bar{T}) = SST(pH,\bar{T}) \times 380 \qquad 4.4$$

where 0.343 and 0.0882 are the values of SST at pH 4.0 and 10.0 respectively. White (1972) gave values for pK_a for six different temperatures which could be used to compute an enthalpy of reaction, $\Delta H°$, of 4.0 kcal. Using this value, the pK_a at a temperature $\bar{T}$, °K, could be computed from the pK_a value at 23°C, 7.6, using the following expression,

$$pK_{\bar{T}} = 7.6 + 86900 \frac{(296 - \bar{T})}{296 \times \bar{T}} \qquad 4.5$$

The dimensionless rate constants, SIT and k_9, used in the numerical solution of the two batch models can be obtained from the values of SST and k_9 given by Equations 4.3 and 4.4 using the following two equations,

$$SIT = \frac{5.272 \times 10^5 \times \mu_{\bar{T}} \times L_p^2 \times SST}{\bar{T}} \qquad 4.6$$

and

$$k_9 = SIT \times 380 \qquad 4.7$$

where $\mu_{\bar{T}}$ is the absolute viscosity at temperature $\bar{T}$, centipoises, and L_p is the pore half length, cm. Because k_8 and k_{10} were constant at 0.000017 and 380, respectively, Equations 4.3-4.7 can be used to calculate the remaining parameters necessary for describing the performance of closed and constant concentration batch reactors as well as packed bed columns using Filtrasorb 400 carbon.

V. CONCLUSIONS AND RECOMMENDATIONS

A. Conclusions

1. Batch experimental data can be used to provide the information necessary for the design of packed bed activated carbon dechlorination reactors. In this study the surface reaction rate constants appearing in the pore diffusion model were evaluated from batch experimental data. These constants were then successfully used to predict packed bed column behavior.

2. In this study an algebraic rate expression, R(X,C), was used to simplify the packed bed reactor mathematical model by eliminating the dimension along the carbon pore from the model. This rate expression was obtained by algebraically fitting constant concentration batch reactor rate data vs. X; the amount of chlorine reacted per unit weight of carbon. The use of such an expression was possible because the two batch models predicted that, for fixed pH, temperature and particle size, the rate of chlorine removal was a function of only the bulk concentration and the amount of chlorine already reacted with the carbon.

3. Pore diffusion was found to be very important, especially when the carbon was relatively fresh. As the extent of reaction increased, the surface reaction became the rate controlling step as was shown in the case of the 60 x 80 and 45 x 50 mesh carbon CCBR experiments.

4. The rate of chlorine removal was found to be very sensitive to particle size, decreasing with increasing granule diameter. This is a direct consequence to the importance of pore diffusion as a rate controlling mechanism especially for low values of X. The mathematical model was

successfully used to predict particle size effects for both batch and packed bed reactors.

5. An analysis of the data showed that the reaction rate approaches zero assymptotically, rather than a steady state value as has been reported by Magee (1956). In terms of the parameters used in this model it was found that k_9/k_{10} was equal to SIT which means that as the amount of chlorine reacted per gram of carbon increases, the surface reaction term approaches zero.

6. The pH was observed to influence the reaction rate only as far as it affects the distribution of free chlorine between HOCl and OCl^-. This finding made it possible to use reaction rate constants obtained separately for HOCl and OCl^- to arrive at the rate constants applicable to mixtures of the two free chlorine species.

7. The effect of temperature on the surface dissociation rate constant, k_3, was found to follow the Arrhenius model. Based on limited data, the activation energy for k_3 was found to be 5.3 kcal for both HOCl and OCl^-.

8. Brown color was observed in solution after extensive oxidation of the carbon. The emergence of the brown color was observed in both constant concentration batch and in packed bed experiments. Little information was obtained on the emergence of the brown color, but based on the limited data available, between 2.8 to 4.2 grams of chlorine had to react with a gram of carbon before the color was visible.

9. Little, if any, mixing occurred in the packed bed reactor experiments carried out in this study. This was shown by the almost

identical results obtained from solving the packed bed model with the axial dispersion coefficient, D_A, equal to 1 cm^2/min and with D_A equal to zero. However, axial dispersion may prove to be important when packed bed declorination reactors are run under conditions other than those studied here.

B. Engineering Significance

1. The particle size of the carbon used in a packed bed reactor has an important influence on the behavior of activated carbon dechlorination reactors. Because the rate of chlorine removal increases with decreasing particle size, shorter columns could be used to achieve a given removal efficiency when smaller carbon granules are used. This advantage should be balanced, however, against the increased cost of obtaining granular carbon smaller than that available commercially and the increased head loss that accompanies such a decrease in carbon size.

2. The design of a dechlorination carbon column should take both the breakthrough effluent chlorine concentration and the appearance of color in the effluent into consideration. The carbon located at the mouth of the packed bed is always exposed to the highest chlorine concentration in the bed and, as a result, the extent of reaction at the mouth of the bed will likely determine when the bed starts producing color. If a column is too long, color will appear in the effluent prior to the emergence of an undesirable chlorine concentration. In such a case, the average amount of chlorine reacted per gram of carbon may be much less than the amount that has reacted with the carbon located at the entrance of the packed bed. In the design of a dechlorination bed, it will be necessary to balance the

cost of more frequent replacement of shallow beds with the cost of more inefficient use of the carbon when longer beds are employed. This aspect remains to be further evaluated however.

C. Further Study

1. The effect of the presence of organic compounds on the rate of uptake of free chlorine by activated carbon has not been investigated. This is a very important parameter which is very difficult to evaluate because of the wide variability of the type of organic compounds present in water and wastewater, and because of the possibility that free chlorine may react with some of the adsorbed and nonadsorbed organic compounds. The model developed in this study should thus be used only as a baseline in any design calculations, and a factor of safety should be used to protect against short filter runs owing to the presence of organic matter and the entrainment of particulate matter present in the water by the carbon. Further research is needed to evaluate the effect of the presence of organic compounds on the process of dechlorination and to give guidelines for factors of safety that are needed when different kinds of water are applied to the carbon.

2. Only one carbon was used in this study. Other carbons have different purity, surface area and pore volume characteristics and the effect of the different characteristics of other carbons on the reaction rate constants remain to be evaluated.

3. Commercial activated carbon is usually manufactured to include a wide range of particle sizes. Before a carbon column is put to use, it is usually fluidized and then allowed to settled by gravity. Such a procedure

results in a stratified bed and the design of such a bed should take this size stratification into account. Further research is needed to evaluate the performance of such beds when chlorinated water is applied to them either in the downflow or the upflow mode.

LIST OF REFERENCES

Baker, R. A., "Dechlorination and Sensory Controls," *Jour. American Water Works Assoc. 56*, 1578 (1964).

Bird, R. B., Stewart, W. E. and Lightfoot, E. N., *Transport Phenomena*, John Wiley & Sons, Inc., New York (1960).

Bischoff, K. B., "A Note on Boundary Conditions for Flow Reactors," *Chem. Eng. Science, 16*, 131 (1961).

Boehm, H. P., "Chemical Identification of Surface Groups," *Advances in Catalysis*, D. D. Eley et al. (eds), *16*, 179-272, Academic Press, New York (1966).

Calgon Corp., "Calgon Activated Carbon Product," Bulletin No. 20-2a, Pittsburgh, PA (1969).

Coughlin, R. W., Ezra, F. and Tan, R. N., "Influence of Chemisorbed Oxygen in Adsorption into Carbon from Aqueous Solution," *J. Coll. Interface Sci. 28*, 386 (1968).

Dean, R. B., "Toxicity of Wastewater Disinfectants," *News of Environmental Research in Cincinnati*, U. S. Environmental Protection Agency, Cincinnati, Ohio, July 5 (1974).

Fair, G. M., Geyer, J. C. and Okun, D. A., *Water and Wastewater Engineering*, Vol. 2, John Wiley & Sons, Inc., New York (1968).

Fogler, H. S., *The Elements of Chemical Kinetics and Reactor Calculations*, Prentice-Hall, Inc., New Jersey (1974).

Hagar, D. G. and Flentje, M. W., "Removal of Organic Contaminants by Granular Carbon Filtration," *Jour. Amer. Water Works Assoc. 57*, 1440 (1965).

Helfferich, F. G., *Ion Exchange*, McGraw-Hill, New York (1962).

Kovach, J. L., "Activated-Carbon Dechlorination," *Ind. Water Eng.*, October/November (1971).

Lapidus, L., *Digital Computations for Chemical Engineers*, McGraw-Hill, New York (1962).

Laubusch, E. J., Chapter in *Water Quality and Treatment*, 3rd edition, American Water Works Assoc., McGraw-Hill, New York (1971).

Levenspiel, O., *Chemical Reaction Engineering*, John Wiley & Sons, Inc., New York (1972).

Magee, V., "The Application of Granular Active Carbon for Dechlorination of Water Supplies," *Proc. Soc. Water Treat. Exam 5,* 17 (1956).

Mishchenko, K. P., Flis, I. E. and Kastodina, V. A., "Thermodynamic Characteristics of Aqueous Solutions of Hydrogen Perioxide and Its Reaction with Chlorine at Different Temperatures," *Zhur. Priklad. Khim 33,* 2671 (1960). In *Chem. Abstracts 55,* 9023 (1961).

Morris, J. C., Chapter in *Water and Wastewater Engineering,* G. M. Fair *et al.* (eds.), *2,* John Wiley & Sons, Inc., New York (1968).

Olson, L. L. and Binning, C. C., "Interaction of Aqueous Chlorine with Activated Carbon," Chapter in *Chemistry of Water Supply Treatment and Distribution,* A. Rubin (ed.), Ann Arbor Science Publishers (1974).

Perry, J. H., *Chemical Engineering Handbook,* McGraw-Hill, New York (1950).

Petersen, E. E., *Chemical Reaction Analysis,* Prentice-Hall, New York (1965).

Puri, B. R., "Surface Complexes on Carbons," *Chemistry and Physics of Carbon,* P. L. Walker (ed.), Vol. VI, 191-282, M. Dekker, New York (1970).

Smisk, M. and Cerny, S., *Active Carbon: Manufacture, Properties and Applications,* Elsevier Publishing Co., New York (1970).

Snoeyink, V. L., Lai, H. T., Johnson, J. H. and Young, J. F., "Active Carbon: Dechlorination and the Adsorption of Organic Compounds", Chapter in *Chemistry of Water Supply, Treatment and Distribution,* A. Rubin, ed., Ann Arbor Science Publishers (1974).

Snoeyink, V. L. and Suidan, M. T., Chapter in *Disinfection of Water and Wastewater,* J. D. Johnson (ed.), Ann Arbor Science Publishers (1975).

Standard Methods for the Examination of Water and Wastewater, 13th edition, American Public Health Association, New York (1970).

White, G. C., *Handbook of Chlorination,* Van Nostrad Reinhold Co., Cincinnati, Ohio (1972).

APPENDIX A

SOLUTIONS OF BATCH AND PACKED BED MODELS

In this study, an implicit finite difference scheme was used to solve the mathematical models as described by sets of nonlinear partial differential equations. This appendix contains the finite difference equations used and an outline of the solution procedures.

1. Closed and Constant Concentration Batch Reactors

Equations 2.27, 2.28, 2.29, 2.30, 2.31 and 2.33 describe the behavior of a closed batch reactor. The distance variable ξ varies between zero and one. This range was divided into N segments, the length, Δr, of each being 1/N. Let r designate the position of each segment. Thus when r is zero, it points to the mouth of the pore and when it is N it refers to the half length of a pore.

A dimensionless time step Δq, was also selected. Let q stand for a position in time, then the dimensionless time is given by $\sum_{i=1}^{q} q_i$.

The difference equations selected to express the different derivatives are

$$\left.\frac{\partial G}{\partial \xi}\right|_{r,q} = \frac{G_{r+1,q} - G_{r,q}}{\Delta r} \qquad \text{A.1}$$

$$\left.\frac{\partial^2 G}{\partial \xi^2}\right|_{r,q} = \frac{G_{r+1,q} - 2G_{r,q} + G_{r-1,q}}{(\Delta r)^2} \qquad \text{A.2}$$

$$\left.\frac{\partial G}{\partial \theta}\right|_{r,q} = \frac{G_{r,q} - G_{r,q-1}}{\Delta q} \qquad \text{A.3}$$

$$\left.\frac{\partial Q}{\partial \theta}\right|_{r,q} = \frac{Q_{r,q} - Q_{r,q-1}}{\Delta q} \qquad A.4$$

Let R represent the nondimensionalized surface rate expression for free chlorine reduction

$$R = \frac{G}{GP_o + k_8} \left(SIT - \frac{k_9 Q}{1 + k_{10} Q}\right) \qquad A.5$$

The surface reaction rate, R, evaluated at time step q + 1 was expressed in terms of the rate at time step q by

$$R_{r,q+1} = R_{r,q} + \left(\frac{\partial R}{\partial G}\right)_{r,q} (G_{r,q+1} - G_{r,q}) + \left(\frac{\partial R}{\partial Q}\right)_{r,q} (Q_{r,q+1} - Q_{r,q}) \qquad A.6$$

Substituting Equations A.1, A.2, A.3, A.4, A.5 and A.6 into the closed batch mathematical model, the following two difference equations are obtained

$$\Delta q\, G_{r-1,q+1} - \left(2\Delta q + (\Delta r)^2 + \Delta q\, (\Delta r)^2 \left(\frac{\partial R}{\partial G}\right)_{r,q}\right) G_{r,q+1} + \Delta q\, G_{r+1,q+1} = \Delta q (\Delta r)^2 R_{r,q} - \left(\Delta q\, (\Delta r)^2 \left(\frac{\partial R}{\partial G}\right)_{r,q} + (\Delta r)^2\right) G_{r,q} + \Delta q\, (\Delta r)^2 \left(\frac{\partial R}{\partial Q}\right)_{r,q} (Q_{r,q+1} - Q_{r,q}) \qquad A.7$$

$$Q_{r,q+1} = \frac{\Delta q\, P_o \left[R_{r,q} + \left(\frac{\partial R}{\partial G}\right)_{r,q} (G_{r,q+1} - G_{r,q}) - \left(\frac{\partial R}{\partial Q}\right)_{r,q} Q_{r,q}\right] + Q_{r,q}}{1 - \Delta q\, P_o \left(\frac{\partial R}{\partial Q}\right)_{r,q}} \qquad A.8$$

Equations A.7 and A.8 are used to evaluate G and Q at position step r and time step q + 1. The Equation A.7 when r equals N is identical to Equation A.7 except in this case, $G_{r-1,q+1}$ is equal to $G_{r+1,q+1}$ because of the symmetry expressed by the boundary condition in Equation 2.31.

At the mouth of the pore, when r = 0, proper boundary condition is given by

$$G_{o,q+1} = G_{o,q} + [m V_p (\frac{G_{1,q+1} - G_{o,q+1}}{\Delta r}) - \frac{k_d L_p^2}{D_c} G_{o,q}] \Delta q \qquad A.9$$

Equation A.9 constitutes the first equation of the set given by Equation A.7.

At the start of the solution, $Q_{r,o}$ was set to zero for all values of r. To obtain the initial distribution of $G_{r,o}$, an approximate distribution was obtained by solving Equation 2.30 assuming GP_o to be much smaller than k_8. This distribution was then corrected by a repeated solution of Equation A.7 with $Q_{r,q+1}$, $Q_{r,q}$ and $(\frac{\partial R}{\partial Q})_{r,q}$ set to zero. After the correct initial distribution of G was obtained, the model was then solved according to the following procedure.

(i) Equation A.8 was solved for $Q_{r,q+1}$ by setting $G_{r,q+1}$ equal to $G_{r,q}$.

(ii) The values of $Q_{r,q+1}$ obtained in step (i) were then used in solving Equation A.7 for $G_{r,q+1}$.

(iii) The values of $G_{r,q+1}$ obtained in step (ii) were then used to recalculate $Q_{r,q+1}$.

(iv) The values of $Q_{r,q+1}$ obtained in step (iii) were then used to recalculate $G_{r,q+1}$.

The above scheme was repeated until convergence was achieved. In this study, however, it was found that, if sufficiently small time steps, Δq were employed, two iterations were sufficient to achieve good convergence. The reason for this begin the slow change in the profile of G.

The solution of the CCBR model was exactly the same as the one outlined above except, in this case, $G_{o,q}$ is always equal to one and consequently Equation A.9 is deleted.

2. Packed Bed Column Reactor with Axial Dispersion

Equations 2.49, 2.50, 2.51, 2.52, 2.53 and 2.54 describe the behavior of a packed bed column reactor with axial dispersion. The distance variable α varies between zero and one. This range was divided into M segments, the length Δh of each being 1/M. Let h designate the position of each segment. Thus when h is zero, it points to the entrance of the carbon bed and when it is equal to M, it refers to the exit of the bed.

A dimensionless time step Δp was also selected. Let p represent a position in time, the dimensionless time is given by $\sum_{i=1}^{p} \Delta p_i$.

The different equations selected to represent the different derivatives are

$$\left.\frac{\partial F}{\partial \alpha}\right|_{h,p} = \frac{F_{h+1,p} - F_{h,p}}{\Delta h} \qquad \text{A.10}$$

$$\left.\frac{\partial^2 F}{\partial \alpha^2}\right|_{h,p} = \frac{F_{h+1,p} - 2F_{h,p} + F_{h-1,p}}{(\Delta h)^2} \qquad \text{A.11}$$

$$\left.\frac{\partial F}{\partial \tau}\right|_{h,p} = \frac{F_{h,p} - F_{h,p-1}}{\Delta p} \qquad \text{A.12}$$

$$\left.\frac{\partial X}{\partial \tau}\right|_{h,p} = \frac{X_{h,p} - X_{h,p-1}}{\Delta p} \qquad \text{A.13}$$

Similarly the rate of chlorine reduction, R(X,F), at time step p + 1 was expressed in terms of the rate at time step p by

$$R(X,F)_{h,p+1} = R(X,F)_{h,p} + \left(\frac{\partial R}{\partial F}\right)_{h,p} (F_{h,p+1} - F_{h,p})$$

$$+ \left(\frac{\partial R}{\partial X}\right)_{h,p} (X_{h,p+1} - X_{h,p+1}) \qquad \text{A.14}$$

Substituting Equations A.10, A.11, A.12, A.13 and A.14 into the packed bed mathematical model, the following two difference equations were obtained

$$-\Delta p\, F_{h-1,p+1} + \left[(\Delta h)^2 P_e + 2\Delta p - \Delta p\, \Delta h\, P_e + \frac{\Delta p (\Delta h)^2 P_e}{S}\right.$$

$$\left. \cdot \left(\frac{\partial R}{\partial F}\right)_{h,p}\right] F_{h,p+1} + (-\Delta p + \Delta p\, \Delta h\, P_e) F_{h+1,p+1}$$

$$= (\Delta h)^2 P_e F_{h,p} - \frac{\Delta p (\Delta h)^2 P_e}{S} R(X,F)_{h,p} + \frac{\Delta p (\Delta h)^2 P_e}{S} \left(\frac{\partial R}{\partial F}\right)_{h,p} F_{h,p}$$

$$- \frac{\Delta p (\Delta h)^2 P_e}{S} \left(\frac{\partial R}{\partial X}\right)_{h,p} (X_{h,p+1} - X_{h,p}) \qquad \text{A.15}$$

$$X_{h,p+1} = \frac{[X_{h,p} + H\Delta p\, R(X,F)_{h,p} - H\Delta p \left(\frac{\partial R}{\partial X}\right)_{h,p} X_{h,p} + H\Delta p \left(\frac{\partial R}{\partial F}\right)_{h,p} (F_{h,p+1} - F_{h,p})]}{[1 - H\Delta p \left(\frac{\partial R}{\partial X}\right)_{h,p}]}$$

A.16

Equations A.15 and A.16 were used to evaluate F and X at position h and time p + 1. The equation for h equal to M is identical to Equation A.15 except, in this case, $F_{h-1,p+1}$ is equal to $F_{h+1,p+1}$. This is because of the boundary condition, at the end of the reactor, given by Equation 2.54. At the entrance of the bed, the boundary condition given by Equation 2.53 contributes the first equation to the set of equations described by Equation A.15. This equation is

$$(\Delta h\, P_e + 1)\, F_{o,p+1} - F_{1,p+1} = \Delta h\, P_e \qquad A.17$$

At the start of the solution, $X_{h,o}$ was set equal to zero for all values of h. To obtain an initial distribution of $F_{h,o}$, the axial dispersion term in Equation 2.49 was dropped and the remaining equation was solved by

$$F_{h+1,o} = F_{h,o} - \frac{\Delta h}{S}\, R(\theta,F)_{h,o} \qquad A.18$$

In the above $F_{o,o}$ is set at one.

Once the initial values of $F_{h,o}$ and $X_{h,o}$ were defined, the finite difference equations were solved in a manner identical to that described previously for the CCBR model.

3. Plug Flow Packed Bed Reactor

Equations 2.55, 2.56, 2.57, 2.58 and 2.59 describe the behavior of a plug flow packed bed reactor. Defining γ to be equal to $\tau - \alpha$ and using the method of characteristics, the system is

$$\frac{\partial F}{\partial \alpha} = -\frac{1}{S} R(X,F); \quad F(0) = 1 \qquad \text{A.19}$$

$$\frac{\partial X}{\partial \gamma} = HR(X,F); \quad X(0) = 0 \qquad \text{A.20}$$

As was done in the case of the packed bed reactor with axial dispersion, the distance variable α was subdivided into M equal segments, the length, Δh, of each being 1/M. Here also h was used to designate the position of a segment.

A dimensionless time step w was also selected. Let w represent a position in the γ dimension, then γ is given by $\sum_{i=1}^{w} \Delta w_i$. The Runge-Kutta-Gill method (Lapidus, 1962) was used to solve the plug flow mathematical model given by Equations A.19 and A.20.

APPENDIX B

COMPUTER PROGRAM LISTINGS

This appendix contains listings of the Constant Concentration Batch Reactor, the Closed Batch Reactor and the Packed Bed with Axial Dispersion Reactor computer programs. Each of the three programs should be solved in conjunction with the subroutine TRIDIR (Section B.4). This subroutine was written by Dr. R. A. Schmitz.

1. Constant Concentration Batch Reactor

```
C     N = NUMBER OF SEGMENTS IN HALF PORE FORMAT(I10)
C     NSTEPS = NUMBER OF TIME STEPS TO BE EXECUTED
C      FORMAT(I10)
C     IINX = A PRINT FLAG, THE SOLUTION IS PRINTED EVERY
C      IINX DK INCREMENTS FORMAT(I10)
C     CO = BULK CONCENTRATION MG/L FORMAT(F20.10)
C     XPV = PORE VOLUME CC/GM FORMAT(F20.10)
C     DA = DIFFUSIVITY COEFFICIENT CM**2/MIN FORMAT(F20.10)
C     XL = PORE HALF LENGTH CM FORMAT(F20.10)
C     CARBON = CONCENTRATION OF CARBON IN REACTOR MG/L
C      FORMAT(F20.10)
C     DK = DIMENSIONLESS TIME STEP FORMAT(F20.10)
C     SIT = AS IN MODEL FORMAT(F20.10)
C     K8 =  AS IN MODEL FORMAT(F20.10)
C     K9 =  AS IN MODEL FORMAT(F20.10)
C     K10 = AS IN MODEL FORMAT(F20.10)
C     AFTER NSTEPS EXECUTIONS OF THE SOLUTION THE
C      PROGRAM READS A NEW VALUE OF NSTEPS AND THEN DK.
C      THIS IS REPEATED UNTIL A VALUE OF ZERO IS
C      ENCOUNTERED FOR NSTEPS WHERE THE PROGRAM IS TERMINATED
```

```
      IMPLICIT REAL*8(A-H,O-Z)
      DIMENSION G(301),G1(301),H(301),H1(301),R(301),
     1DRH(301),DRG(301),A(301),AL(301),AU(301),B(301),
     2QS(301)
      COMMON QS,AU,AL,A,G1,B
      COMMON N
      CALL UNDERZ('OFF')
      REAL K8,K9,K10
    1 FORMAT(I10)
    2 FORMAT(F20.10)
  150 FORMAT(1X,6(E15.8,5X))
  151 FORMAT(4(E15.8,5X))
      READ(5,1) N
      READ(5,1) NSTEPS
      READ(5,1) IINX
      READ(5,2) CO
      READ(5,2) XPV
      READ(5,2) DA
      READ(5,2) XL
      READ(5,2) CARBON
      READ(5,2) DK
      READ(5,2) SIT
      READ(5,2) K8
      READ(5,2) K9
      READ(5,2) K10
C      CO IS CONVERTED FROM MG/L TO GMS/CC
      CO = CO*0.000001
C      XPO IS THE DIMENSIONLESS CONCENTRATION AT PORE MOUTH
      XPO = XPV*CO
      N1 = N-2
      TM = DSQRT(SIT/K8)
      DO 12 K = 1,N
      XI = DH*K
      G(K) = -DTANH(TM)*DSINH(TM*XI)+DCOSH(TM*XI)
   12 CONTINUE
      DH = 1./N
      NF = N-1
      DO 9 I=1,NF
      AU(I)=DK
      AL(I)=DK
    9 CONTINUE
      AL(NF)=2.*DK
      DO 16 J = 1,20
      DO 15 I=1,N
      DRR = SIT*K8/((G(I)*XPO+K8)**2)
      RR = SIT*G(I)/(G(I)*XPO+K8)
      B(I) = DK*(DH**2)*RR-(DK*(DH**2)*DRR+(DH**2))*G(I)
      A(I) = -(2.*DK+(DH**2)+DK*(DH**2)*DRR)
   15 CONTINUE
      B(1) = B(1)-DK
```

```
      CALL TRIDIR
      DO 17 K = 1,N
      G(K) = G1(K)
   17 CONTINUE
      RATE = (-G(2)+4.*G(1)-3.)*DA*XPO*CARBON/
     1(2.*DH*(XL**2))
      WRITE(6,18) RATE
   16 CONTINUE
   18 FORMAT(2X,'THE INITIAL RATE IS ',E15.8,5X,
     1'MG/L-MIN',//)
      DO 8 I = 1,N1
      AU(I) = DK
      AL(I) = DK
    8 CONTINUE
      AU(N-1) = DK
      AL(N-1) = 2.*DK
      NN = N+1
      G(NN) = 1.
      G1(NN) = 1.
      DH = 1./N
C      NN REFERS TO MOUTH OF PORE,  N REFERS TO END OF PORE
      DO 3  I = 1,NN
      H(I) = 0.
    3 CONTINUE
  100 FORMAT(E15.8)
      WRITE(6,10)N,CO,XPO,XPV,DA,XL,CARBON,DH,DK,SIT,
     1K8,K9,K10
   10 FORMAT(2X,'THE NUMBER OF SEGMENTS PER PORE IS  ',
     1I10,/,2X,'THE BULK CONCENTRATION IS ',F20.10,
     2'   GRAMS/CC',/,2X,
     2'THE DIMENSIONLESS CONCENTRATION AT PORE MOUTH IS',
     3F20.10,/,
     32X,'THE PORE VOLUME IS ',F20.10,'  CC/GRAM',/,
     42X,'THE DIFFUSIVITY IS ',F20.10,'  CM**2/MIN',/,
     52X,'THE PORE LENGTH IS',F20.10,'  CM',/,
     62X,'THE CARBON CONCENTRATION IS',F20.10,'  MG/L',/,
     72X,'THE DISTANCE STEP IS',F20.10,/,
     82X,'THE TIME STEP IS',F20.10,/,
     92X,'SIT = ',F20.10,'     K8 = ',F20.10,/,
     12X,'K9 = ',F20.10,'     K10 = ',F20.10)
      TIM = 0.
      AMREM = 0.
      WRITE(6,21)
   21 FORMAT(//,6X,'TIME MIN',9X,'AMT.REM. GM/GM',4X,
     1'AMT.REC. GM/GM',5X,'RATE MG/L-MIN',/)
      IIT = IINX - 1
   13 DO 20 JJ = 1,NSTEPS
      DO 4 I = 1,NN
      R(I) = G(I)*(SIT-K9*XPO*H(I)/(1.+K10*XPO*H(I)))/
     1(G(I)*XPO+K8)
```

```
      DRG(I) = K8*(SIT-K9*XPO*H(I)/(1.+K10*XPO*H(I)))/
     1((G(I)*XPO+K8)**2)
      DRH(I) = -K9*XPO*G(I)/((G(I)*XPO+K8)*
     1((1.+K10*XPO*H(I))**2))
      H1(I)= (H(I)+DK*(R(I)-DRH(I)*H(I)))/(1.-DK*DRH(I))
    4 CONTINUE
      DO 5 I = 1,N
      A(I) = -(2.*DK+(DH**2)+DK*(DH**2)*DRG(I))
      B(I) = (DH**2)*(DK*R(I)-(DK*DRG(I)+1.)*G(I) +
     1DK*DRH(I)*(H1(I)-H(I)))
    5 CONTINUE
      B(1) = B(1)-DK*G(NN)
      CALL TRIDIR
      DO 6 I = 1,N
      B(I) = B(I) - DK*(DH**2)*H1(I)*DRH(I)
      H1(I) = (DK*(R(I)+DRG(I)*(G1(I)-G(I))-DRH(I)*H(I))
     1+H(I))/(1.-DK*DRH(I))
      B(I) = B(I) + DK*(DH**2)*H1(I)*DRH(I)
    6 CONTINUE
      CALL TRIDIR
      DO 7 I = 1,NN
      H(I) = H1(I)
      G(I) = G1(I)
    7 CONTINUE
      RATE =(-G1(2) + 4.*G1(1) - 3.*G1(NN))*DA*XPO*CARBON/
     1(2.*DH*(XL**2))
      AMREM = AMREM+RATE*DK*(XL**2)/(DA*CARBON)
      AMREC = (H(NN) + H(N))/2.
      NS = N-1
      DO 11 I = 1,NS
      AMREC = AMREC + H(I)
   11 CONTINUE
      AMREC = AMREC*XPO/N
      TIM = TIM + DK*(XL**2)/DA
      IIT = IIT +1
      IF(IIT.NE.IINX) GO TO 20
      WRITE(6,150)TIM,AMREM,AMREC,RATE
      IIT = 0
   20 CONTINUE
      READ(5,1)NSTEPS
      IF(NSTEPS.EQ.0) GO TO 14
      READ(5,2)DK
      DO 25 I = 1,N1
      AU(I) = DK
      AL(I) = DK
   25 CONTINUE
      AU(N-1) = DK
      AL(N-1) = 2.*DK
      GO TO 13
   14 STOP
      END
```

2. Closed Batch Reactor

```
C     N = NUMBER OF SEGMENTS IN HALF PORE FORMAT(I10)
C     NSTEPS = NUMBER OF TIME STEPS TO BE EXECUTED
C      FORMAT(I10)
C     IINX = A PRINT FLAG, THE SOLUTION IS PRINTED EVERY
C      IINX DK INCREMENTS FORMAT(I10)
C     CO = INITIAL BULK CONCENTRATION MG/L FORMAT(F20.10)
C     XPV = PORE VOLUME CC/GM FORMAT(F20.10)
C     DA = DIFFUSIVITY COEFFICIENT CM**2/MIN FORMAT(F20.10)
C     XL = PORE HALF LENGTH CM FORMAT(F20.10)
C     CARBON = CONCENTRATION OF CARBON IN REACTOR MG/L
C      FORMAT(F20.10)
C     DK = DIMENSIONLESS TIME STEP FORMAT(F20.10)
C     SIT = AS IN MODEL FORMAT(F20.10)
C     K8 =  AS IN MODEL FORMAT(F20.10)
C     K9 =  AS IN MODEL FORMAT(F20.10)
C     K10 = AS IN MODEL FORMAT(F20.10)
C     STRIP = FIRST ORDER RATE CONSTANT FOR CHLORINE
C      DISAPPEARANCE 1/MIN FORMAT(F20.10)
C     AFTER NSTEPS EXECUTIONS OF THE SOLUTION THE
C      PROGRAM READS A NEW VALUE OF NSTEPS AND THEN DK.
C      THIS IS REPEATED UNTIL A VALUE OF ZERO IS
C      ENCOUNTERED FOR NSTEPS WHERE THE PROGRAM IS TERMINATED
       IMPLICIT REAL*8(A-H,O-Z)
       DIMENSION G(301),G1(301),H(301),H1(301),R(301),
      1DRH(301),DRG(301),A(301),AL(301),AU(301),B(301),
      2QS(301)
       COMMON QS,AU,AL,A,G1,B
       COMMON NN
       CALL UNDERZ('OFF')
       REAL K8,K9,K10
     1 FORMAT(I10)
     2 FORMAT(F20.10)
   150 FORMAT(1X,6(E15.8,5X))
   151 FORMAT(4(E15.8,5X))
       READ(5,1)N
       READ(5,1)NSTEPS
       READ(5,1)IINX
       READ(5,2)CO
       READ(5,2)XPV
       READ(5,2)DA
       READ(5,2)XL
       READ(5,2)CARBON
       READ(5,2)DK
       READ(5,2) SIT
       READ(5,2) K8
       READ(5,2) K9
       READ(5,2) K10
```

```
      READ(5,2)STRIP
C      CO IS CONVERTED FROM MG/L TO GMS/CC
      CO = CO*0.000001
C      XPO IS THE DIMENSIONLESS CONCENTRATION AT PORE MOUTH
      XPO = XPV*CO
      STM = SIT/K8
      TM = DSQRT(STM)
      DH = 1./N
      DO 12 K=1,N
      XI = DH*K
      G(K) = -DTANH(TM)*DSINH(TM*XI)+DCOSH(TM*XI)
   12 CONTINUE
      NN = N
      NF = N-1
      DO 9 I=1,NF
      AU(I) = DK
      AL(I) = DK
    9 CONTINUE
      AL(NF) = 2.*DK
      DO 16 J=1,20
      DO 15 I=1,N
      RR = SIT*G(I)/(G(I)*XPO+K8)
      DRR = SIT*K8/((G(I)*XPO+K8)**2)
      B(I) = DK*(DH**2)*RR-(DK*(DH**2)*DRR+(DH**2))*G(I)
      A(I) = -(2.*DK+(DH**2)+DK*(DH**2)*DRR)
   15 CONTINUE
      B(1) = B(1)-DK
      CALL TRIDIR
      DO 17 K=1,N
      G(K) = G1(K)
   17 CONTINUE
      RATE  = (-G(2)+4.*G(1)-3.)*DA*XPO*CARBON/
     1(2.*DH*(XL**2))
      WRITE(6,18)RATE
   16 CONTINUE
   18 FORMAT(2X,'THE INITIAL RATE IS ',E15.8,5X,
     1'MG/L-MIN',//)
      WRITE(6,10)N,CO,XPO,XPV,DA,XL,CARBON,DH,DK,SIT,
     1K8,K9,K10,STRIP
   10 FORMAT(2X,'THE NUMBER OF SEGMENTS PER PORE IS  ',
     1I10,/,2X,'THE BULK CONCENTRATION IS ',F20.10,
     2'   GRAMS/CC',/,2X,
     2'THE DIMENSIONLESS CONCENTRATION AT PORE MOUTH IS',
     3F20.10,/,
     32X,'THE PORE VOLUME IS ',F20.10,'  CC/GRAM',/,
     42X,'THE DIFFUSIVITY IS ',F20.10,'  CM**2/MIN',/,
     52X,'THE PORE LENGTH IS',F20.10,'  CM',/,
     62X,'THE CARBON CONCENTRATION IS',F20.10,'  MG/L',/,
     72X,'THE DISTANCE STEP IS',F20.10,/,
     82X,'THE TIME STEP IS',F20.10,/,
```

```
  92X,'SIT = ',F20.10,'      K8 = ',F20.10,/,
  12X,'K9 = ',F20.10,'     K10 = ',F20.10,/,
  22X,'STRIPPING RATE CONSTANT = ',F20.10,'   1/MIN' )
   IIT = IINX-1
   WRITE(6,21)
21 FORMAT(//,6X,'TIME MIN',9X,'AMT.REM. GM/GM',4X,
  1'AMT.REC. GM/GM',5X,'RATE MG/L-MIN',6X,
  2'CONC. GM/CC'/)
   TIM = 0.
   AMREM = 0.
   CM = CARBON*.000001
   NN = N+1
   DO 50 I = 1,N
   KII = N+2-I
   H(KII) = 0.
   G(KII) = G(KII-1)
50 CONTINUE
   H(1) = 0.
   G(1) = 1.
55 DO 8 I=2,NF
   AU(I) = DK
   AL(I) = DK
 8 CONTINUE
   AU(N) = DK
   AL(N) = 2.*DK
   AU(1) = -CM*XPV*DK
   AL(1) = DK
   A(1) = DH+CM*XPV*DK
   DO 20 JJ=1,NSTEPS
   B(1) = DH*G(1)-G(1)*DH*STRIP*DK*(XL**2)/DA
   DO 4 I=1,NN
   R(I) = G(I)*(SIT-K9*H(I)/(1.+K10*H(I)))/(G(I)*XPO+K8)
   DRG(I) = K8*(SIT-K9*H(I)/(1.+K10*H(I)))/
  1((G(I)*XPO+K8)**2)
   DRH(I) = -K9*G(I)/((G(I)*XPO+K8)*((1.+K10*H(I))**2))
   H1(I) = (H(I)+DK*XPO*(R(I)-DRH(I)*H(I)))/
  1(1.-DK*XPO*DRH(I))
 4 CONTINUE
   DO 5 I=2,NN
   A(I) = -(2.*DK+(DH**2)+DK*(DH**2)*DRG(I))
   B(I) = (DH**2)*(DK*R(I)-(DK*DRG(I)+1.)*G(I)+
  1DK*DRH(I)*(H1(I)-H(I)))
 5 CONTINUE
   CALL TRIDIR
   DO 6 I=2,NN
   B(I) = B(I)-DK*(DH**2)*H1(I)*DRH(I)
   H1(I) = (XPO*DK*(R(I)+DRG(I)*(G1(I)-G(I))-DRH(I)*
  1H(I))+H(I))/(1.-DK*XPO*DRH(I))
   B(I) = B(I)+DK*(DH**2)*H1(I)*DRH(I)
 6 CONTINUE
```

```
      CALL TRIDIR
      DO 7 I=1,NN
      H(I) = H1(I)
      G(I) = G1(I)
    7 CONTINUE
      RATE = (-G1(3)+4.*G1(2)-3.*G1(1))*DA*XPO*CARBON/
     1(2.*DH*(XL**2))
      AMREM = AMREM+RATE*DK*(XL**2)/(DA*CARBON)
      AMREC = (H(1)+H(NN))/2.
      DO 11 I=2,N
      AMREC = AMREC+H(I)
   11 CONTINUE
      AMREC = AMREC/N
      TIM = TIM+DK*(XL**2)/DA
      CN = G(1)*CO
      IIT = IIT+1
      IF(IIT.NE.IINX)GO TO 20
      WRITE(6,150) TIM,AMREM,AMREC,RATE,CN
      IIT = 0
   20 CONTINUE
      READ(5,1) NSTEPS
      IF(NSTEPS.EQ.0)GO TO 14
      READ(5,2) DK
      GO TO 55
   14 STOP
      END
```

3. Packed Bed Reactor

```
C     N = NUMBER OF SEGMENTS IN PACKED BED FORMAT(I10)
C     NSTEPS = NUMBER OF TIME STEPS TO BE EXECUTED
C      FORMAT(I10)
C     INDEX = A PRINT FLAG, THE SOLUTION IS PRINTED
C      EVERY INDEX DK INCREMENTS FORMAT(I10)
C     CO = INFLUENT CONCENTRATION MG/L FORMAT(20.10)
C     DA = AXIAL DISPERSION COEFFICIENT CM**2/MIN
C      FORMAT(20.10)
C     XL = BED LENGTH CM FORMAT(20.10)
C      FORMAT(20.10)
C     AREA = PACKED BED CROSS-SECTIONAL AREA CM**2
C     XPORO = POROSITY FORMAT(20.10)
C      VOLUME FORMAT(20.10)
C     CARBON = GRAMS OF CARBON IN ONE CUBIC CM OF BED
```

```
C     FLOW = TOTAL INFLUENT FLOW RATE CM**3/MIN
C      FORMAT(F20.10)
C     DK = DIMENSIONLESS TIME STEP FORMAT(F20.10)
C     XJ(I) = NINE CONSTANTS FOR THE ALGEBRAIC RATE
C      EXPRESSION R(X,C) , THE UNITS FOR THE RATE
C      EXPRESSION ARE 1./MIN AND THE CONSTANTS ARE READ
C      USING FORMAT(E15.8)
C     AFTER NSTEPS EXECUTIONS OF THE SOLUTION THE PROGRAM
C      READS A NEW VALUE FOR NSTEPS AND THEN DK. THIS IS
C      REPEATED UNTIL A VALUE OF ZERO IS ENCOUNTERED FOR
C      NSTEPS WHERE THE PROGRAM IS TERMINATED
       IMPLICIT REAL*8(A-H,O-Z)
       DIMENSION AU(301),AL(301),TEMP(301),A(301),B(301),
      1R(301),DRX(301),DRP(301),P(301),P1(301),X(301),
      2X1(301),QS(301),XJ(9)
       COMMON QS,AU,AL,A,P1,B
       COMMON NP
       CALL UNDERZ('OFF')
     1 FORMAT(I10)
     2 FORMAT(F20.10)
   150 FORMAT(1X,6(E15.8,5X))
   151 FORMAT(E15.8)
   152 FORMAT(10(1X,E15.8))
       READ(5,1) N
       READ(5,1) NSTEPS
       READ(5,1) INDEX
       READ(5,2) CO
       READ(5,2) DA
       READ(5,2) XL
       READ(5,2) CARBON
       READ(5,2) XPORO
       READ(5,2) AREA
       READ(5,2) FLOW
       READ(5,2) DK
       DO 99 I=1,9
       READ(5,151)XJ(I)
    99 CONTINUE
C      CO IS CONVERTED FROM MG/L TO GMS/CC
       CO = CO*0.000001
       DH = 1./N
       NP = N+1
       N1 = NP-2
       V = FLOW/(AREA*XPORO)
       WRITE(6,10) N,CO,DA,XL,CARBON,XPORO,AREA,FLOW,V,
      1DH,DK
    10 FORMAT(2X,'THE NUMBER OF POINTS IN BED IS ',I10,/,
      12X,'THE BULK CONCENTRATION IS ',F20.10,'  GRAMS/CC'
      2,/,2X,'THE AXIAL DISPERSION COEFFICIENT IS ',
      3F20.10,'CM**2/MIN',/,2X,'THE BED LENGTH IS ',F20.10
      4,'  CM',/,2X,'THE CARBON CONCENTRATION IS',F20.10,
```

```
     5'  GM/CC',/,2X,'THE POROSITY IS',F20.10,/,
     62X,'THE CROSS SECTIONAL AREA IS',F20.10,'  CM**2',/,
     72X,'THE FLOW RATE IS',F20.10,'  CC/MIN',/,
     82X,'THE PORE VELOCITY IS',F20.10,'  CM/MIN',/,
     92X,'THE DISTANCE STEP IS',F20.10,/,
     12X,'THE TIME STEP IS',F20.10,///)
      WRITE(6,21)
  21 FORMAT(6X,'TIME MIN',7X,'VOLUME IN L/CM**2',3X,
     1'TOT. VOL. IN L',7X,'AMT.REM. GM    ',6X,
     2'CONC.EFF. MG/L',6X,'AMT.REAC. GM    ',/)
      XPECLE = XL*V/DA
      DO 3 I = 1,NP
      X(I) = 0.
    3 CONTINUE
      CONST = -DH*CARBON*XL*XJ(1)/(V*XPORO)
      P(1) = 1.
      DO 7 KKK = 2,NP
      P(KKK) = P(KKK-1)+CONST*P(KKK-1)/(XJ(2)+CO*P(KKK-1))
    7 CONTINUE
      V1 = XJ(1)*CO
      V2 = V1*XJ(2)
      V5 = -XJ(4)*CO
      V6 = XJ(3)*XJ(5)
      V7 = V5*V6
      V8 = XJ(7)*CO
      V9 = (XJ(6)**XJ(8))*XJ(8)*XJ(9)
      S = CARBON*XL/(V*CO*XPORO)
      T = XL/V
      TIM = 0.
      AMREM = 0.
      AU(1) = -1.
      A(1) = DH*XPECLE+1.
      B(1) = DH*XPECLE
   13 TT1 = DK*DH*XPECLE-DK
      TT2 = -DK
      TT3 = (DH**2)*XPECLE+2.*DK-DK*DH*XPECLE
      AU(N) = TT1
      AL(1) = TT2
      AL(N) = 2.*TT2
      DO 8 I = 2,N1
      AU(I) = TT1
      AL(I) = TT2
      TEMP(I) = TT3
    8 CONTINUE
      TEMP(N) = TT3
      TEMP(NP) = (DH**2)*XPECLE+2.*DK
      TT4 = T*DK
      TT5 = DK*(DH**2)*XPECLE*S
      TT6 = (DH**2)*XPECLE
      IIT = INDEX-1
```

```
      DO 20 JJ = 1,NSTEPS
   22 DO 4 I = 1,NP
      W1 = XJ(2)+C0*P(I)
      W3 = DEXP(V5*P(I))
      W4 = 1.+XJ(3)*W3*X(I)
      W5 = X(I)*DEXP(V8*P(I))
      W6 = 1.+((XJ(6)*W5)**XJ(8))
      G1 = V1*P(I)/W1
      G2 = W4**XJ(5)
      G3 = W6**XJ(9)
      G4 = V2/(W1**2)
      G5 = V6*W3*(W4**(XJ(5)-1.))
      G6 = V9*(W5**(XJ(8)-1.))*DEXP(V8*P(I))*
     1(W6**(XJ(9)-1.))
      G7 = V7*X(I)*W3*(W4**(XJ(5)-1.))
      G8 = G6*V8*X(I)
      G10 = G2*G3
      G11 = (G10**2)
      G12 = -G1*G3
      G13 = -G1*G2
      R(I) = G1/G10
      DRX(I) = (G13*G6+G12*G5)/G11
      DRP(I) = (G10*G4+G12*G7+G13*G8)/G11
      X1(I) = (X(I)+TT4*R(I)-TT4*DRX(I)*X(I))/(1.-TT4
     1*DRX(I))
    4 CONTINUE
      DO 5 I= 2,NP
      A(I) = TEMP(I) + TT5*DRP(I)
      B(I) = TT6*P(I) -TT5*(R(I)-DRP(I)*P(I)+DRX(I)*
     1(X1(I)-X(I)))
    5 CONTINUE
      CALL TRIDIR
      DO 6 I = 2,NP
      B(I) = B(I)+TT5*DRX(I)*X1(I)
      X1(I) = X1(I) + TT4*DRP(I)*(P1(I)-P(I))/(1.-TT4*
     1DRX(I))
      B(I) = B(I) - TT5*DRX(I)*X1(I)
    6 CONTINUE
      X1(1) = X1(1) + TT4*DRP(1)*(P1(1)-P(1))/(1.-TT4*
     1DRX(1))
      CALL TRIDIR
      CLAST = P(NP)
      DO 25 I = 1,NP
      X(I) = X1(I)
      P(I) = P1(I)
   25 CONTINUE
      TIM = TIM+DK*XL/V
      AMREM = AMREM + FLOW*(1.-(CLAST+P(NP))/2.)*C0*DK*XL/V
      CEF = P(NP)*1000000.*C0
      Q = V*TIM*XPORO/1000.
```

```
      F = FLOW*TIM/1000.
      IIT = IIT+1
      IF(IIT.NE.INDEX) GO TO 20
      WRITE(6,150) TIM,Q,F,AMREM,CEF
      IIT = 0
   20 CONTINUE
      AMREC = (X(1) + X(NP))/2.
      DO 11 I = 2,N
      AMREC = AMREC + X1(I)
   11 CONTINUE
      AMREC = AMREC*CARBON*AREA*XL/N
      WRITE(6,152) AMREC
      READ(5,1) NSTEPS
      IF(NSTEPS.EQ.0) GO TO 14
      READ(5,2) DK
      IIT = INDEX - 1
      GO TO 13
   14 STOP
      END
```

4. Tridiagonal Matrix Solver (TRIDIR)

```
      SUBROUTINE TRIDIR
      IMPLICIT REAL*8(A-H,O-Z)
      DIMENSION QS(301),AL(301),AU(301),A(301),
     1P1(301),B(301)
      COMMON QS,AU,AL,A,P1,B
      COMMON N
      N1 = N-1
  100 QS(1) = AU(1)/A(1)
      DO 110 J = 2,N1
      QDEN = A(J)-AL(J-1)*QS(J-1)
  110 QS(J) = AU(J)/QDEN
      P1(1) = B(1)/A(1)
      DO 120 J = 2,N
      GNUM = B(J)-AL(J-1)*P1(J-1)
      GDEN = A(J)-AL(J-1)*QS(J-1)
  120 P1(J) = GNUM/GDEN
      DO 130 J = 1,N1
      M = N-J
  130 P1(M) = P1(M)-QS(M)*P1(M+1)
      RETURN
      END
```